



**UNIVERSITY OF  
BIRMINGHAM**

**Anti-leukemic action of Bezafibrate and Medroxyprogesterone acetate in  
Myeloid Leukemia Cells  
and  
Analysis of Putative cis-Regulatory Elements in Type 2 Diabetes Associated  
Genes using Zebrafish Model**

**By**

**Julia Constantinou**

**A combined research thesis submitted to the University of Birmingham as  
part of the requirement for the degree of MASTER OF RESEARCH in  
Molecular and Cellular Biology**

**College of Life and Environmental Sciences**

**School of Biosciences**

**University of Birmingham**

**December 2014**

UNIVERSITY OF  
BIRMINGHAM

**University of Birmingham Research Archive**

**e-theses repository**

This unpublished thesis/dissertation is copyright of the author and/or third parties. The intellectual property rights of the author or third parties in respect of this work are as defined by The Copyright Designs and Patents Act 1988 or as modified by any successor legislation.

Any use made of information contained in this thesis/dissertation must be in accordance with that legislation and must be properly acknowledged. Further distribution or reproduction in any format is prohibited without the permission of the copyright holder.



**UNIVERSITY OF  
BIRMINGHAM**

**Anti-leukemic action of Bezafibrate and Medroxyprogesterone acetate in  
Myeloid Leukemia Cells**

**By**

**Julia Constantinou**

**Part 1 of 2: A research thesis submitted to the University of Birmingham as  
part of the requirement for the degree of MASTER OF RESEARCH in  
Molecular and Cellular Biology**

**College of Life and Environmental Sciences**

**School of Biosciences**

**University of Birmingham**

**December 2014**

# CONTENTS

## ABSTRACT

---

<b>1. INTRODUCTION</b>	<b>1</b>
<b>1.1 LEUKAEMIA</b>	<b>1</b>
<b>1.2 ACUTE MYELOID LEUKAEMIA</b>	<b>4</b>
<b>1.3 CURRENT TREATMENT</b>	<b>4</b>
<b>1.4 DRUG REDEPLOYMENT</b>	<b>5</b>
<b>1.5 CANCER CELL METABOLISM</b>	<b>7</b>
1.5.1 FATTY ACID SYNTHESIS	8
1.5.2 CARNITINE PALMOYLTRANSFERASE I	10
1.5.3 STEAROYL-CoA DESATURASE	11
<b>1.6 AIMS AND OBJECTIVES</b>	<b>13</b>
<b>2. MATERIALS AND METHODS</b>	<b>14</b>
<b>2.1 TISSUE CELL CULTURE</b>	<b>14</b>
<b>2.2 PREPARATION OF PALMITATE – BSA SOLUTION</b>	<b>15</b>
<b>2.3 PREPARATION OF BEZAFIBRATE (BEZ) AND MEDROXYPROGESTERONE ACETATE (MPA)</b>	
<b>STOCK SOLUTIONS</b>	<b>16</b>
<b>2.4 CONTROL AND BAP TREATED SAMPLES</b>	<b>17</b>
<b>2.5 FLOW CYTOMETRY OF K562 AND HL60 TREATMENTS</b>	<b>17</b>
<b>2.6 WESTERN BLOT</b>	<b>18</b>
2.6.1 PROTEIN PREPARATION	18
2.6.2 LYSATE PREPARATION	19
2.6.3 PROTEIN DETERMINATION USING BIO-RAD DC REAGENT	19
2.6.4 SDS-PAGE ELECTROPHORESIS	20
2.6.5 SEMI-DRY BLOTTING TRANSFER	22
2.6.6 IMMUNOBLOTTING	22
<b>2.7 ALAMAR BLUE VIABILITY TEST</b>	<b>24</b>
<b>2.8 INHIBITING ANTI-LEUKEMIC ACTION OF BAP BY FATTY ACID SUPPLEMENTATION</b>	<b>26</b>
<b>2.9 REAL-TIME PCR</b>	<b>27</b>
2.9.1 RNA EXTRACTION	27
2.9.2 cDNA SYNTHESIS	28
2.9.3 B-ACTIN PCR	28
2.9.4 cDNA REAL-TIME PCR	29

---

**3. RESULTS** **30****3.1 BAP TREATMENT INDUCES APOPTOSIS IN LEUKEMIC CELL LINES** **30****3.2 BAP ALTERS EXPRESSION OF PROTEINS INVOLVED IN UP-REGULATION OF FATTY ACID SYNTHESIS IN LEUKEMIC CELL LINES** **33****3.3 PALMITIC ACID PROVIDES PARTIAL RESCUE TO BAP TREATED CELLS** **40****3.4 PALMITIC ACID PLUS OLEIC ACID PROVIDES BETTER RESCUE THAN PALMITIC ACID ALONE** **41**

---

**4. DISCUSSION** **42****4.1 COMBINED BEZAFIBRATE AND MEDROXYPROGESTERONE ACETATE HAVE POTENT ANTI-LEUKEMIC ACTION IN LEUKEMIC CELL LINES** **42****4.2 BAP REDUCES CELL PROLIFERATION BY INHIBITING FATTY ACID SYNTHESIS** **43**4.2.1 BAP DOWN-REGULATES FATTY ACID SYNTHASE (FASN) **43**4.2.2 BAP INHIBITS ACC BY INCREASING PHOSPHORYLATION **44**4.2.3 BAP UP-REGULATES CARNITINE PALMITOYLTRANSFERASE I (CPTI) **46**4.2.4 STEAROYL-CoA DESATURASE (SCDI) IS DECREASED IN BAP TREATED SAMPLES **48**4.2.5 PALMITIC ACID AND OLEIC ACID PROVIDE RESCUE TO BAP TREATED CELLS **49**

---

**5. CONCLUSION** **52**

---

**REFERENCES** **54**

---

**APPENDIX I – ADDITIONAL DATA** **I**AI.1 FACSCALIBUR ANNEXIN V/PROPIDIUM IODIDE DATA (96-HOUR TREATMENT) **I**AI.2 FACSCALIBUR FORWARD/SIDE SCATTER DATA (96-HOUR TREATMENT) **III**AI.3 PALMITIC ACID RESCUE DATA **V**

## **ACKNOWLEDGEMENTS**

I would like to thank my supervisor Dr Andrew Southam for giving me the opportunity to be a part of this project, whose constant support and guidance through-out the duration of the project made the process both enjoyable and successful.

I would also like to thank the rest of the group, namely Laura Cronin, Nikos Batis, Katarzyna Koczula, Matthew Fenton, Hawwa Shillingford, Dr Farhat Khanim and Prof Christopher Bunce for their support and welcoming, friendly attitude that made the experience so easy to enjoy.

## FIGURES AND TABLES

### List of Figures

<b>Figure 1.1:</b> Glycolysis, TCA Cycle and Fatty Acid Metabolism	8
<b>Figure 1.2:</b> Carnitine Palmitoyltransferase I Metabolism and Transportation	10
<b>Figure 1.3:</b> Steroyl-CoA-Desaturase Mechanism of Action	11
<b>Figure 2.1:</b> Semi-Dry Blotting Transfer	21
<b>Figure 3.1:</b> Apoptosis in Control and BaP Treated Samples	29
<b>Figure 3.2</b> Annexin V and Propidium Iodide expression in 96-hour treated samples	30
<b>Figure 3.3</b> Forward Scatter and Side Scatter Data of 96-hour treated samples	31
<b>Figure 3.3</b> Fatty Acid Synthase Western Blot Results	32
<b>Figure 3.4</b> Acetyl-CoA-Carboxylase (ACC) and Phosphorylated-ACC Western Blot Results	33
<b>Figure 3.5</b> Carnitine Palmitoyltransferase IA Western Blot Results	34
<b>Figure 3.6</b> Total AMP-Kinase Western Blot Results	34
<b>Figure 3.7:</b> Steroyl-CoA Desaturase I Western Blot Results	35
<b>Figure 3.8:</b> Western Blot Densitometry Significance Analysis	35
<b>Figure 3.9:</b> Fold Change between Control and BaP treated samples	36
<b>Figure 3.10:</b> RT-PCR Analysis	37
<b>Figure 3.11:</b> Palmitic Acid Rescue Data	38

### List of Tables

<b>Table 1.1:</b> Drug Redeployment Therapies	5
<b>Table 2.1:</b> Composition of Control and BaP Treated Samples	16
<b>Table 2.2:</b> Composition of Acrylamide Gel	19
<b>Table 2.3:</b> Volume of primary and secondary antibody added to 10ml 5% blotto	22
<b>Table 2.4:</b> Antibody Product Information	22
<b>Table 2.5:</b> Composition of palmitic acid rescue experiments	25

## ABBREVIATIONS

ACC – Acyl CoA Carboxylase	FASN – Fatty Acid Synthase
ALL – Acute Lymphoid Leukemia	HL – Hodgkin Lymphoma
AML – Acute Myeloid Leukemia	MM – Multiple Myeloma
AMPK – Adenosine Monophosphate Kinase	MPA – Medroxyprogesterone Acetate
ATP – Adenine Triphosphate	MUFA – Mono-unsaturated Fatty Acid
BaP – Combined bezafibrate and medroxyprogesterone acetate	NaCl – Sodium Chloride
BEZ – Bezafibrate	NHL – Non-hodgkin Lymphoma
BL – Burkitt Lymphoma	OA – Oleic Acid
BSA – Bovine Serum Albumin	PA – Palmitic Acid
CLL – Chronic Lymphoid Leukemia	P-ACC – Phosphorylated Acyl CoA Carboxylase
CML – Chronic Myeloid Leukemia	P-AMPK – Phosphorylated Adenosine Monophosphate Kinase
CPT1 – Carnitine Palmitoyltransferase I	RNA – Ribose Nucleic Acid
CPT1A - Carnitine Palmitoyltransferase IA	SCDI – Steroyl Co-A Desaturase
DLBCL – Diffuse Large B-Cell Lymphoma	MUFA – Mono-unsaturated Fatty Acid
DNA – Deoxyribose Nucleic Acid	SFA – Saturated Fatty Acid

## **ABSTRACT**

Acute Myeloid Leukemia (AML) is an aggressive cancer that occurs most commonly in people over the age of 60. Current treatment comprises intrusive non-specific chemotherapy that is often poorly tolerated by patients and frequently leads to other complications. Drug redeployment technologies have identified anti-leukemic activity of combined bezafibrate and medroxyprogesterone acetate (BaP). BaP induces apoptosis in leukemic cells whilst exerts no toxic effect in healthy cells. It has been suggested that the mode of action that BaP undertakes to exercise anti-leukemic activity is the disruption of the lipogenic/lipolytic balance needed to maintain cell growth and proliferation.

Western blot and RT-PCR analysis of 24-hour BaP-treated samples were performed across myeloid cell lines HL60 and K562, and lymphoma cell lines GLOR and BL31.

Enzymes important for lipogenesis include ACC and FASN. Levels of the inactive phosphorylated-ACC are increased in BaP-treated samples therefore limiting production of Malonyl-CoA. Malonyl-CoA is the substrate for FASN which catalyses the final step of biogenesis and levels of FASN were shown to be decreased. The product of FASN catalysis can be converted into monounsaturated fatty acids via SCDI for the production of phospholipids, triglycerides, etc. SCDI expression was reduced in BaP-treated samples therefore production of these is likely to be inhibited. Furthermore, lipolysis appears to be increased as CPTI levels are increased in BaP-treated samples indicating the lipogenic/lipolysis balance is disrupted by BaP. Rescue of BaP-treated samples was possible by supplementing with palmitic acid and oleic acid thus suggesting that lipid metabolism is an important target for the anti-leukemic activity of BaP.

# 1. INTRODUCTION

## 1.1 Leukaemia

Leukaemia is the term for ‘cancer of the blood’ and relates to a group of associated malignant conditions that inhibit the formation of mature healthy white blood cells in the bone marrow. This results in the failure of cells to undergo regulated cell death (apoptosis), the uncontrolled proliferation of new cells, or a combination of both (Leukaemia and Lymphoma Research, 2011).

The abnormal survival and accumulation of immature haemopoietic cells in the bone marrow (known as blasts) are a result of biological properties of leukemic cells. These include decelerated differentiation, deregulation of apoptosis, and ability to spread (Wang and Chen, 2008), resulting in inhibited production of mature cells.

The disease can be sub-divided into acute or chronic and myeloid or lymphoid. Acute and chronic relate to the time frame that the disease exists in. Acute has a short, severe time frame with short life expectancy once the disease is contracted, whilst chronic has a longer more persistent time frame which allows better control of the disease. See below for statistical life expectancy. The disease can be classified as either myeloid or lymphoid depending on blasts existing as myeloblasts or lymphoblasts (Hoffbrand et al., 2006).

Chronic Lymphoid Leukaemia (CLL) is a disease where an excess of neoplastic B lymphoblasts are produced and occupy the lymphatic system (blood, bone marrow, lymphnodes and spleen), interfering with the production of mature lymphocytes (Rozman and Monsterrat, 1995). This mass production of lymphoblasts inhibits the body’s ability to deal

with infection and disease and to drain fluid from tissues. The production of lymphoblasts in CLL is considered slow and many sufferers can live numerous years without any serious symptoms, however in Acute Lymphoid Leukemia (ALL), the production and accumulation of lymphoblasts is significantly more rapid causing severe symptoms to occur much sooner (Macmillan<sup>a</sup>, accessed February 2014). CLL is often split into stages A, B and C. For patients diagnosed in stage A, life expectancy is typically a minimum of 10 years. For patients diagnosed in stage B, life expectancy ranges averagely between 5-8 years whilst those diagnosed in stage C are expected to live between 1-3 years (Cancer research UK<sup>b</sup>, accessed November 2014), for patients suffering from ALL the life expectancy is much shorter with only 40% of sufferers surviving to 5 years (Cancer research UK<sup>c</sup>, accessed November 2014).

Chronic Myeloid Leukaemia (CML) is a disease where excess granulocytes are produced. Clear phases in the development have been identified through extensive research. 'Chronic phase' is the initial step, where myeloid progenitor cells (myeloblasts) are present in peripheral blood, whilst mature granulocytes are still produced. This is followed by 'acceleration phase' and concluded by 'blast crisis' where haematopoietic differentiation has stopped and the accumulation of myeloblasts in the bone marrow spills over in to circulation (Melo and Barnes, 2007). More than 90% of CML cases are caused by the Philadelphia chromosome (Pc)(Kurzrock et al., 2003). The Pc develops when the *Abl* gene located on chromosome 9 is translocated to chromosome 22 and combined with the *Bcr* gene. The *Abl-Bcr* fusion results in the production of tyrosine kinase which leads to blood and bone marrow deficiencies characteristic of CML (Macmillan<sup>b</sup>, accessed February 2014). For patients suffering from CML, 90% often live for 5 years or more from the onset of the disease (Cancer research UK<sup>d</sup>, accessed November 2014).

Other related diseases include lymphoma. This blood cancer is specifically a dysfunction of the lymphocytes and is divided into Non-Hodgkin (NHL) and Hodgkin (HL).

Four out of five cases of lymphoma are NHL (Cancer Research UK<sup>a</sup>, accessed December 2013); of these, Diffuse Large B – Cell Non-Hodgkin Lymphoma (DLBCL) is the most prevalent type accounting for approximately 40% of all cases (Alizadeh et al., 2000). This disease causes swelling of the lymph nodes and can spread to organs such as lungs, kidneys and bones and is ultimately fatal to 60% of sufferers (Macmillan<sup>c</sup>, accessed December 2013).

Historically, distinction between DLBCL and a more rare type of NHL, Burkitt Lymphoma (BL) was largely non-reproducible as both were characterised as mature aggressive B-Cell Lymphomas that when left untreated proved fatal within a period of months.

BL was described as a distinctive entity due to translocations which juxtapose the *myc* oncogene loci and one of three immunoglobulin loci being present in almost all BL, resulting in endemic and sporadic cases associated with immunodeficiency or immunosuppression.

However, confusion arose by the presence of *myc* translocations in other lymphomas, including DLBCL (Hummel et al., 2006).

More recently, distinction between histology, molecular alterations, prognosis and treatment of these lymphomas has become possible. Specifically, DLBCL commonly contains translocation t(14;18)(q32;q21), which juxtaposes BCL2 gene to the immunoglobulin heavy chain gene enhancer. This translocation is absent in BL. Moreover, translocations involving 8(q24) are characteristic of BL whilst only present in a subset of DLBCL (Edwards et al., 2014). BL is described as prevalent in males and can present at all ages, and is often associated with the Epstein-Barr virus, malaria and immunodeficiency (Brady et al., 2007).

## **1.2 Acute Myeloid Leukaemia**

Acute Myeloid Leukaemia (AML) is an aggressive cancer which causes deficits and loss of normal function in erythrocytes (red blood cells), thrombocytes (platelets) and neutrophils (most abundant type of white blood cell), and is prevalent in people ages 60+ (Khanim et al., 2009, Murray et al., 2010). AML is clinically identified by the presence of >20% blast cells in bone marrow and blood (Hoffbrand et al. 2006) and has a rapid onset of symptoms such as infection, bleeding and anaemia which can ultimately be fatal within weeks (Khanim et al., 2009).

The proliferation of blast cells and decreased number of mature leukocytes results in a lowered immune system. The production of blast cells in the bone marrow results in a reduction in the production of other cell types causing other diseases such as anaemia and low platelet count. The blast cells are in such high numbers in the bone marrow that they eventually disseminate and spread in to circulation which can then be detected (Leukaemia and Lymphoma Research, 2012).

## **1.3 Current Treatment**

Current treatment for AML comprises intrusive and non-specific treatments including chemotherapy, radiotherapy, and in severe cases blood transfusion. Treatments include anthracyclines daunorubicin and adriamycin which exert antiproliferative and cytotoxic effects in cancerous cells (Minotti et al., 2004, Pefani et al., 2012).

## **1.4 Drug Redeployment**

Drug Redeployment, also known as Drug Repurposing or Drug Repositioning, offers an alternative to finding new drug treatments. Where empirical data suggests that a drug yields apparent spin-off benefits; above that for which it was originally prescribed; then this offers an opportunity for new avenues of treatment to be promoted. Using readily available products removes the time and costs associated with the discovery, development and registration stages of a new drug (Pessetto et al., Gupta et al.), which takes on average approximately 13.5 years (Gaulton et al., 2010).

The redeployment option provides a substance that has been toxicity tested and has proved stable and clinically safe for human administration. This aspect is particularly beneficial in the treatment of cancers where conventional treatments of chemotherapy are highly toxic and patients require a high degree of care.

The probability of success is also higher than when developing a brand new drug (Thomson Reuters, 2012). By lowering time and costs it makes the treatment more affordable at the application stage and so can be used by poorer countries (Tiziani et al., 2009) but it also allows the development of treatments for 'orphan' diseases that do not capture the attention of larger pharmaceutical companies (Manara et al., 2013, Pessetto et al., 2013)

Examples of successful drug redeployment therapies can be seen in Table 1.1.

**Table 1.1:** Drug Redeployment Therapies

<b>Drug</b>	<b>Original Use</b>	<b>Redeployed Use</b>
<b>Amphotericin B</b>	Fungal Infections	Leishmaniasis
<b>Aspirin</b>	Inflammation, pain	Antiplatelet
<b>Bromocriptine</b>	Parkinson's disease	Diabetes mellitus
<b>Finasteride</b>	Prostate hyperplasia	Hair loss
<b>Gemcitabine</b>	Viral infections	Cancer
<b>Methotrexate</b>	Cancer	Psoriasis, rheumatoid arthritis
<b>Minoidill</b>	Hypertension	Hair loss
<b>Raloxifene</b>	Cancer	Osteoporosis
<b>Thalidomide</b>	Morning Sickness	Leprosy, multiple myeloma
<b>Sildenafil</b>	Angina	Erectile dysfunction, pulmonary hypertension

Table 1.1 adapted from Thomas Reuters, 2012

The most widely recognised drug redeployment operation was that of thalidomide. This particular drug was of great public interest due to causing severe birth defects after being prescribed as a treatment for morning sickness. Singhal *et al* (Singhal et al., 1999) identified that thalidomide caused such defects by inhibiting embryonic angiogenesis, and that in models thalidomide induced apoptosis in newly formed blood vessels. The paper then went on to discuss the key role of angiogenesis and neovascularisation in tumour progression in multiple myeloma (MM), thus identifying thalidomide as a potential treatment. Later studies supported thalidomide as a treatment for MM, including identifying its ability to cause apoptosis in MM cells that are resistant to other treatments such as melphalan and doxorubicin, both *in vivo* and *in vitro* (Hideshima et al., 2000).

Drug redeployment technologies have identified that the combination of the contraceptive drug medroxyprogesterone acetate (MPA) with cholesterol lowering bezafibrate (BEZ); denoted as BaP, as having anti-leukemic activity *in vivo* when using Acute Myeloid Leukaemia (AML) cell lines. An important aspect to note about BaP treatment is that unlike current treatments it has shown anti-leukemic activity without toxicity (Khanim et al., 2009).

Southam et al (unpublished) found that BaP exerts anti-leukemic activity by disrupting *de novo* phospholipid and glycolipid synthesis. The redistribution of incorporating  $^{13}\text{C}$ -D-glucose from phospholipids and glycolipids into glycerol 3-phosphate suggests BaP disrupts synthesis at the acyl chain-addition stage resulting in higher sensitivity to  $\text{H}_2\text{O}_2$ -induced lipid peroxidation and apoptosis. This suggested that BaP increases endogenous reactive oxygen species (ROS) whilst making cells more susceptible to the negative impacts of ROS. BaP may also increase fatty acid  $\beta$ -oxidation of saturated fatty acids therefore disrupting phospholipid synthesis. Southam et al (unpublished) identified the disruption of cellular lipogenic/lipolytic balance as a likely mechanism of anti-leukemic activity exerted by BaP.

## **1.5 Cancer cell metabolism**

Cellular metabolism controls the production of ATP to provide energy for normal cell function, and in cancer cells for rapid division. Metabolism is responsible for the biosynthesis of carbohydrates, proteins, lipids and nucleic acids, in addition to the maintenance of the cells Redox Status (Cairns et al., 2011).

A key phenotype shown by cancer cells is the Warburg effect, characterised as a shift towards anabolic metabolism under aerobic conditions. ATP production moves from oxidative phosphorylation to glycolysis, resulting in high consumption of glucose and producing large quantities of lactic acid when under normoxic conditions. The high consumption of glucose via glycolysis can provide precursors for DNA/RNA and protein synthesis in addition to increased *de novo* fatty acid synthesis. The glucose via glycolysis can also act as an energy supply (Menendez and Lupu, 2007).

Importantly, the metabolism of cancer cells differs greatly to normal quiescent cells.

Although ATP production via oxidative phosphorylation is more efficient in terms of ATP

production per glucose metabolised, production of ATP via glycolysis is much faster and therefore provides energy for proliferation of cancerous cells. Such a shift creates stresses within the cells and changes in metabolism are necessary to deal with these.

For the purpose of this report, lipid metabolism and the Warburg effect shall be focussed upon.

### **1.5.1 Fatty Acid Synthesis**

Fatty acids are essential for the survival of cells and can be derived exogenously or endogenously. Exogenous fatty acids are provided by diet whereas endogenous fatty acids are biosynthesised.

For healthy cells, exogenously derived fatty acids provide a sufficient level of energy, therefore reducing endogenous production to a minimum. In these conditions Fatty Acid Synthase (FASN) converts excess carbohydrates in to fatty acids which are then esterified and stored as triacylglycerols in adipose tissue. These stored triacylglycerols can release fatty acids, typically via the influence of lipases, to undergo  $\beta$ -oxidation and provide energy when needed (Menendez and Lupu, 2007).

**Figure 1.1:** Glycolysis, TCA Cycle and Fatty Acid Metabolism

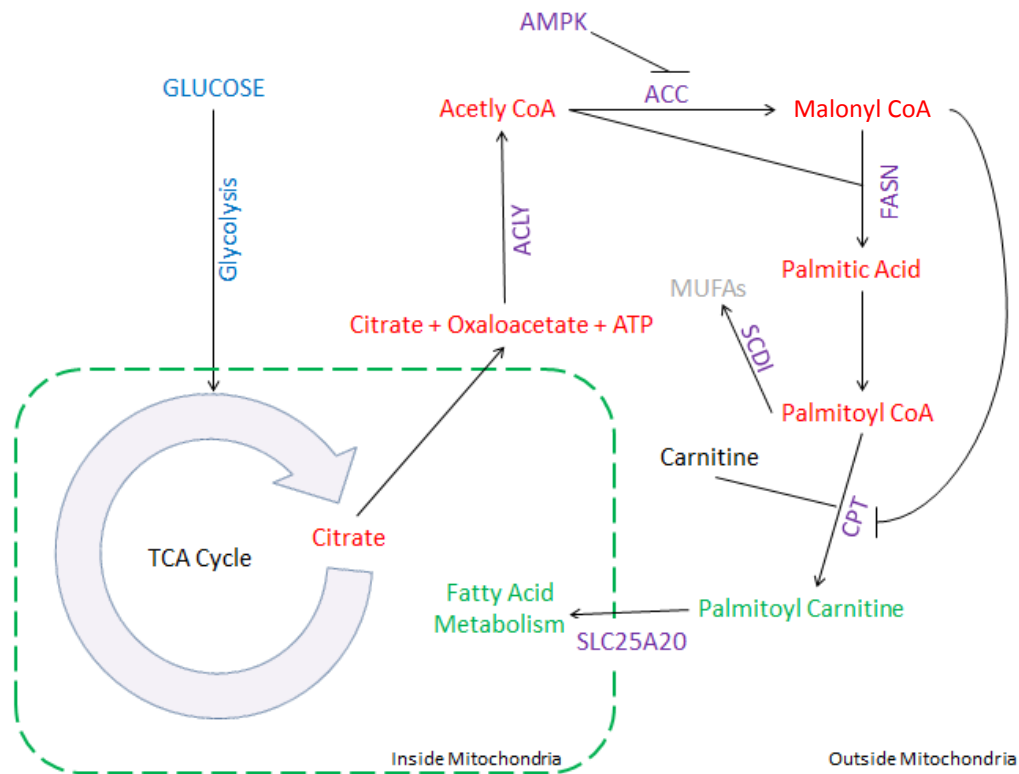


Figure 1.1: Cell metabolism with focus on metabolism of fatty acids as visualised by Southam et al (unpublished). Fatty acids are synthesised via the following mechanism; ATP citrate lyase (ACYL) catalyses citrate from the TCA cycle in to Acetyl CoA. Acetyl CoA is then converted in to Malonyl CoA via the enzyme Acetyl CoA Carboxylase (ACC). The Acetyl CoA and Malonyl CoA are utilised by Fatty Acid Synthase (FASN) to produce the fatty acid, palmitic acid.

In cancerous cells however, proteins involved in the up-regulation of endogenous fatty acid synthesis have been shown to be accelerated, including fatty acid synthase (Pizer et al., 1996, Kuhajda, 2000). Fatty acid synthase (FASN) is a lipogenic enzyme that regulates *de novo* synthesis of fatty acids by catalysing the final stage of biogenesis. An increased level of *de novo* lipogenesis has been associated with many cancers and is a trademark of aggressive cancers (Menendez and Lupu, 2007, Louie et al., 2013) including AML.

Another enzyme shown to be up-regulated in cancers is ACC, of which two isoforms have been identified (designated  $\alpha$  and  $\beta$  or 1 and 2). ACC is a rate limiting step in *de novo* lipid synthesis and produces fatty acid substrate Malonyl CoA in addition to inhibiting

mitochondrial fatty acid  $\beta$ -oxidation by allosteric regulation, and inhibiting Carnitine Palmitoyltransferase I (CPTI) (see section 1.5.2). The  $\alpha$ -isoform has been shown to be up-regulated in cancer cells and has been linked to increased lipogenesis prevalent in human cancers, aiding growth and proliferation of cancer cells (Wang et al., 2010). Whilst both isoforms produce Malonyl-CoA, the subcellular location results in ACC- $\alpha$  producing Malonyl-CoA for *de novo* lipogenesis and ACC- $\beta$  producing Malonyl-CoA for the inhibition of CPTI and mitochondrial fatty acid  $\beta$ -oxidation (Jump et al., 2011). Jump *et al* (2011) showed that in cancer cells the use of Soraphen A, a pharmacological inhibitor of ACC resulted in reduced *de novo* lipid synthesis, including synthesis of long chain saturated and mono- and poly unsaturated fatty acids, as well as inducing  $\beta$ -oxidation thus proving ACC to play an important role in cancer cell metabolism.

### **1.5.2 Carnitine Palmitoyltransferase I**

Carnitine Palmitoyltransferase I (CPTI) is an enzyme coded by the gene located at 11q13.2 and is the rate limiting step in mitochondrial  $\beta$ -oxidation of long chain fatty acids, specifically involved in the uptake of these fatty acids into the mitochondria. This enzyme catalyses the reaction between long chain fatty acid – acyl CoA conjugates with the transporter molecule carnitine. Acyl CoA Synthase modulates the addition of the ‘acyl’ group on the fatty acid. CPTI then acts on the resultant fatty acid – acyl CoA conjugate, and exchanges the acyl CoA moiety with carnitine forming an acyl-carnitine. The newly formed conjugates can then pass through the inner membrane of the mitochondria where the carnitine is removed by CPTII and the fatty acid can be metabolised via  $\beta$ -oxidation to produce energy (McGarry and Brown, 1997, Morash et al., 2008)

**Figure 1.2:** Carnitine Palmitoyltransferase I Metabolism and Transportation

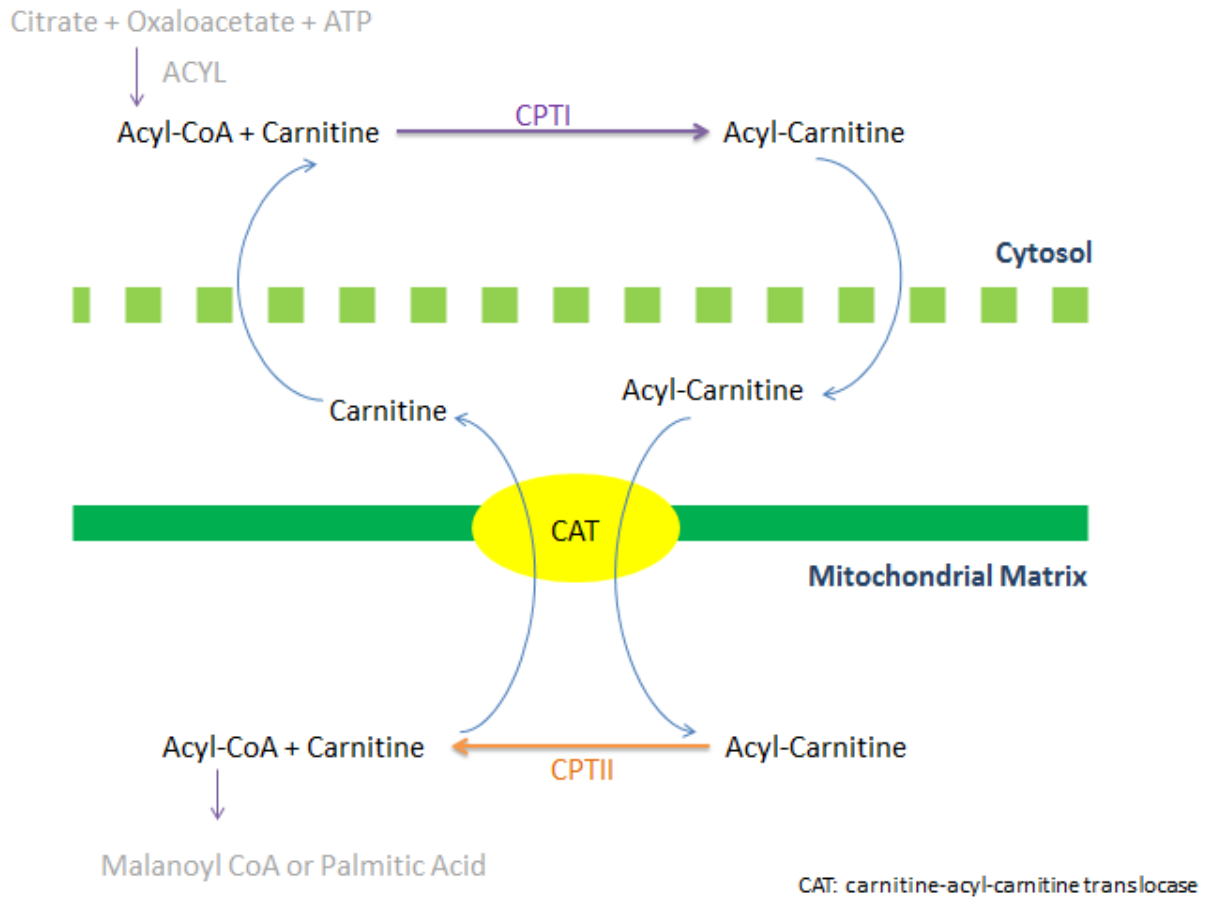


Figure 1.2: Transportation of fatty acid-acyl CoA occurs by conjugation with transporter molecule carnitine catalysed by Carnitine Palmitoyltransferase I. The carnitine allows the movement of acyl-carnitine moiety to pass through the membrane with the help of carnitine-acyl-carnitine translocase. Once successfully transported through the membrane and in to the mitochondria the carnitine is removed by Carnitine Palmitoyltransferase II leaving the resultant fatty acid available to undergo  $\beta$ -oxidation. The carnitine is recycled by the cell.

CPTI is not only regulated by transcription, but also undergoes allosteric modulation and can be modified by pH (Morash et al., 2008).

### 1.5.3 Stearoyl-CoA Desaturase

Stearoyl-CoA Desaturase I (SCDI) is a membrane-bound protein located in the endoplasmic reticulum. SCDI catalyses the desaturation of saturated fatty acids (SFAs) by introducing a bond between carbons 9 and 10 of acyl-CoAs to produce monounsaturated fatty acids (MUFAs).

**Figure 1.3:** Steroyl-CoA-Desaturase Mechanism of Action

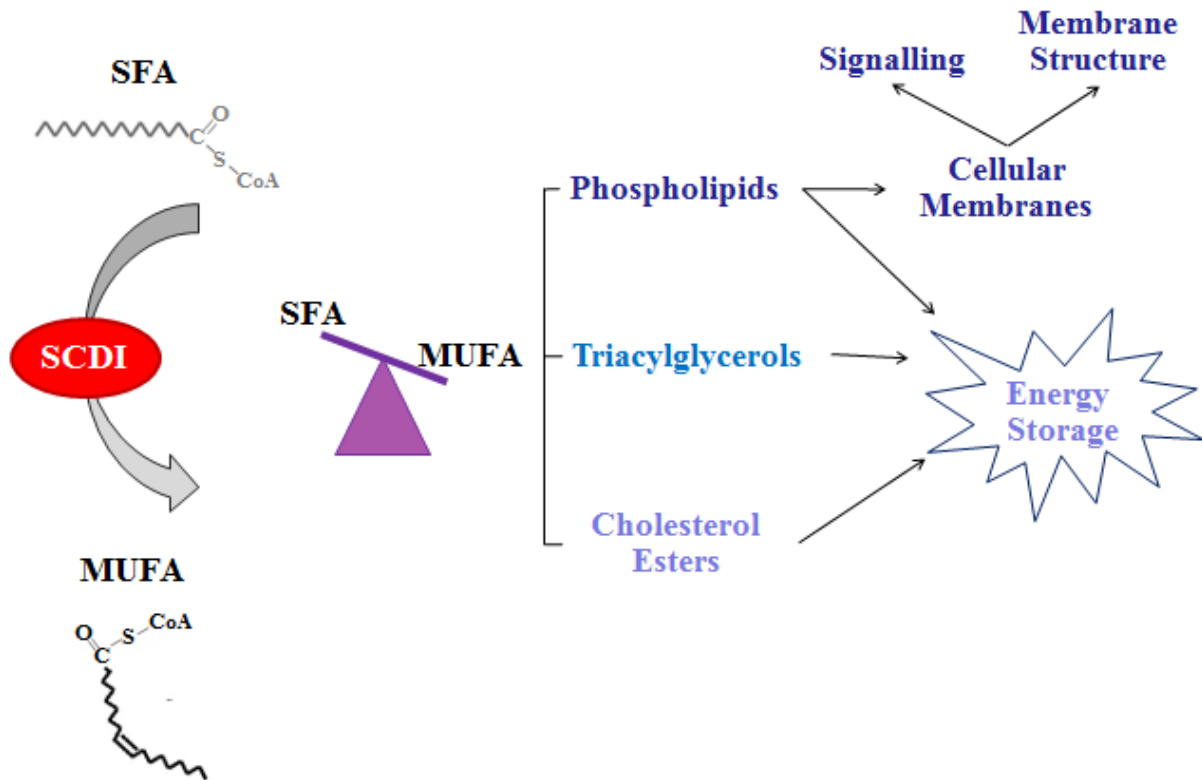


Figure 1.3: Steroyl CoA Desaturase I catalyses the desaturation of saturated fatty acids by introducing a bond between carbons 9 and 10 of acyl-CoAs to produce monounsaturated fatty acids (MUFAs). The MUFAs produced are then used for multiple purposes, including synthesis of phospholipids, triglycerides, cholesterol esters, wax esters and alkyldiacylglycerols. Modified from (Igal, 2010).

Often the substrates are palmitoyl-CoA (16:0) and stearoyl-CoA (18:0) which are desaturated to become palmitoleoyl-CoA (16:1) and oleoyl-CoA (18:1) respectively. The MUFAs produced are then used for multiple purposes, including synthesis of phospholipids, triglycerides, cholesterol esters, wax esters and alkyldiacylglycerols .

Oleic acid is of particular importance in the production of triglycerides and cholesterol esters as it is the preferred substrate for the enzymes that catalyse their production: cholesterol acyltransferase and diacylglycerol acyltransferase. Furthermore, oleate is the primary MUFA in human adipose tissue and in erythrocyte membranes (Miyazaki and Ntambi, 2003).

The importance of MUFAs in the synthesis of lipids means that SCDI plays a key role in lipid metabolism. Cancer cells undergo rapid replication and to do so an increased level of phospholipids are required, for which MUFAs are also required. Scaglia *et al* (2009) showed that SCDI knockdown reduced the rate of lipid synthesis and of cancer cell proliferation. Furthermore, knockdown of SCDI increased the activation of AMPK which is known to inhibit ACC.

## **1.6 Aims and Objectives**

BaP treatment has been shown to effectively terminate leukemic cells without damaging healthy cells, unlike current cancer treatments. Extensive research has shown that lipid metabolism plays an essential role in the proliferation of cancer cells and Southam *et al* (unpublished) identified the disruption of lipogenic/lipolytic balance as a potential mechanism by which BaP exerts anti-leukemic activity. This research aims to identify changes in lipid metabolism of BaP treated cells to investigate the hypothesis proposed by Southam *et al*. To achieve this aim, changes in protein and mRNA levels of key enzymes involved in lipogenesis and lipolysis have been explored. A second objective was to assess whether providing increased levels of exogenous fatty acids provided changes to lipid metabolism, cell survival and cell proliferation in BaP treated samples.

## **2. MATERIALS AND METHODS**

### **2.1 Tissue Cell Culture**

#### **Materials for making Complete Media:**

500ml RPMI 1640

50ml Foetal Bovine Serum (FBS)

5ml penicillin/streptomycin

#### **Method:**

Complete media was made using a base of 500ml RPMI 1640 (ordered from GIBCO, product reference 21875). 10% Foetal Bovine Serum (v/v) was added, thus in this instance 50ml, in addition to 5ml penicillin/streptomycin (1% v/v). This was completed inside a fully operational fume cupboard with sterile pipettes to avoid contamination.

An FBS free media was also made using the same method, with the substitution of FBS with ITS+ (ordered from Sigma, product reference I2521-5ML). ITS+ is a defined product that does not contain the fatty acids considered within this report.

#### **Materials for culturing HL60, K562, BL31 and GLOR cells:**

Stock of each cell line

Complete media

**Method:**

Cell lines HL60, K562, BL31 and GLOR mature and multiply most effectively when population exists at approximately  $\frac{1}{4}$  million cells per millilitre (ml) of media. From stock solutions of the cell lines, the approximate number of cells was calculated using a haemocytometer.

In sterile conditions, 10 $\mu$ l of the cells were inserted on to the haemocytometer and then counted using a microscope. From these results it was possible to work out the ratio of the current cell line stock to fresh complete media needed to equal approximately  $\frac{1}{4}$  million cells per ml to ensure survival and effective growth of the cells. This process occurred every 2 days to certify the survival of the cell line for use in later testing.

**2.2 Preparation of Palmitate – BSA Solution****Materials:**

155mM Sodium Chloride (NaCl) in water

150mM Palmitic Acid in ethanol

10% Bovine Serum Albumen (BSA)

**Method:**

As described by Kuhajda *et al* (1996), 155mM NaCl was made by adding 0.45g NaCl to 50ml deionised water (dH<sub>2</sub>O) (0.9% v/v).

To make 150mM palmitic acid, 38.4mg of palmitic acid should be added to 1ml ethanol. A supply of 3ml was made using 116.4mg acid in 3ml ethanol. Due to the nature of palmitic acid it does not dissolve readily, however it must be completely in solution before use. The mixture was vigorously shaken whilst being held under a stream of hot water until the

solution turned clear to be sure the acid was in solution.

5g BSA was added to the 50ml NaCl solution to make 10% BSA. This was mixed at 37°C until completely dissolved.

1ml 150mM palmitic acid was added to 19ml 10% BSA, and a control set up adding 1ml ethanol to 19ml 10% BSA. These were both stirred continuously at 37°C for 1 hour. Both solutions were clear and ready for use by the end of this process. When not in use the stock was sterile filtered and frozen as aliquots.

### **2.3 Preparation of Bezafibrate (BEZ) and Medroxyprogesterone Acetate (MPA)**

#### **Stock Solutions**

##### **Materials:**

BEZ, molecular weight 362

MPA, molecular weight 387

Dimethylsulfoxide (DMSO)

Ethanol

##### **Method:**

Stock solutions were made at 1000 times more concentrated than the desired target value when inside the cell culture mix.

To achieve a 0.5mM concentration of BEZ in the cell culture mix, a stock of 0.5M BEZ was created. The following molar equation was used:

$$\frac{\text{Grams}}{\text{Molar Mass}} = \text{Moles} > \frac{x \text{ grams}}{362} = 0.5 > 0.5 \times 362 = \text{grams} > 0.5 \times 362 = 181\text{g/l}$$

Therefore to create a 0.5M solution using 181mg/ml, a 4ml stock was made by adding 724mg BEZ to 4ml DMSO.

A 0.5µM concentration of MPA in cell culture mix was reached via a stock solution of 0.5mM MPA. The same method of calculation was used for MPA as was used for BEZ, therefore utilising 1.935mg/ml, a stock of 10.5ml MPA was produced by adding 20.3g MPA to 10.5ml ethanol.

Particulates occasionally gather at the base of the stock solution and so were heated under a hot tap whilst being shaken to ensure all of the MPA and BEZ were in solution prior to use.

The stocks were stored in a freezer when not in use.

## 2.4 Control and BaP Treated Samples

Four replicates of the following reactions were set up for 24, 48 and 96-hour periods as shown in Table 2.1.

**Table 2.1:** Composition of Control and BaP Treated Samples

	<b>Cells in Complete Media</b>	<b>Ethanol</b>	<b>DMSO</b>	<b>BEZ</b>	<b>MPA</b>
<b>Control</b>	8ml	8µl	8µl	-	-
<b>BaP Treated</b>	8ml	-	-	8µl	8µl
<b>Control + PA</b>	8ml	8µl	8µl	-	-
<b>BaP + PA</b>	8ml	-	-	8µl	8µl

## 2.5 Flow Cytometry of K562 and HL60 Treatments

### Materials:

Annexin V Apoptosis Detection Kit (BD Biosciences, catalogue ref 556547);

includes 10x Annexin V Binding Buffer, Annexin V and Propidium Iodide

Sterile distilled water

## **Method:**

Approximately 0.5 million cells from each of the above reactions were required for flow cytometry, equating to approximately 0.5ml. These were transferred in to labelled tubes and 2ml PBS was added to each then centrifuged at 1500rpm for 5 minutes.

A master mix was created using 6ml sterile distilled water, 625µl binding buffer, 62.5µl Annexin V and 62.5µl Propidium Iodide. A master mix creates consistency as it allows the same mixture to be added to each test.

Once removed from the centrifuge, the supernatant was discarded from each tube ensuring the pellet remained at the bottom. The pellets were then re-suspended in 0.5ml master mix and placed in the dark for 15 minutes. This allows the fluorescence markers to bind to the markers on the cell surface, in this instance Annexin V will bind to cell markers for apoptosis, cells either under-going or that have completed the apoptosis procedure (Annexin V), whilst Propidium Iodide identifies non-viable cells, which if not expressing Annexin V must have undergone necrosis.

After 15 minutes in the dark, flow cytometry was performed for each sample using a BD FACSCalibur.

## **2.6 Western Blot**

### **2.6.1 Protein Preparation**

100ml RIPA Buffer was made by combining the following in an eppendorf tube;

1ml [1% v/v] NP40 (IGEPAL)

0.5g [0.5% w/v] Sodium Deoxycholate

1ml [0.1% w/v] 10% SDS

Up to 100ml ddH<sub>2</sub>O

1 x Complete Protease Inhibitor.

### **2.6.2 Lysate Preparation**

#### **Materials**

PBS (Pre-chilled)

RIPA Buffer

Samples

#### **Method**

Drug treated and control cells were transferred in to falcon tubes and centrifuged at 1,000rpm for 5 minutes. The supernatant was removed and the pellet re-suspended in 1ml PBS and then transferred in to a clean eppendorf tube. PBS is isotonic much like the human body and is also non-toxic to cells whilst maintaining the cells natural osmotic movement and is therefore ideal for cell-washing procedures (Medicago AB, accessed October 2013). The samples were centrifuged at 14,000rpm for 10 seconds and 100µl RIPA buffer was added to lyse the cells. These were then incubated on a rotator at 4°C for 1 hour. The samples were again centrifuged at 14,000rpm at 4°C for 10 minutes to pellet the cell membranes. The supernatant was transferred in to clean eppendorf tubes and were stored at -70°C until used.

### **2.6.3 Protein Determination using Bio-Rad DC Reagent**

#### **Materials**

Bio-Rad DC Protein Assay;

Reagent S

Reagent A

Reagent B

Protein standards (0mg/ml, 0.625mg/ml, 1.25mg/ml, 2.5mg/ml, 5mg/ml, 10mg/ml)

## **Method**

To determine the level of protein in each sample, the Bio-Rad DC Protein Assay protocol was applied. Of each sample and protein standard, 2µl was added to duplicate wells in a 96 well plate, thus overall 28 samples were exposed to the determination. To each millilitre of reagent A, 20µl reagent S was added and 25µl of this solution was added to each well, followed by 200µl of reagent B. The samples were agitated for 15 minutes at room temperature to allow the reactions to occur before absorbance readings at 645nm were taken.

From these results a graph was plotted using the protein standards. Using the equation for the line of best fit, the amount of protein in the samples could be determined.

### **2.6.4 SDS-PAGE Electrophoresis**

SDS-PAGE Electrophoresis was performed to determine protein expression in control and 24 hour-BaP treated groups of HL60, K562, GLOR and BL31 for the proteins identified previously.

#### ***2.6.4.1 Preparing gels for SDS-PAGE Electrophoresis***

A 7.5% gel was used for FASN whilst a 10% gel was used for CPT1A due to the size of each protein. FASN is approximately 270kb whilst CPT1A is approximately 76kb. The gels were made using materials shown in Table 2.2;

**Table 2.2:** Composition of Acrylamide Gel

	<b>Resolving Gel 7.5%</b>	<b>Resolving Gel 10%</b>	<b>Stacking Gel</b>
<b>Arcyl/bis</b>	2.5ml	3.3ml	440ul
<b>4xbuffer</b>	2.5ml	2.5ml	830ul
<b>10% SDS</b>	0.1ml	0.1ml	33ul
<b>ddH2O</b>	5.0ml	4.1ml	2.03ml
<b>10% APS</b>	50ul	50ul	16.7ul
<b>TEMED</b>	3.3ul	3.3ul	1.7ul

**Table 2.2:** Composition of acrylamide gels with quantities relative to making one gel 1.5mm thick

8ml of resolving gel was poured between glass plates with a gap 1.5mm wide and water was layered on top to remove any air bubbles. The gel was allowed to set for approximately 40 minutes. Once the resolving gel had solidified the water was removed and the stacking gel added. A 10-well comb was placed in the stacking gel and more stacking gel was added to fill any gaps or air bubbles. This was then allowed to set for approximately 30 minutes to allow complete polymerisation. The gels were then secured in a tank with 1 x running buffer ready for use.

Premade 4-15% gradient gels (BioRad) were used to aid separation of larger proteins.

#### **2.6.4.2 Preparing samples for SDS-PAGE Electrophoresis**

Using information gained from the protein determination, the following calculation was performed to determine the amount of each reagent needed to load 20 $\mu$ g of protein in a total volume of 20 $\mu$ l in to each well:

To determine amount of protein sample;

20 $\mu$ g /protein concentration

5 $\mu$ l 4 x SDS Gel Loading Buffer (GLB) was added to all samples

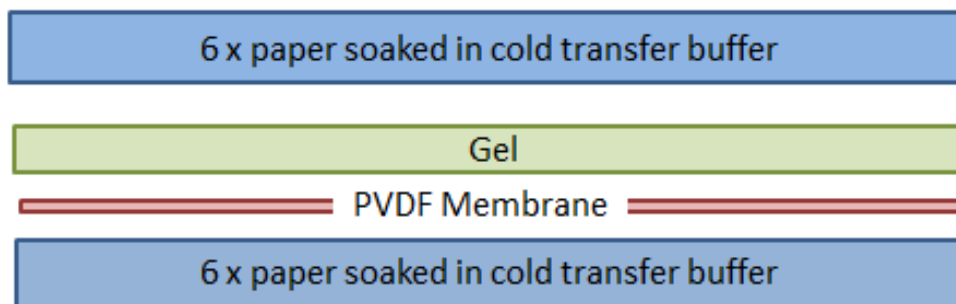
To make the final volume to 20 $\mu$ l, RIPA buffer as described earlier was added.

Once the samples were mixed, they were boiled for 10 minutes to ensure complete linearization. The combs were removed from the gels and 5µl pre-stained Bio-Rad Precision Blue marker was loaded in to the first well, followed by the samples. Electrophoresis was performed at 120V until the dye front reached the bottom of the gel.

### 2.6.5 Semi-Dry Blotting Transfer

1 x Transfer buffer was made using 25mM Tris, 192mM glycine and 20% methanol and stored at 4°C. PVDF membrane was cut to fit the size of the gel (approx. 8cm by 6cm) and soaked in methanol for 5 minutes, whilst 12 pieces of filter paper were soaked in the cold transfer buffer. The transfer was set up as below;

**Figure 2.1:** Semi-Dry Blotting Transfer



The transfer was run at 25V for 90 minutes. Once complete, the membrane was removed and soaked for 3 minutes in Ponceau stain to determine if an equal amount of protein had been loaded in each well. The stain was cleared by washing the membrane firstly in ddH<sub>2</sub>O followed by being washed 3 times for 5 minutes in TBS-T (40ml 1.0M Tris HCl pH 7.5, 16g NaCl, 20ml Tween 20 and filled to 2L with ddH<sub>2</sub>O).

### 2.6.6 Immunoblotting

The membranes were washed in TBS-T and then blocked in 5% blotto made up of milk powder and TBS-T for 45 minutes. The appropriate dilution of the primary antibody was

made in 5% blotto (see Table 2.3) and the membranes incubated in the appropriate antibody overnight at 4°C.

Following this the membranes were washed in TBS-T and incubated in a 1 in 1000 dilution of secondary-HRP antibodies in 5% blotto (see Table 2.3). Again, the membranes were washed in TBS-T and exposed to 2ml Supersignal West Pico ECL reagent A and B combined for 5 minutes. The excess ECL was drained and the membranes were then exposed to film for various amounts of time.

**Table 2.3:** Volume of primary and secondary antibody added to 10ml 5% blotto

<b>Antibody (Ab)</b>	<b>µl added to 10ml 5% blotto</b>	<b>Mouse Secondary Ab</b>	<b>Rabbit Secondary Ab</b>
<b>FASN</b>	10		X
<b>CPT1A</b>	10		X
<b>α-AMP-Kinase</b>	10		X
<b>Phosphorylated –α-AMP-Kinase</b>	10		X
<b>Acyl-Co-Carboxylase</b>	10		X
<b>Phosphorylated Acyl-Co-Carboxylase</b>	10		X
<b>SDC1</b>	10	X	
<b>B-Actin</b>	1	X	

B-actin was used as a loading control, with the membranes being incubated in a 1 in 10,000 dilution of the primary antibody for 45 minutes, then washed in TBS-T before being incubated in a 1 in 20,000 dilution of the secondary Anti-Mouse for a further 45 minutes. The membranes were then re-exposed to 2ml Supersignal West Pico ECL reagent A and B combined for 5 minutes and exposed to film. If the Pico ECL did not return any results the stronger Dura ECL was adopted.

**Table 2.4:** Antibody Product Information

<b>Antibody (Ab)</b>	<b>Supplier</b>	<b>Product Code</b>
<b>FASN</b>	Abcam	ab22759
<b>CPT1A</b>	Abcam	ab128568
<b>AMPK and ACC Antibody Sampler Kit</b>	New England Biolabs	#9957S
<b>SDC1</b>	Abcam	ab19862
<b>B-Actin</b>	Sigma Aldrich	A5441

## **2.7 Alamar Blue Viability Test**

The active ingredient of Alamar Blue is Resazurin. This is a non-toxic, cell permeable compound that is non-fluorescent, which in the cytosol of viable cells is reduced to a red fluorescent resorufin. This reducing activity allows viable cells to fluoresce red therefore an overall fluorescence that is more red indicates more live, viable cells (Life Technologies, accessed October 2013)

The following exposures were set-up in a flat-bottomed 96-well plate (6 wells/replicates of each) for cells lines HL60, K562, GLOR and BL31;



## 2.8 Inhibiting anti-leukemic action of BaP by Fatty Acid Supplementation

### Materials:

BEZ stock solution

MPA stock solution

Ethanol

DMSO

K562 cell culture

ITS+ media (FBS free)

### Method:

Approximately 26 million cells were obtained in a total of 52ml cell culture to provide a supply of 0.25 million cells/ml for each of the reactions shown in Table 2.5. This was centrifuged for 5 minutes at 1000rpm at 22°C, after which the supernatant removed and the pellet re-suspended in 26ml ITS+ media (fatty acid free) which had been incubated at 37°C. Triplicates of the following reactions were set up;

**Table 2.5:** Composition of palmitic acid rescue experiments

	<b>ITS+ Media</b>	<b>Ethanol</b>	<b>DMSO</b>	<b>BEZ</b>	<b>MPA</b>	<b>Palmitic Acid</b>
<b>Control</b>	8ml	8µl	8µl	-	-	-
<b>BaP Treated</b>	8ml	-	-	8µl	8µl	-
<b>Control + PA</b>	8ml	8µl	8µl			16µl
<b>BaP + PA</b>	8ml	-	-	8µl	8µl	16µl

BEZ and MPA were incubated at 37°C and when added to the reaction, the solution was gently shaken to ensure maximum incorporation in to the solution. The palmitic acid was also incubated at 37°C for 5 minutes prior to use.

A reaction using HL60 cells was also set up using 8ml ITS+ media, 8µl BEZ, 8µl MPA and 16µl palmitic acid. This acts as a control as this reaction showed a positive result in previous experiments performed by Southam *et al* (unpublished). Alamar Blue viability test was undertaken as previously described to determine cell viability.

## **2.9 Real-Time PCR**

### **2.9.1 RNA Extraction**

24-hour control and BaP treatments were set up for GLOR and BL31 cell lines so that a total of approximately 5 million cells were present at the time of extraction.

The cells were centrifuged at 1000rpm for 5 minutes, the supernatant was removed and the pellet re-suspended in 1ml PBS. Following this the Qiagen RNeasy protocol for RNA extraction was performed as follows;

600µl RLT buffer was added to the sample followed by vortexing to disrupt the cells. The lysate was pipetted directly in to a QIAshredder spin column placed in a 2ml collection tube and centrifuged at 14,000rpm for 2 minutes. 600µl of 70% ethanol was then mixed with the homogenised lysate and 700µl was transferred in to an RNeasy spin column placed in a 2ml collection tube. This was centrifuged for 15s at 10,000rpm and the flow-through discarded.

The spin column membrane was washed by adding 350µl Buffer RW1 and centrifuging at 10,000rpm for 15s. The flow-through was discarded. DNase I incubation mix was made by adding 10µl DNase I stock solution to 70µl Buffer RDD. 80µl of this mix was added directly on to the spin column membrane and left to stand at room temperature for 15min. The membrane was then again washed by adding 350µl Buffer RW1 and centrifuging at 10,000rpm for 15s.

500µl Buffer RPE was added to the spin column and centrifuged for 15s, followed by adding another 500µl to the column and centrifuging for 2min at 10,000rpm and the flow-through discarded. To ensure any residual Buffer RPE or flow-through is eliminated, the collection tube wash changed and the spin column centrifuged at 10,000rpm for 1 min.

The RNeasy spin column was then transferred in to a new collection tube and 50µl RNase free water was added to the column membrane. RNA was eluted by centrifuging at 10,000rpm for 1 min. The supernatant was transferred back on to the column membrane and centrifuged again to ensure as much RNA had been eluted.

Levels of RNA were determined by applying 1µl to a nanophotometer. The RNA was stored at -80°C until used.

### **2.9.2 cDNA Synthesis**

A master mix containing 0.5µl random primers and 1µl 10µM dNTPs for each sample was made. 10.5µl ddH<sub>2</sub>O and 1.5µl master mix were added to 3µg of each RNA extraction. The samples were mixed well and heated to 65°C for 6 minutes before being placed on ice for 10 minutes. Whilst on ice, 8µl of a second master mix (4µl 5x first strand buffer, 2µl 0.1M DTT, 1µl Rnaseri plus, 1µl Superscrit II per sample) was added to each sample. The samples then underwent PCR amplification.

### **2.9.3 β-actin PCR**

β-actin was used as means of identifying the production of cDNA from the PCR process. The following PCR reactions were set up;

5µl	10x Buffer
1.5µl	50mM MgCl <sub>2</sub>
1µl	10mM dNTPs
1µl	10µM β-actin primer mix

0.75µl Biotaq Red

39.75µl ddH<sub>2</sub>O

1µl cDNA (1 in 10 dilution)

Once mixed, these samples underwent PCR amplification in addition to a negative control.

20µl 5x DNA loading buffer was added to each of the resultant PCR products and were run on a 1% agarose gel at 120V for approx. 90 min.

#### **2.9.4 cDNA Real-Time PCR**

A master mix was created containing 10µl Low ROX Sensimix, 2µl 10 x primers for protein of interest and 6µl dH<sub>2</sub>O for each sample. 18µl master mix was added to 2µl diluted cDNA in a 96-well PCR plate. The plate was sealed, centrifuged for 3 minutes followed by Real-Time measurements.

Real-Time PCR was set up for both GLOR and BL31 24hour RNA extractions for the following proteins;

18S (control)

FASN

CPTIA

SCDI

ACC-α

ACC-β

ALCY

SLC25A20

### 3. RESULTS

#### 3.1 BaP Treatment induces Apoptosis in Leukemic Cell Lines

**Figure 3.1:** Apoptosis in Control and BaP Treated Samples

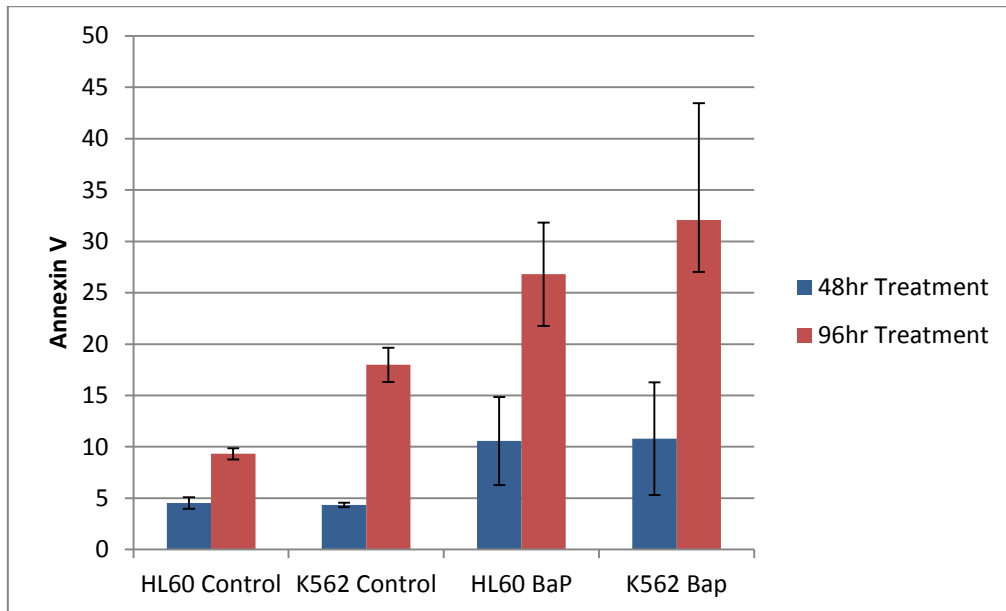


**Figure 3.1:** BaP has potent anti-leukemic activity across a short time-frame in HL60 and K562 cell lines. Control samples were treated with DMSO and ethanol in replacement for BaP treatment where 0.5mM Bezafibrate in DMSO and 0.5 $\mu$ M Medroxyprogesterone Acetate in ethanol were added. Four replicates of each underwent Annexin V-Propidium Iodide (AV-PI) treatment as described and 10,000 cells counted using FACSCalibur. FACS monitored the number of cells expressing AV (apoptotic), PI (necrotic) and neither (viable). The above graph represents the average number of cells expressing AV from all four replicates after 48 hour and 96 hour treatment.

After 48-hour treatment, cell viability in BaP treated samples was decreased by >50% of control samples in both HL60 and K562 cell lines. After 96-hour treatment cell viability for HL60 had declined to 40%, whilst K562 had been reduced to approximately 33% of control samples.

**Figure 3.2** Annexin V and Propidium Iodide expression in 96-hour treated samples

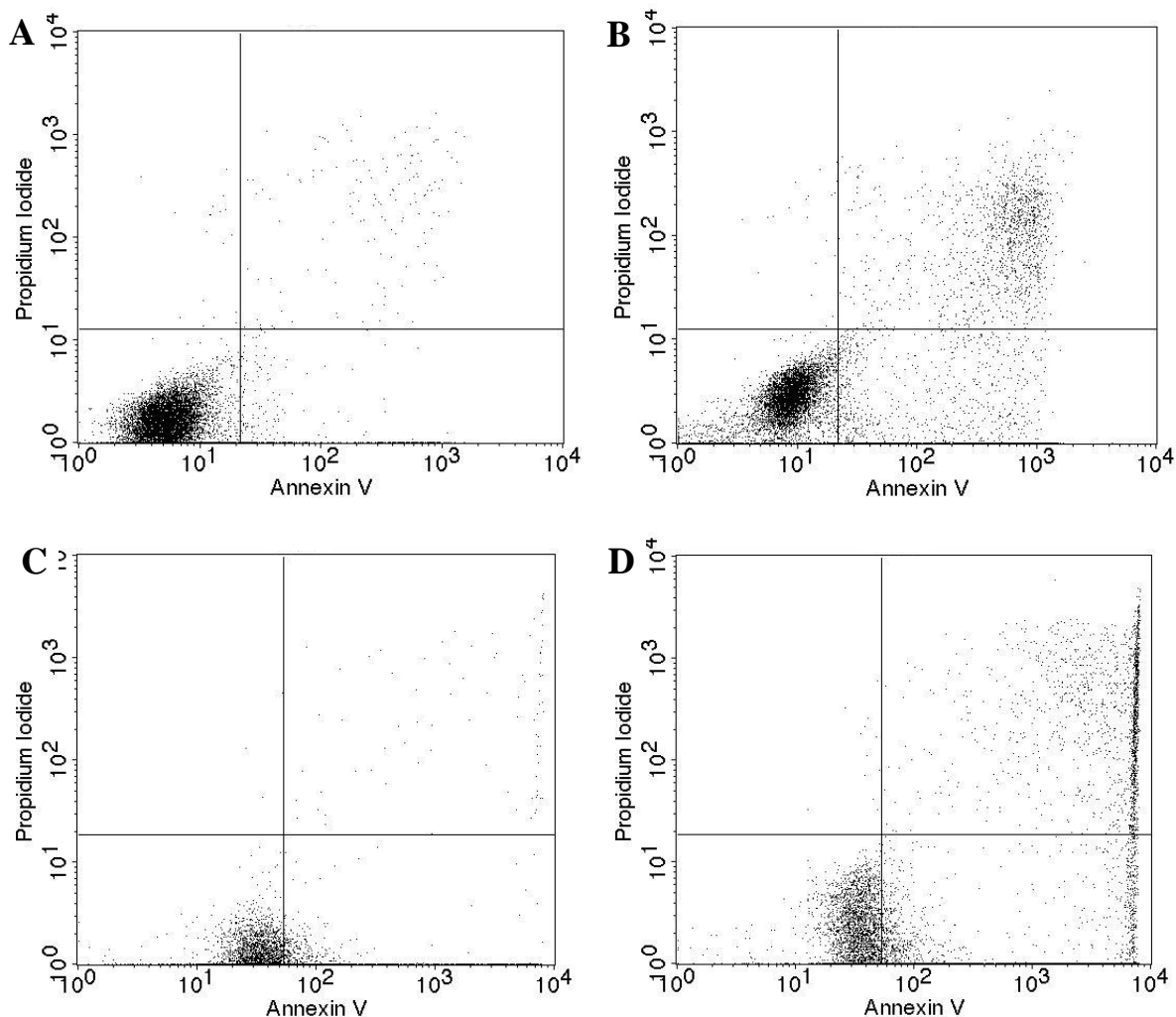


**Figure 3.2:** A: FACSCalibur data of 96-hour HL60 Control sample (treated with DMSO and ethanol only) (C1). B: FACSCalibur data of 96-hour HL60 BaP treated sample (D1). C: FACSCalibur data of 96-hour K562 Control sample (treated with DMSO and ethanol only) (C1). D: FACSCalibur data of 96-hour K562 BaP treated sample (D1). Lower left fraction represents viable cells, lower right represents cells undergoing apoptosis, upper right visualises cells that have undergone apoptosis and upper left represents cells expressing PI without AV therefore cells that have undergone necrosis. Further 96-hour AV and Pi FACS data can be found in Appendix I in addition to forward scatter and side scatter data.

HL60 and K562 control samples represented by Figure 3.2 A and C show a dense cluster of cells in the lower left bracket. The dense cluster represents viable cells as they do not express Annexin V or Propidium Iodide. In the respective drug treated samples, B and D, the cluster of viable cells is dispersed and increased levels of cells in the lower right fraction (undergoing apoptosis) and upper right fraction (having undergone apoptosis) are recorded.

**Figure 3.3:** Forward Scatter and Side Scatter Data of 96-hour treated samples

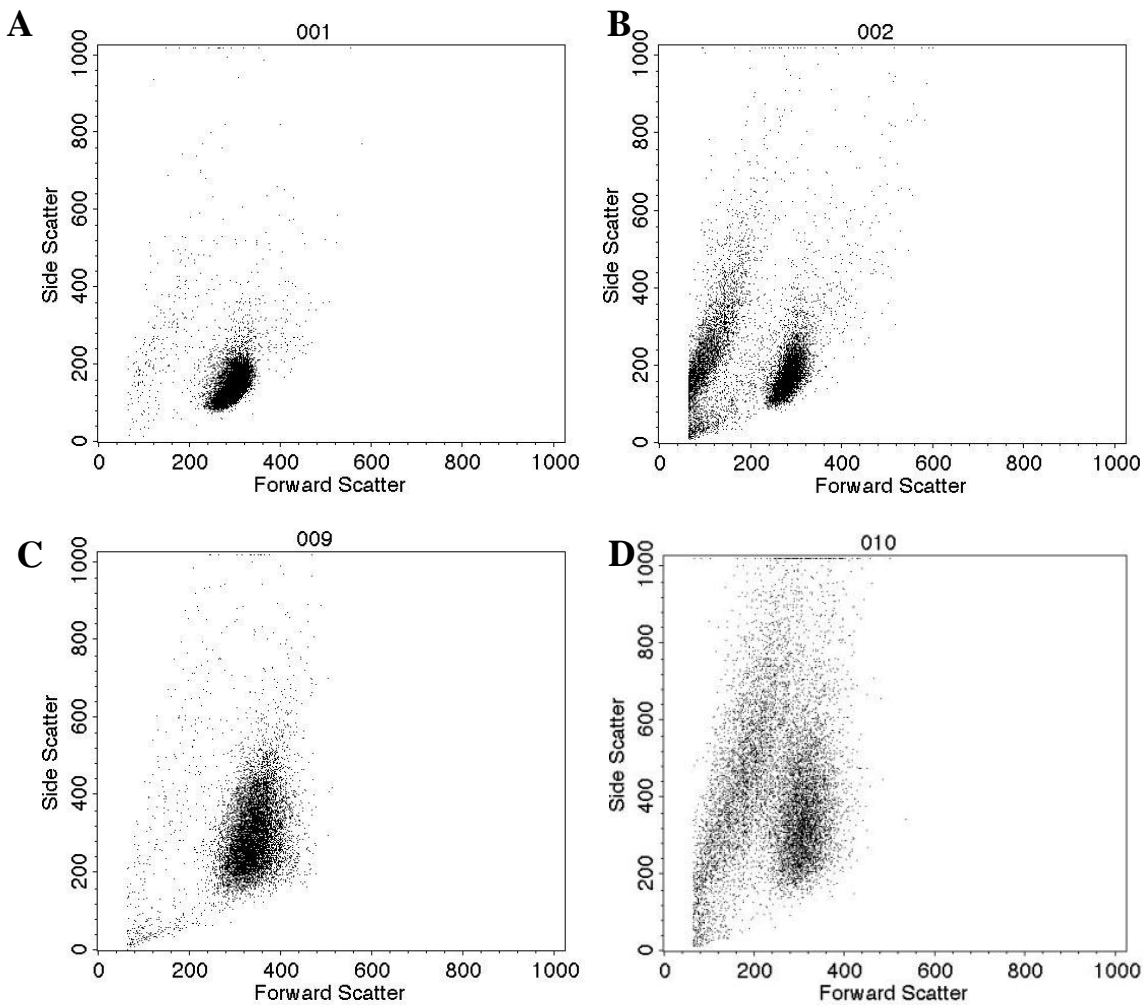


**Figure 3.3:** A: FACSCalibur data of 96-hour HL60 Control sample (treated with DMSO and ethanol only) (Control Replicate 1). B: FACSCalibur data of 96-hour HL60 BaP treated sample (Drug Treated Replicate 1). C: FACSCalibur data of 96-hour K562 Control sample (treated with DMSO and ethanol only) (Control Replicate 1). D: FACSCalibur data of 96-hour K562 BaP treated sample (Drug Treated Replicate 1). The changes in forward and side scatter recorded between control and drug treated samples represents the changes in cell physiology most likely due to the morphological changes that have occurred in the drug treated samples after an increased number of cells having undergone apoptosis. For forward and side scatter data of a further three replicates of control and drug treated samples for both cells see **Appendix I**.

HL60 and K562 control samples, represented by Figure 3.3 A and C respectively, identify a high number of cells falling within a close range of forward and side scatter showing cells to be of a similar shape. Figure 3.3 B and D represent drug treated samples and show fewer areas of high density and the pattern of forward and side scatter is far more dispersed identifying cells of irregular shape, supporting the notion of higher levels of apoptosis present in these samples.

### 3.2 BaP alters expression of proteins involved in up-regulation of fatty acid synthesis in leukemic cell lines

**Figure 3.3:** Fatty Acid Synthase Western Blot Results

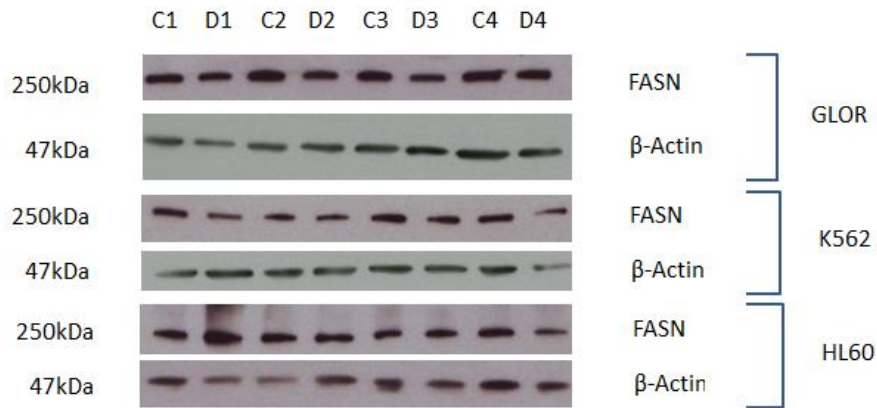


**Figure 3.3:** Western blot results obtained for GLOR, K562 and HL60 cell lines for levels of enzyme Fatty Acid Synthase (FASN). Western blots shown were run on a 4-15% pre-made gradient gel (Bio-Rad) and exposed to gel electrophoresis at 120V for 140 minutes. Protein was transferred from the gel on to PVDF membrane at 25V for 90 minutes. Lanes labelled C 1-4 represent 4 replicates of control samples treated with DMSO and ethanol only. Lanes labelled D 1-4 represent 4 replicates of cells treated with 0.5mM Bezafibrate in DMSO and 0.5µM Medroxyprogesterone in ethanol.

Western blot analysis identified a decreased expression of FASN in drug treated samples compared to control samples (where n=4) in GLOR and K562 cell lines. Although the decrease appears small and image J analysis gave p values of 0.222 (GLOR) and 0.07 (K562) (see Figure 3.8 for image J analysis results), a trend can clearly be seen across all 4 replicates of control and drug treated samples in both cell lines.  $\beta$ -actin has been used as a loading control and shows an even level of sample protein was loaded in to each well. No significant change was observed for HL60 samples.

**Figure 3.4:** Acetyl-CoA-Carboxylase (ACC) and Phosphorylated-ACC Western Blot Results

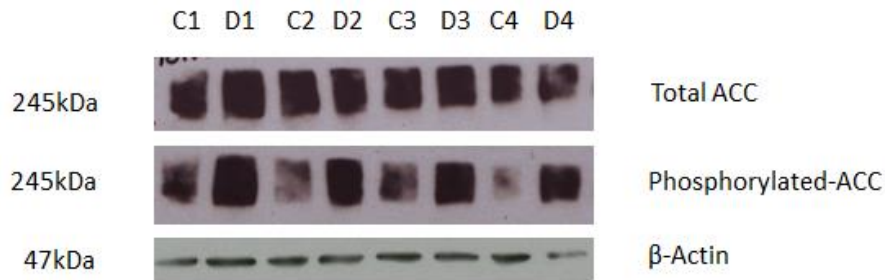


**Figure 3.4:** Acetyl-CoA-Carboxylase (ACC) and phosphorylated-ACC western blot results obtained for K562. Western blots shown were run on a 4-15% pre-made gradient gel (Bio-Rad) and exposed to gel electrophoresis at 120V for 140 minutes. Protein was transferred from the gel on to PVDF membrane at 25V for 90 minutes. Lanes labelled C 1-4 represent 4 replicates of control samples treated with DMSO and ethanol only. Lanes labelled D 1-4 represent 4 replicates of cells treated with 0.5mM Bezafibrate in DMSO and 0.5µM Medroxyprogesterone in ethanol.

Western blot analysis showed the presence of total ACC in both control and drug treated samples to be fairly consistent after 24-hour treatment, with a p-value of 0.54 suggesting no significant change had occurred. Phosphorylated-ACC is clearly present at lower levels in control groups and at higher levels in drug treated samples at the 24-hour time point. ACC- $\alpha$  has a molecular mass of 245kDa whilst ACC- $\beta$  has a mass of 280kDa causing a large spot to appear on the western blot as opposed to a thin band.  $\beta$ -actin has been used as a loading control and shows an even level of sample protein was loaded in to each well.

**Figure 3.5:** Carnitine Palmitoyltransferase IA Western Blot Results

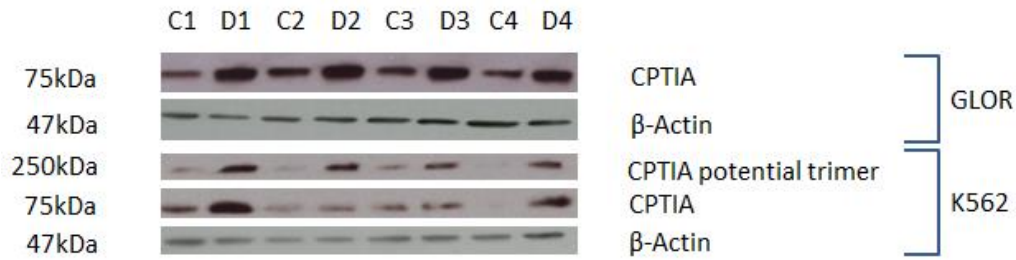


**Figure 3.5:** Carnitine Palmitoyl Transferase IA (CPTIA) western blot results obtained for GLOR and K562. Western blots shown were run on a 4-15% pre-made gradient gel (Bio-Rad) and exposed to gel electrophoresis at 120V for 140 minutes. Protein was transferred from the gel on to PVDF membrane at 25V for 90 minutes. Lanes labelled C 1-4 represent 4 replicates of control samples treated with DMSO and ethanol only. Lanes labelled D 1-4 represent 4 replicates of cells treated with 0.5mM Bezafibrate in DMSO and 0.5µM Medroxyprogesterone in ethanol.

BaP treated GLOR cells show increased levels of CPTIA when compared to control groups after 24-hour treatment. At the same time point, K562 shows partial evidence of the same pattern at the expected size of CPTIA (75kDa), but also shows bands at 250kDa that may be a trimer of CPTIA at increased levels in drug treated samples.  $\beta$ -actin has been used as a loading control and shows an even level of sample protein was loaded in to each well.

**Figure 3.6:** Total AMP-Kinase Western Blot Results

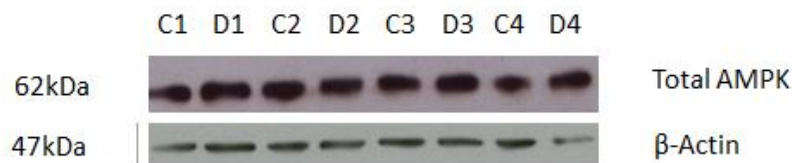


**Figure 3.6:** Total AMP-Kinase western blot results obtained for K562. Western blots shown were run on a 4-15% pre-made gradient gel (Bio-Rad) and exposed to gel electrophoresis at 120V for 140 minutes. Protein was transferred from the gel on to PVDF membrane at 25V for 90 minutes. Lanes labelled C 1-4 represent 4 replicates of control samples treated with DMSO and ethanol only. Lanes labelled D 1-4 represent 4 replicates of cells treated with 0.5mM Bezafibrate in DMSO and 0.5µM Medroxyprogesterone in ethanol.

Levels of total AMP-Kinase appears unchanged between control and drug treated samples after 24-hour exposure across 4 replicates.  $\beta$ -actin has been used as a loading control and shows an even level of sample protein was loaded in to each well.

**Figure 3.7:** Steroyl-CoA Desaturase I Western Blot Results

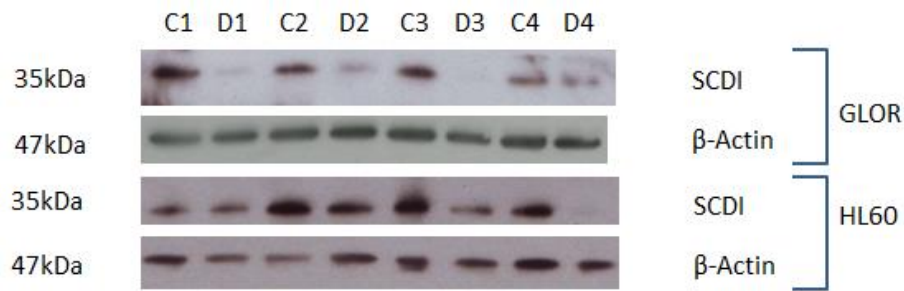


**Figure 3.7:** Steroyl-CoA Desaturase I (SCDI) western blot results obtained for GLOR and HL60 cell lines. Western blots shown were run on a 4-15% pre-made gradient gel (Bio-Rad) and exposed to gel electrophoresis at 120V for 140 minutes. Protein was transferred from the gel on to PVDF membrane at 25V for 90 minutes. Lanes labelled C 1-4 represent 4 replicates of control samples treated with DMSO and ethanol only. Lanes labelled D 1-4 represent 4 replicates of cells treated with 0.5mM Bezafibrate in DMSO and 0.5 $\mu$ M Medroxyprogesterone in ethanol.

SCDI is down regulated in BaP treated samples when compared to control groups in cell lines GLOR and HL60.  $\beta$ -actin has been used as a loading control and shows an even level of sample protein was loaded in to each well.

**Figure 3.8:** Western Blot Densitometry Significance Analysis

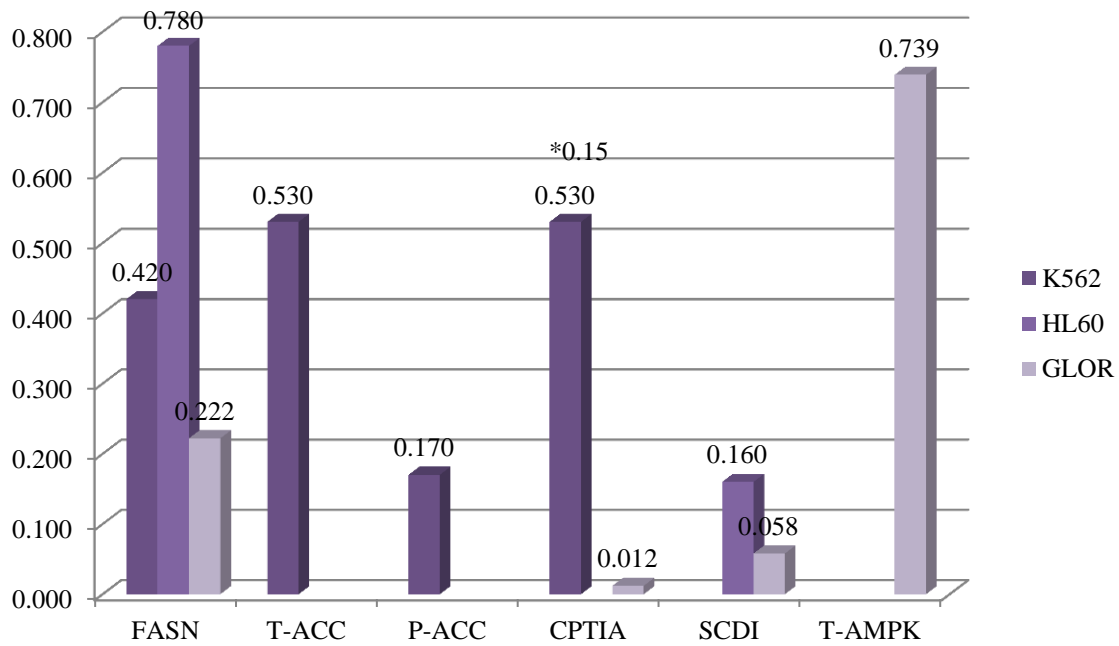


**Figure 3.8:** ImageJ software was used to apply densitometry analysis to western blots. Once the density of the band was obtained, result were normalised to the density of corresponding  $\beta$ -actin bands that act as a loading control for the well. A paired T-Test provided significance values for control-drug pairs.

\*Western blot analysis showed a band at 250kDa for K562, CPT1A. This is potentially a trimer and the pattern shown by the trimer was consistent with what would be expected of CPT1A therefore ImageJ analysis was also performed for these bands.

Densitometry analysis using ImageJ software indicates the change in levels of CPT1A and SCD1 observed between control and BaP treated sample in GLOR cell line are significant ( $\leq 0.05$ ).

**Figure 3.9:** Fold Change between Control and BaP treated samples (Western Blot)

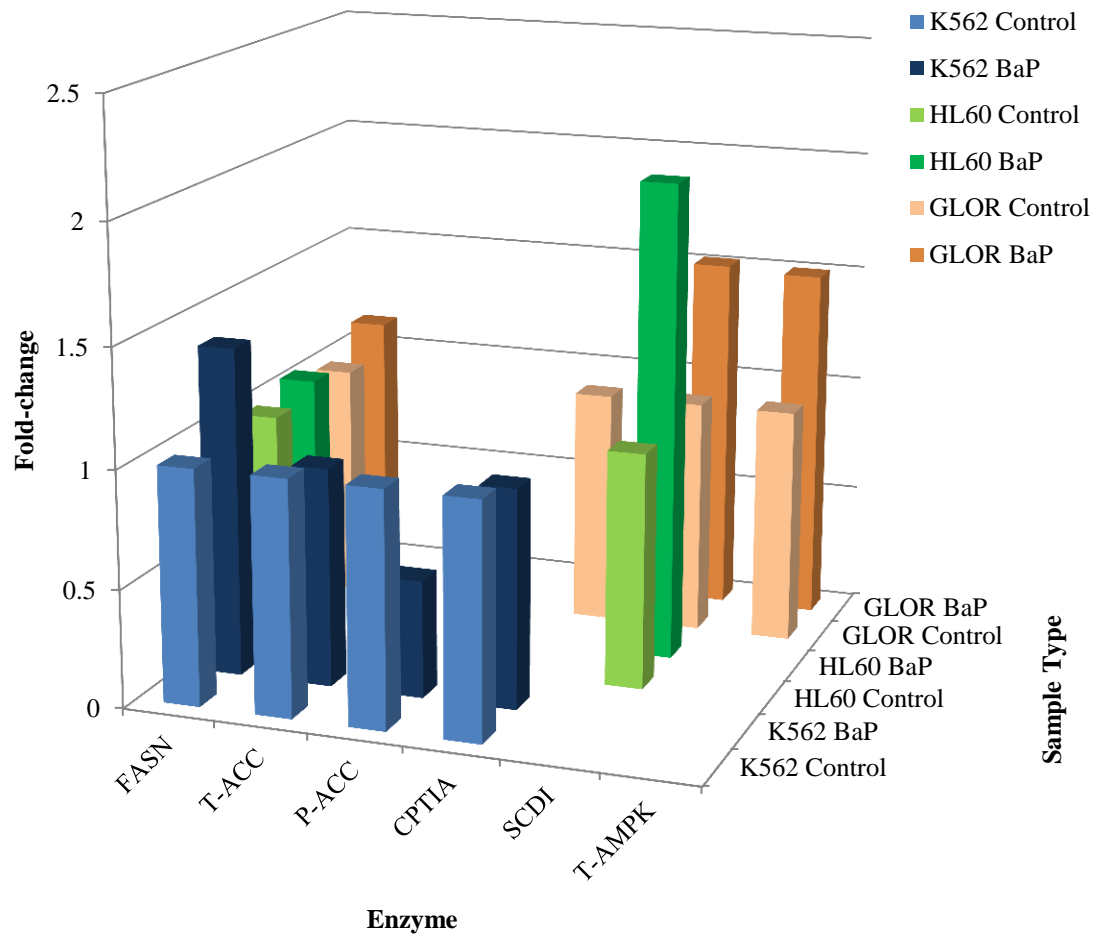


**Figure 3.9:** Fold change between control and drug-treated samples were calculated by using densitometry results. \*Western blot analysis showed a band at 250kDa for K562, CPTIA. This is potentially a trimer and the pattern shown by the trimer was consistent with what would be expected of CPTIA therefore fold change analysis was also performed for these bands. Fold change for the trimer identified a fold change of 0.67.

Fold-change is a method of quantifying the level of change in the drug treated sample from the control group, thus the control group fold-change is a baseline value and therefore is represented as 1. Fold-change ranges between 0.50 and 2.03, with the majority of enzymes across all cell lines showing a fold-change between 0.90 and 1.50 for drug treated samples. For enzymes showing approximately 0.90 fold-change, for example Total-ACC (0.93), this represents a negligible change on the drug treated sample. At the upper limit, a two-fold change in SCD1 levels can be observed in HL60 cell line, whilst at the lower limit a fold-change of 0.50 is shown for phosphorylated-ACC in K562 cell line.

**Figure 3.10: RT-PCR Analysis**

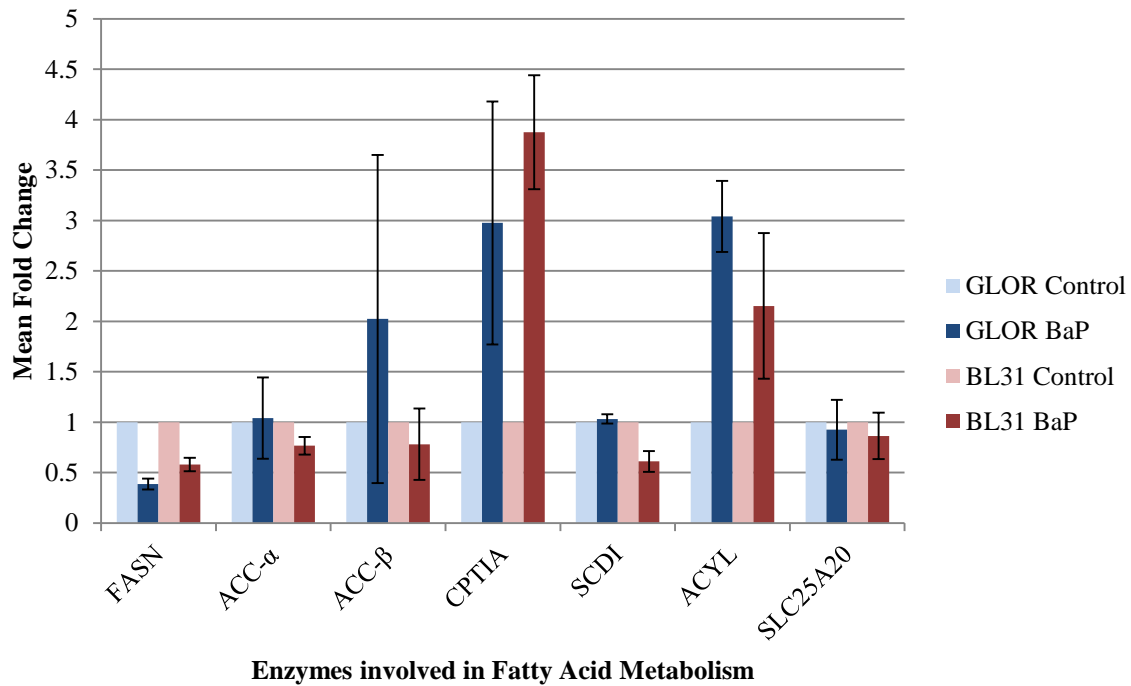


**Figure 3.10:** Quantitative Real-Time analysis of mRNA from 24-hour control and BaP treated samples for cells lines BL31 and GLOR for key enzymes involved in fatty acid synthesis. Results were normalised to 18S ribosomal RNA.

Fold-change of the RNA levels of the enzymes of interest in drug treated samples ranges between 0.39 and 3.04 across all cell lines when analysed via RT-PCR. RT-PCR analysis identified a significant increase in RNA levels of CPT1A and ACYL in BaP treated samples for both GLOR and BL31 cell lines analysed, whilst a notable decrease of FASN can be observed.

### 3.3 Palmitic Acid provides partial rescue to BaP treated cells

**Figure 3.11:** Palmitic Acid Rescue Data

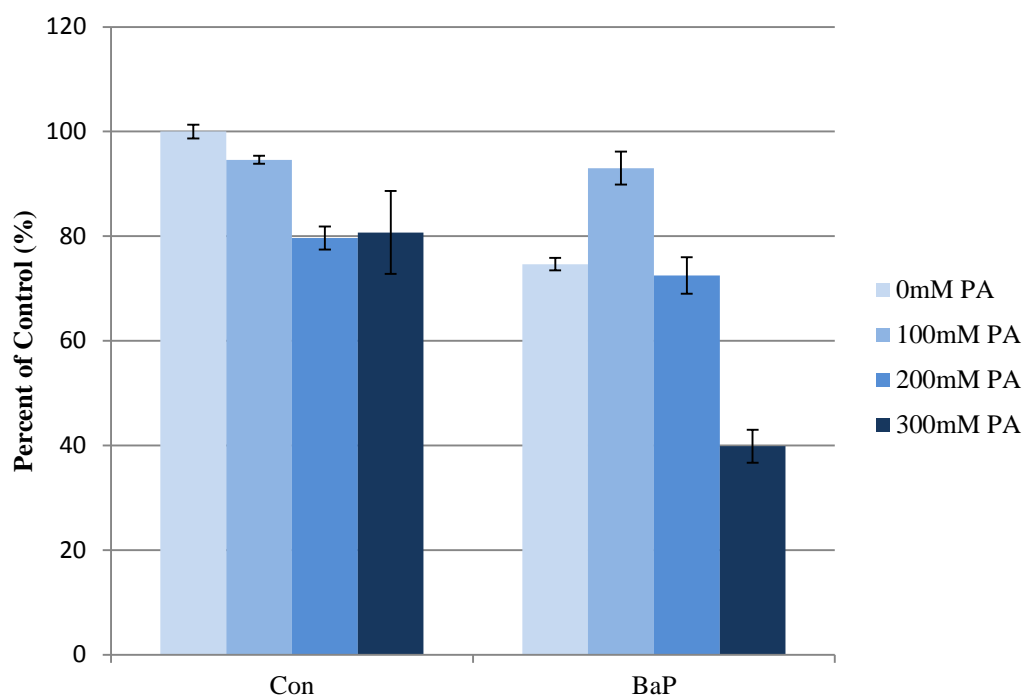


**Figure 3.3.11:** 100mM palmitic acid provided rescue to BaP treated HL60 cells after 48-hour treatment. Control and BaP treated samples were set up in a 96-well plate and 0mM, 100mM, 200mM and 300mM palmitic acid were added to 6 wells each. Alamar Blue was added to the wells and fluorescence was read at 630nm excitation and 690nm emission. Results were analysed and expressed as a percentage of the control group exposed to 0mM palmitic acid. For palmitic acid rescue data of other cell lines see Appendix I.

Cell viability was determined by calculating the percentage of each sample group treated with the stated concentrations of palmitic acid, in comparison to a control group treated with 0mM palmitic acid. Drug treated samples treated with 100mM palmitic acid showed 93.01% rescue when compared to the control sample treated with 0mM palmitic acid, however when compared to the control sample similarly treated with 100mM palmitic acid the results are almost indistinct (control 94.06%, drug-treated 93.01%). In contrast, higher doses decreased cell viability, for example at 300mM treatment cell viability was reduced to 40% of the 0mM palmitic acid control group (equivalent to 50% of the 300mM treated control group).

### 3.4 Palmitic Acid plus Oleic Acid provides better rescue than palmitic acid alone

**Figure 3.12:** Palmitic Acid and Oleic Acid Rescue Data

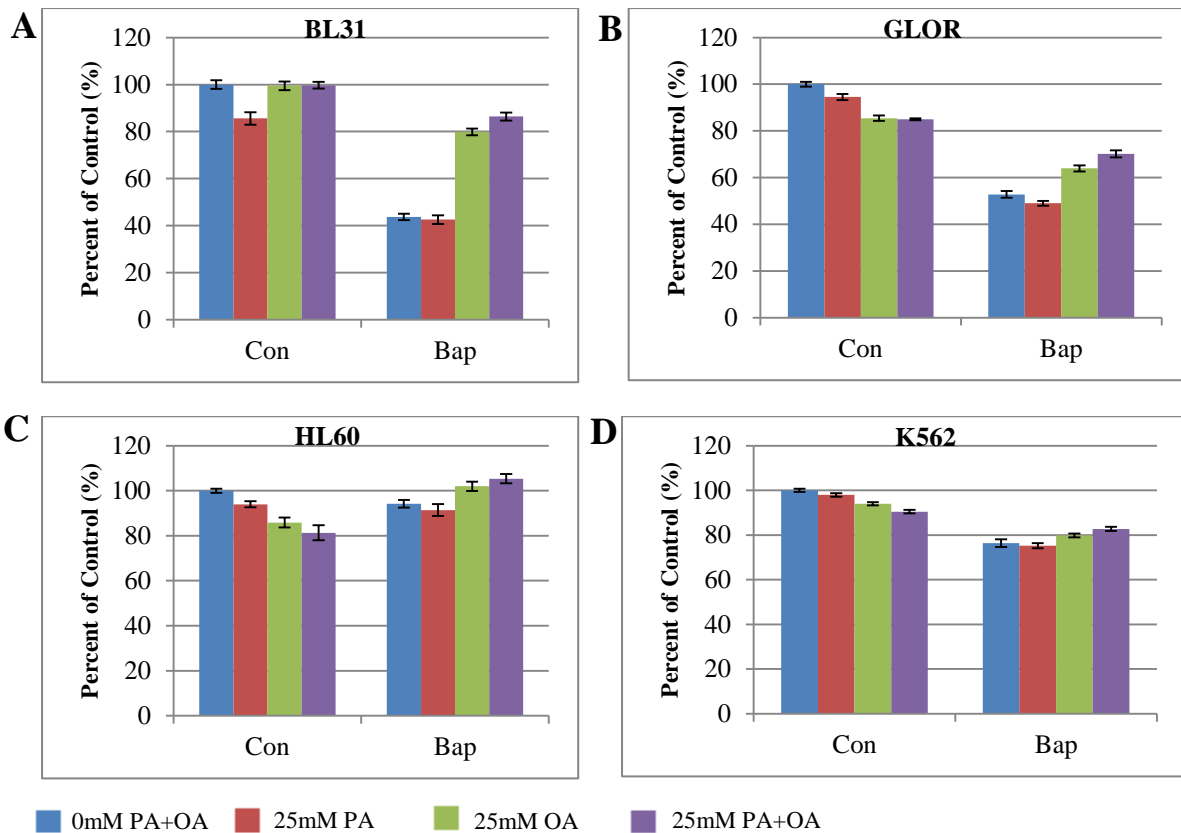


**Figure 3.12:** A: BL31. B: GLOR. C: HL60. D: K562. Control and BaP treated samples were set up in a 96-well plate and 0mM Fatty Acids, 25mM PA, 25mM OA and 25mM PA plus OA were added. Alamar Blue was added to the wells and fluorescence was read at 630nm excitation and 690nm emission. Results were analysed and expressed as a percentage of the control group exposed to 0mM Fatty Acid. This research was undertaken by Southam et al (unpublished).

Combined Palmitic acid (PA) and Oleic acid (OA) provided clear rescue to BaP-treated cells after 120-hour treatment for BL31 and GLOR cell lines. The combined agents appear to provide only a slight improved rescue result for HL60 and K562 cell lines than OA alone, however. Cell viability was increased to between 70-100% in BaP treated samples when supplemented with both acid agents, with GLOR showing 70% rescue whilst HL60 showed 100% viability. Palmitic acid alone provided variable rescue, between 40-90% whilst oleic acid provided a rescue range of 60-100%. Combined agents were overall more successful than singular agents.

## 4. DISCUSSION

### 4.1 Combined Bezafibrate and Medroxyprogesterone Acetate have potent anti-leukemic action in leukemic cell lines

The combination of 5mM Bezafibrate and 5 $\mu$ M Medroxyprogesterone acetate (BaP) when added to leukemic cell lines clearly induces apoptosis, as shown by Figures 3.1 and 3.2. After 48-hour treatment, cell viability in BaP treated samples was decreased by >50% of control samples in both HL60 and K562 cell lines. After 96-hour treatment cell viability for HL60 had declined to 40%, whilst K562 had been reduced to approximately 33% of control samples. Similar results were observed by Khanim *et al* (2009) which also showed that after 10 days of BaP treatment a complete loss of cell viability had almost been achieved.

HL60 is defined as a 'leukemic-like' cell line and is an immortalised line derived from a patient with acute promyelocytic leukaemia (Collins, 1987). Its characteristics are distinctive of myeloid cells and so act as an ideal model for primary drug response research for AML treatment.

K562 is derived from pleural fluid of a chronic myeloid leukaemia patient in blast crisis (Collins et al., 1977). Although derived from a patient with chronic leukaemia K562 expresses myeloid characteristics, therefore the response to BaP treatment is indicative of how AML patients may respond to BaP treatment.

Furthermore, BaP has been shown to exert potent effects in Burkitts-Lymphoma cell lines, GLOR and BL31 (data not shown). The anti-leukemic activity of BaP across AML, CML and lymphoid leukemic cell lines suggests the pathway BaP is affecting is important for cancer cell survival and proliferation and is not just specific to AML.

## **4.2 BaP reduces cell proliferation by inhibiting fatty acid synthesis**

It is widely accepted that fatty acid synthesis is important for the proliferation of cancer cells. There are many steps involved in the production and metabolism of fatty acids utilising many enzymes, as denoted by Figure 1.1. Western blots were performed using protein extracted from 24-hour control and drug treated samples as described in Section 2 and changes in the fatty acid synthesis pathway were identified in drug treated samples compared to control samples.

### **4.2.1 BaP down-regulates Fatty Acid Synthase (FASN)**

Western blot analysis identified a decreased expression of FASN in drug treated samples compared to control samples (where n=4). Although the decrease appears small and image J analysis gave p values of 0.222 (GLOR) and 0.420 (K562), a trend can clearly be seen across all 4 replicates of control and drug treated samples in both cell lines.

Western blot is an important method for the separation and identification of a particular protein from a mixture of proteins, however data analysis of western blots is considered semi-quantitative due to variation in loading and transfer rates (Mahmood and Yang, 2012). This variation is partially mitigated by using a loading control, in this instance  $\beta$ -actin, to identify if changes observed between samples are representative of changes in the protein levels, or if it is simply due to variable loading. However, the analysis still represents a relative comparison between samples but cannot provide absolute quantification. What appears to be a small change on western blot analysis could have a far greater significance on a molecular level. Therefore an additional analytical method of Real-Time PCR (RT-PCR) was used to gain discriminatory evidence.

RT-PCR analysis of GLOR and BL31 identified a >50% and approx.40% decrease in FASN expression in BaP treated samples compared to control groups respectively at 24-hours

(Figure 3.4A). Additionally, RT-PCR data collected by Southam et al (unpublished) identified a significant decrease in FASN expression in 24-hour BaP treated HL60 cells when compared to control cells, however, RT-PCR data for K562 did not show much change at the 24-hour period.

The combination of western blot results and RT-PCR data strongly indicates FASN expression is down in all cell lines; however additional replicates of RT-PCR analysis for K562 and western blot analysis of 24-hour HL60 and BL31 samples could be undertaken to complete the data set and provide clarity. Furthermore, a later time point, for example 48-hour and 72-hour samples, could be analysed using the same methods to determine if the changes become greater and therefore more significant at this point.

As previously described, FASN is responsible for the regulation of *de novo* fatty acid synthesis by catalysing the final stage of biogenesis. BaP inhibits this mechanism by reducing FASN expression resulting in the cells inability to synthesise large quantities of fatty acids required by the cancer cells to survive and proliferate.

#### **4.2.2 BaP inhibits ACC by increasing ACC phosphorylation**

Western blot densitometry analysis showed the presence of total ACC in both control and drug treated samples to be fairly consistent, with a p-value of 0.54 (K562) suggesting no significant change had occurred. ACC- $\alpha$  has a molecular mass of 245kDa whilst ACC- $\beta$  has a mass of 280kDa causing a large spot to appear on the western blot as opposed to a thin band. Additionally, a fold-change value of 0.928 was calculated showing little deviation from the control value of 1, again suggesting no significant change between control and drug-treated samples. Research has shown ACC- $\alpha$  to be slightly up-regulated in cancer cells (Morash et al., 2008) and so may account for slightly higher values obtained for some of the control groups, however over all little difference was observed.

Notably, there was an increase of phosphorylated-ACC (P-ACC) in BaP treated samples (Figure 3.4), with very little shown to be present in control samples. An anti-log fold-change value of 0.498 represents the doubled level of P-ACC in BaP treated samples compared to control samples. Phosphorylation is a post-translation modification used to regulate gene-expression and in this instance causes the ACC gene to become inactive. Active ACC is vital for the production of the fatty acid substrate Malonyl-CoA. The phosphorylation of ACC and consequent silencing of the gene results in a decrease in the production of Malonyl-CoA and therefore reduces production of fatty acids without which the cancer cells cannot survive.

AMPK is activated via phosphorylation in response to cellular metabolic stresses (GeneCards, accessed February 2014). Once active, AMPK inhibits ACC via inducing phosphorylation, therefore it is reasonable to expect phosphorylated-AMPK to also be up-regulated in BaP treated samples. Western blot analysis has shown the total AMPK (inactive) expression to be fairly consistent across control and drug treated samples, however phosphorylated-AMPK (active) data was not obtained. It is unknown if this was due to the anti-body batch being faulty or if it was due to the levels of phosphorylated-AMPK in all cell lines being too low to be detected thus a positive control test needs to be undertaken. The positive control to determine if the phosphorylated-AMPK antibody is working is to pre-treat cells with hydrogen peroxide for 1 hour before extraction (extraction method as described in Section 2). The hydrogen peroxide causes increased levels of reactive oxygen species (ROS) inside the cell which stimulates the activation of AMPK (Zmijewski et al., 2010). This test would need to be undertaken to validate the apparent negative result observed.

RT-PCR data was obtained for ACC- $\alpha$  and ACC- $\beta$  however the information obtained was insufficiently discriminatory to provide an unambiguous correlation. This may be due to variability in loading the wells. It would therefore be beneficial to repeat this experiment to clarify if this was due to any error in the process. Although the western blot analysis shows

little change between control and drug treated samples of total ACC, changes in the level of each isoform are not clear (if present) and so a more sensitive analysis approach could provide greater differentiation. Each isoform is responsible for different modes of action as described in Section 1.5.1, hence if RT-PCR data showed significant change between control and drug treated of one isoform but negligible change in another for example, it could provide more detail in to how BaP treatment effectively kills leukemic cells.

#### **4.2.3 BaP up-regulates Carnitine Palmitoyltransferase I (CPTI)**

CPTIA is significantly higher in 24-hour BaP treated samples when compared to control groups, with densitometry analysis identifying a significant change between control and BaP treated groups in GLOR cell line (significance value 0.012). Western blot analysis proved this for K562 and GLOR cell lines (Figure 3.5), whilst RT-PCR data supports this for GLOR and BL31 (Figure 3.10). Additionally, K562 western blot analysis showed a consistent pattern for what appears to be a trimer of CPTIA (Figure 3.5). CPTI is a membrane-bound protein and research has shown that these can form conjugates when heated. Samples were boiled for 10 minutes prior to loading which may have caused these trimers to form. To reduce the likelihood of polymers forming,  $\beta$ -mercaptoethanol needed to be added to the loading dye.

ACC- $\beta$  produces Malonyl-CoA that is inhibitory to CPTI (Jump et al., 2011). Western data showed high levels of inactive ACC in BaP treated samples therefore inhibitory action of Malonyl-CoA on CPTI had decreased, however western data is not exemplary of enzyme activity but represents the quantity of protein present. A feedback loop is believed to exist between ACC and CPTI whereby a decrease in ACC results in an increase in oxidation (Lopaschuk and Gamble, 1994) for which an increase of CPTI may be required to transfer acyl carnitine conjugates across the membrane and in to the mitochondria where oxidation is undertaken.

When levels of Malonyl-CoA rise, allosteric inhibition of CPTI occurs reducing the rate of fatty acid oxidation, instead directing them toward production of triglycerides which are then stored as adipose tissue. When levels of Malonyl-CoA decrease, synthesis of fatty acids decreases and levels of CPTI rise (McGarry and Brown, 1997) which is likely to be a homeostatic mechanism.

As previously mentioned, CPTI is also regulated via transcription. The transcription factor peroxisome proliferated-activated receptor (PPAR), in this case PPAR $\alpha$ , regulates gene expression and is thought to modulate mRNA in CPTI due to the presence of PPAR response elements (Morash et al, 2008). Fibrates have been identified as PPAR ligands (Michalik and Wahli, 2006) and cause an increase in the transcriptional activity of PPAR $\alpha$  (Inoue et al., 2002) therefore it is likely that the use of BEZ in BaP influences the increase in CPTI levels identified via western blot and RT-PCR analysis. However, Southam et al (unpublished) determined that optimal anti-leukemic activity of BaP utilised BEZ (and MPA) at much higher concentrations than those used for their initial purpose; therefore suggestive of additional mechanisms exerted by BaP being ultimately responsible for the anti-leukemic activity.

Southam *et al* (unpublished) suggests that the similar structure of BEZ and fatty acids means BEZ can mimic high levels of fatty acid inside the cell. As a response to these 'high levels', ACC becomes inactivated causing CPTI to in-turn become more active.

It is reasonable to believe that the increased levels of CPTI caused by PPAR activity in addition to the silencing of ACC resulting in increased CPTI activity would lead to an increased transport of fatty acids across the membrane and into the mitochondria where it undergoes  $\beta$ -oxidation. The increased fatty acid metabolism without the fatty acid content of

the cell being replaced would cause a disruption in the lipogenic/lipolytic balance of the cell, ultimately leading to apoptosis.

#### **4.2.4 Stearoyl-CoA Desaturase (SCDI) is decreased in BaP treated samples**

SCDI is down-regulated in BaP treated samples as shown by HL60 and GLOR western blot analysis, see Figure 3.7. Anti-log fold-change calculated a two-fold change in BaP treated samples showing BaP treated samples to express SCDI levels at half that of control groups.

Decreased levels of SCDI lead to an increased level of saturated fatty acids (SFA) within the cell as they are not being converted in to monounsaturated fatty acids (MUFA) (Miyazaki and Ntambi, 2003). SFAs are allosteric inhibitors of ACC and although the total levels of ACC appear consistent across control and BaP treated samples, activity of the enzyme may differ between the two groups. The inhibition of ACC from accumulating SFA acts as a negative feedback loop for biosynthesis of fatty acids therefore regulation of the SFA:MUFA ratio by SCDI is crucial for the continuous production of fatty acids and lipogenesis required by cancerous cells to survive and proliferate (Scaglia et al., 2009). The clear down-regulation of SCDI in BaP treated samples results in the disruption of lipogenesis due to the decreased production of MUFAs. Scaglia et al suggested the down-regulation of fatty acid synthesis noted when SCDI activity is decreased may be a safeguard mechanism used to adapt to the changing cellular environment when a harmful build-up of SFA occurs (Scaglia et al., 2009).

Much research has shown down-regulation of SCDI to cause up-regulation of PPAR $\alpha$  target genes responsible for lipid oxidation whilst down-regulating genes important for lipid synthesis, therefore the action of BaP on SCDI also explains the changes observed in CPTI and FASN (enzymes that contain PPAR $\alpha$  response elements) (Miyazaki and Ntambi, 2003). Furthermore, regulation of SCDI expression has been strongly linked to sterol regulatory element binding protein 1 (SREBP-1) (Ntambi, 1999). It has been suggested that fibrates

cause partial inhibition of SREBP-1 activation (König et al., 2009); therefore BEZ may be causing inactivation of SREBP-1 leading to a reduced expression of SCDI. It would be beneficial to determine levels of SREBP-1 in control and BaP treated samples to observe any changes.

It may be that BaP utilises the feedback loop regulated by SCDI to disrupt the lipogenic/lipolytic balance. BaP may induce the down-regulation of SCDI as an initial action, resulting in the changes observed in CPTI and FASN, in addition to allosteric inhibition of ACC. The decrease in MUFA production decreases lipogenesis, whilst increased levels of CPTI results in higher levels of lipolysis, disrupting the healthy balance maintained by the cell to allow growth and proliferation, ultimately resulting in apoptosis.

In addition, the ratio of SFA:MUFA regulated by SCDI is important for membrane phospholipid composition (Miyazaki and Ntambi, 2003). The down-regulation of SCDI caused by BaP could cause a change in the membrane composition which leads to the increased sensitivity to ROS observed by Southam et al (unpublished).

#### **4.2.5 Palmitic Acid and Oleic Acid provide rescue to BaP treated cells**

BaP clearly affects fatty acid synthesis, however it still remains unclear if this is a primary action or is a secondary result of something occurring elsewhere in the cell that results in the overall anti-leukemic activity. To determine if the inhibition of fatty acid synthesis is an important mode of action, fatty acid supplement experiments were performed. Complete rescue via supplementation should be possible if the inhibition of synthesis is one of the main causes for the potency of BaP in leukemic cells.

Figure 3.11 shows that 100mM palmitic acid alone provided almost 100% rescue to HL60 cells after 48 hours, whilst higher concentrations appeared to increase toxicity. Figure 3.12

illustrates the rescue activity of palmitic acid (PA), oleic acid (OA) and PA plus OA in all four cell lines at a much lower concentration of 25mM across a 120-hour time period.

PA alone did not provide high levels of rescue to all cell lines when a variety of concentrations and time frames were tested (see Appendix I.3). Differences between the cell lines would account for such a difference in response to rescue via PA alone. PA produces palmitoyl-CoA that can either go on to produce MUFA via SCDI or it can go on to be transported in to the mitochondria via CPTI to undergo  $\beta$ -oxidation. The rate at which both of these occur will differ across the cell lines therefore the importance of each varies depending on cell metabolism of each cell line.

If an increased level of oxidation, caused by BEZ creating a 'high fatty acid' environment within the cell, has a greater apoptotic effect than the limited production of MUFAs in HL60 then it provides an explanation as to why PA alone gives high levels of rescue for this cell line and not for the others. However, all four cell lines exert similar responses to BaP therefore rescue via the same method should be achievable.

The high levels of inactive ACC in addition to potential decreased ACC activity (via allosteric inhibition) provides limited SCDI substrates palmitoyl-CoA (16:0) and stearoyl-CoA (18:0) due to reduced production of Malonyl-CoA. Malonyl-CoA goes on to produce PA, which becomes elongated to produce OA in addition to other acids which then go on to produce the SCDI substrates, therefore by substituting the cells with PA and OA it should bypass the need for Malonyl-CoA production and provide the substrates necessary for MUFA production thus mitigating the effect caused by lower SCDI levels.

It is believed that BaP still causes the down-regulation of SCDI in the rescue experiments but because the inhibition of substrate production is overcome by substitution, the lessened activity of SCDI is still able to produce MUFA and increase lipogenesis. To determine SCDI

levels of rescued cells, protein should be extracted from post-rescue cell cultures and undergo western blot analysis.

Figure 3.12 clearly shows that addition of PA alone does not always provide rescue, but the addition of OA does which suggests SCDI activity may play an important role in the anti-leukemic activity of BaP. However, the combination of both PA and OA provides rescue across all cell lines indicative of combined SCDI and CPTI alterations caused by BaP resulting in apoptosis.

OA alone provides similar rescue to the combined PA and OA supplementation for myelocytic cell lines HL60 and K562, whilst the Burkitt lymphoma (BL) cell lines GLOR and BL31 have slightly greater rescue when both fatty acids are supplemented. Notably, the BL lines show an overall greater level of rescue when treated with OA alone and combined agents when compared to myelocytic lines. This may reflect the differences in the diseases. The burkitts lines *in vitro* grow much faster than the myelocytic lines which may suggest a more imminent demand for both fatty acids, hence a slightly greater rescue when either one or both fatty acids are supplemented. However, a more likely reason for the differences between the myeloid and the BL cells is that at this time point, BaP is having a more potent effect on the BL lines and therefore the rescue in Burkitts lines is apparently much greater because the magnitude of the killing by BaP was much greater.

## 5. CONCLUSION

The combination of 5mM Bezafibrate (BEZ) and 5 $\mu$ M Medroxyprogesterone acetate (MPA), denoted as BaP, causes alterations to expression and activity of enzymes crucial for the maintenance of the lipogenic/lipolytic balance within leukemic cells. The results obtained clearly identify the down-regulation of SCDI and FASN, whilst phosphorylated-ACC and CPTI are up-regulated across multiple cell lines (where n=4). These alterations in lipid metabolism ultimately reduce the cells ability to grow and proliferate, resulting in apoptosis.

It is clear that BaP induces apoptosis in leukemic cell lines. FACSCalibur analysis using Annexin V and Propidium Iodide showed BaP induced apoptosis by >50% in both HL60 and K562 after 48 hours when compared to control samples.

After 24-hours of BaP treatment alterations in lipid metabolism can be seen by western blot and RT-PCR analysis. SCDI expression is decreased resulting in lesser conversion of fatty acid substrates in to monounsaturated fatty acids (MUFA). MUFA are used for the production of phospholipids, triglycerides, cholesterol esters, wax esters, etc., which are important for the maintenance of the cell membrane fluidity. Decreased SCDI activity has been shown to lead to reduced expression of FASN and increased expression of CPTI as observed by the western blots and RT-PCR data obtained within this research. It is unknown if BaP acts directly on SCDI, however a regulator of SCDI expression, SREBP-1, is known to be inhibited by fibrates therefore it is possible that the action of BEZ of SREBP-1 is adding to the down-regulation of SCDI.

Lipogenesis is inhibited by BaP treatment. Levels of phosphorylated-ACC are increased in BaP treated samples resulting in decreased activity of ACC therefore inhibiting the production of Malonyl-CoA, a key substrate for the production of fatty acids. This, combined with reduced FASN levels, resulting in disrupted lipid synthesis.

BaP increases lipolysis in leukemic cells. Malonyl-CoA is an inhibitor of CPTI, therefore the inactivity of ACC observed in BaP treated samples would suggest lower levels of Malonyl-CoA therefore a heightened activity of CPTI is expected. Increased activity in combination with amplified CPTI levels as a response to decreased SCDI results in  $\beta$ -oxidation activity also increasing.

Cell viability for BaP treated samples of HL60, K562, GLOR and BL31 was significantly increased when treatments were supplemented with a combination of the fatty acids palmitic acid (PA) and oleic acid (OA) at a concentration of 25mM. PA and OA alone did not provide rescue across all cell lines, however OA alone was more effective than PA alone. The combination of both was by far a more effective treatment. The substitution of PA and OA bypasses the need for malonyl-CoA production therefore the inhibitory action BaP exerts on ACC is overcome. PA can provide substrate for SCDI to produce MUFA for the creation of phospholipids, triglycerides, etc. or it can go on to produce substrate to be transported in to the mitochondria via CPTI. OA provides one of the preferred substrates for SCDI to produce triglycerides and cholesterol esters. The limited rescue provided by the acid agents separately indicates the divergent pathways that it is expected each agent rectifies is not singularly responsible for the anti-leukemic activity of BaP, therefore only provides partial rescue. Therefore it is likely that the combined action of PA and OA supplying substrate for both arms of the divergent pathway that causes rescue to BaP treated cells across all cell lines.

It is reasonable to suggest the increased  $\beta$ -oxidation activity in addition to the decreased production on MUFAs caused by BaP creates an imbalance in lipogenic/lipolytic activity in the cell which is necessary for the growth and proliferation of cancerous cells. The effect of BaP across AML, CLL and lymphoma cell lines indicates this mechanism is not only important for AML but also for other cancers.

## REFERENCES

- ALIZADEH, A. A., EISEN, M. B., DAVIS, R. E., MA, C., LOSSOS, I. S., ROSENWALD, A., BOLDRICK, J. G., SABET, H., TRAN, T., YU, X., POWELL, J. I., YANG, L. M., MARTI, G. E., MOORE, T., HUDSON, J., LU, L. S., LEWIS, D. B., TIBSHIRANI, R., SHERLOCK, G., CHAN, W. C., GREINER, T. C., WEISENBURGER, D. D., ARMITAGE, J. O., WARNKE, R., LEVY, R., WILSON, W., GREVER, M. R., BYRD, J. C., BOTSTEIN, D., BROWN, P. O. & STAUDT, L. M. 2000. Distinct types of diffuse large B-cell lymphoma identified by gene expression profiling. *Nature*, 403, 503-511.
- CAIRNS, R. A., HARRIS, I. S. & MAK, T. W. 2011. Regulation of cancer cell metabolism. *Nat Rev Cancer*, 11, 85-95.
- COLLINS, S. 1987. *The HL-60 promyelocytic leukemia cell line: proliferation, differentiation, and cellular oncogene expression.*
- GAULTON, K. J., NAMMO, T., PASQUALI, L., SIMON, J. M., GIRESI, P. G., FOGARTY, M. P., PANHUIS, T. M., MIECZKOWSKI, P., SECCHI, A., BOSCO, D., BERNEY, T., MONTANYA, E., MOHLKE, K. L., LIEB, J. D. & FERRER, J. 2010. A map of open chromatin in human pancreatic islets. *Nature Genetics*, 42, 255-U41.
- GUPTA, S. C., SUNG, B., PRASAD, S., WEBB, L. J. & AGGARWAL, B. B. Cancer drug discovery by repurposing: teaching new tricks to old dogs. *Trends in pharmacological sciences*, 34, 508-17.
- HIDESHIMA, T., CHAUHAN, D., SHIMA, Y., RAJE, N., DAVIES, F. E., TAI, Y. T., TREON, S. P., LIN, B., SCHLOSSMAN, R. L., RICHARDSON, P., MULLER, G., STIRLING, D. I. & ANDERSON, K. C. 2000. Thalidomide and its analogs overcome drug resistance of human multiple myeloma cells to conventional therapy. *Blood*, 96, 2943-2950.
- IGAL, R. A. 2010. Stearoyl-CoA desaturase-1: a novel key player in the mechanisms of cell proliferation, programmed cell death and transformation to cancer. *Carcinogenesis*, 31, 1509-1515.
- INOUE, I., ITOH, F., AOYAGI, S., TAZAWA, S., KUSAMA, H., AKAHANE, M., MASTUNAGA, T., HAYASHI, K., AWATA, T., KOMODA, T. & KATAYAMA, S. 2002. Fibrate and statin synergistically increase the transcriptional activities of PPAR alpha/RXR alpha and decrease the transactivation of NF kappa B. *Biochemical and Biophysical Research Communications*, 290, 131-139.
- JUMP, D. B., TORRES-GONZALEZ, M. & OLSON, L. K. 2011. Soraphen A, an inhibitor of acetyl CoA carboxylase activity, interferes with fatty acid elongation. *Biochemical Pharmacology*, 81, 649-660.
- KHANIM, F. L., HAYDEN, R. E., BIRTWISTLE, J., LODI, A., TIZIANI, S., DAVIES, N. J., RIDE, J. P., VIANT, M. R., GUNTHER, U. L., MOUNTFORD, J. C., SCHREWE, H., GREEN, R. M., MURRAY, J. A., DRAYSON, M. T. & BUNCE, C. M. 2009. Combined Bezafibrate and Medroxyprogesterone Acetate: Potential Novel Therapy for Acute Myeloid Leukaemia. *Plos One*, 4.
- KÖNIG, B., KOCH, A., SPIELMANN, J., HILGENFELD, C., HIRCHE, F., STANGL, G. I. & EDER, K. 2009. Activation of PPAR $\alpha$  and PPAR $\gamma$  reduces triacylglycerol synthesis in rat hepatoma cells by reduction of nuclear SREBP-1. *European journal of pharmacology*, 605, 23-30.
- KUHAJDA, F. P. 2000. Fatty-acid synthase and human cancer: new perspectives on its role in tumor biology. *Nutrition*, 16, 202-208.
- KURZROCK, R., KANTARJIAN, H. M., DRUKER, B. J. & TALPAZ, M. 2003. Philadelphia chromosome-positive leukemias: From basic mechanisms to molecular therapeutics. *Annals of Internal Medicine*, 138, 819-830.
- LOPASCHUK, G. D. & GAMBLE, J. 1994. ACETYL-COA CARBOXYLASE - AN IMPORTANT REGULATOR OF FATTY-ACID OXIDATION IN THE HEART. *Canadian Journal of Physiology and Pharmacology*, 72, 1101-1109.

- LOUIE, S. M., ROBERTS, L. S., MULVIHILL, M. M., LUO, K. & NOMURA, D. K. 2013. Cancer cells incorporate and remodel exogenous palmitate into structural and oncogenic signaling lipids. *Biochimica Et Biophysica Acta-Molecular and Cell Biology of Lipids*, 1831, 1566-1572.
- MANARA, M. C., GAROFALO, C., FERRARI, S., BELFIORE, A. & SCOTLANDI, K. 2013. Designing Novel Therapies Against Sarcomas in the Era of Personalized Medicine and Economic Crisis. *Current Pharmaceutical Design*, 19, 5344-5361.
- MCGARRY, J. D. & BROWN, N. F. 1997. The mitochondrial carnitine palmitoyltransferase system - From concept to molecular analysis. *European Journal of Biochemistry*, 244, 1-14.
- MELO, J. V. & BARNES, D. J. 2007. Chronic myeloid leukaemia as a model of disease evolution in human cancer. *Nature Reviews Cancer*, 7, 441-453.
- MENENDEZ, J. A. & LUPU, R. 2007. Fatty acid synthase and the lipogenic phenotype in cancer pathogenesis. *Nature Reviews Cancer*, 7, 763-777.
- MICHALIK, L. & WAHLI, W. 2006. Involvement of PPAR nuclear receptors in tissue injury and wound repair. *The Journal of clinical investigation*, 116, 598-606.
- MINOTTI, G., MENNA, P., SALVATORELLI, E., CAIRO, G. & GIANNI, L. 2004. Anthracyclines: Molecular advances and pharmacologic developments in antitumor activity and cardiotoxicity. *Pharmacological Reviews*, 56, 185-229.
- MIYAZAKI, M. & NTAMBI, J. M. 2003. Role of stearoyl-coenzyme A desaturase in lipid metabolism. *Prostaglandins Leukotrienes and Essential Fatty Acids*, 68, 113-121.
- MORASH, A. J., KAJIMURA, M. & MCCLELLAND, G. B. 2008. Intertissue regulation of carnitine palmitoyltransferase I (CPTI): Mitochondrial membrane properties and gene expression in rainbow trout (*Oncorhynchus mykiss*). *Biochimica Et Biophysica Acta-Biomembranes*, 1778, 1382-1389.
- MURRAY, J. A., KHANIM, F. L., HAYDEN, R. E., CRADDOCK, C. F., HOLYOAKE, T. L., JACKSON, N., LUMLEY, M., BUNCE, C. M. & DRAYSON, M. T. 2010. Combined bezafibrate and medroxyprogesterone acetate have efficacy without haematological toxicity in elderly and relapsed acute myeloid leukaemia (AML). *British Journal of Haematology*, 149, 65-69.
- NTAMBI, J. M. 1999. Regulation of stearoyl-CoA desaturase by polyunsaturated fatty acids and cholesterol. *Journal of lipid research*, 40, 1549-1558.
- PEFANI, E., PANOSKALTSIS, N., MANTALARIS, A., GEORGIADIS, M. C. & PISTIKOPOULOS, E. N. 2012. Design of optimal disease and patient-specific chemotherapy protocols for the treatment of Acute Myeloid Leukaemia (AML). *11th International Symposium on Process Systems Engineering, Pts a and B*, 31, 1717-1721.
- PESSETTO, Z. Y., WEIR, S. J., SETHI, G., BROWARD, M. A. & GODWIN, A. K. Drug Repurposing for Gastrointestinal Stromal Tumor. *Molecular Cancer Therapeutics*, 12, 1299-1309.
- PESSETTO, Z. Y., WEIR, S. J., SETHI, G., BROWARD, M. A. & GODWIN, A. K. 2013. Drug Repurposing for Gastrointestinal Stromal Tumor. *Molecular Cancer Therapeutics*, 12, 1299-1309.
- PIZER, E. S., JACKISCH, C., WOOD, F. D., PASTERNAK, G. R., DAVIDSON, N. E. & KUHAJDA, F. P. 1996. Inhibition of fatty acid synthesis induces programmed cell death in human breast cancer cells. *Cancer research*, 56, 2745-2747.
- SCAGLIA, N., CHISHOLM, J. W. & IGAL, R. A. 2009. Inhibition of stearoylCoA desaturase-1 inactivates acetyl-CoA carboxylase and impairs proliferation in cancer cells: role of AMPK. *PloS one*, 4, e6812.
- TIZIANI, S., LODI, A., KHANIM, F. L., VIANT, M. R., BUNCE, C. M. & GUENTHER, U. L. 2009. Metabolomic Profiling of Drug Responses in Acute Myeloid Leukaemia Cell Lines. *Plos One*, 4.
- WANG, Z.-Y. & CHEN, Z. 2008. Acute promyelocytic leukemia: from highly fatal to highly curable. *Blood*, 111, 2505-2515.
- ZMIJEWSKI, J. W., BANERJEE, S., BAE, H., FRIGGERI, A., LAZAROWSKI, E. R. & ABRAHAM, E. 2010. Exposure to Hydrogen Peroxide Induces Oxidation and Activation of AMP-activated Protein Kinase. *Journal of Biological Chemistry*, 285, 33154-33164.

## Other Sources

Brady, G., MacArthur, G. J., & Farrell, P. J. (2007). Epstein–Barr virus and Burkitt lymphoma. *Journal of Clinical Pathology*, 60(12), 1397–1402. doi:10.1136/jcp.2007.047977

Cancer Research UK<sup>a</sup>. Available at: <http://www.cancerresearchuk.org/cancer-help/type/hodgkins-lymphoma/about/what-is-hodgkins-lymphoma> [Accessed October 2013]

Cancer Research UK<sup>b</sup>. Available at: <http://www.cancerresearchuk.org/about-cancer/type/cll/treatment/statistics-and-outlook-for-chronic-lymphocytic-leukaemia> [Accessed November 2014]

Cancer Research UK<sup>c</sup>. Available at: <http://www.cancerresearchuk.org/about-cancer/type/all/treatment/statistics-and-outlook-for-acute-lymphoblastic-leukaemia> [Accessed November 2014]

Cancer Research UK<sup>d</sup>. Available at: <http://www.cancerresearchuk.org/about-cancer/type/cml/treatment/statistics-and-outlook-for-chronic-myeloid-leukaemia> [Accessed November 2014]

Collins. SJ. Gallo. RC. Gallagher. RE. 1977. “Continuous growth and differentiation of human myeloid leukaemic cells in suspension culture.” *Nature* **270**: 347-349

Genecards. Available at: <http://www.genecards.org/cgi-bin/carddisp.pl?gene=PRKAB1&search=AMPK> [Accessed February 2014].

Genecards<sup>b</sup>. Available at: <http://www.genecards.org/cgi-bin/carddisp.pl?gene=CPT1A> [Accessed February 2014]

Hoffbrand. V. Moss. P. Pettit. JE. (2006). *Essential Haematology*. Blackwell Publishing : London.

Hummel. M. Bentink. S. Berger H. Klapper. W. Wessendorf. S. Barth. T. Bernd. HW. Cogliatti. DB. Dierlamm. J. Feller. AC. Hansmann. ML. Haralambieva. E. Harder. L. Hasenclever. D. Kuhn. M. Lenze. D et al. 2006. "Abiological definition of Burkitt's Lymphoma from Transcriptional and Genomic Profiling" *The New England Journal of Medicine* **354 (23)**: 2419 – 2430

Leukaemia and Lymphoma Research. 2011. “Leukemia and Related Diseases.”

Leukaemia and Lymphoma Research. 2012. “Adult Acute Myeloid Leukaemia AML).”

Life Technologies. Available at <http://www.lifetechnologies.com/uk/en/home/references/protocols/cell-and-tissue-analysis/cell-proliferation-assay-protocols/cell-viability-with-alamarblue.html> [Accessed October 2013]

Macmillan<sup>a</sup>. Available at:

<http://www.macmillan.org.uk/Cancerinformation/Cancertypes/Leukaemiachronicmyeloid/AboutCML/WhatisCML.aspx> [Accessed February 2014]

Macmillan<sup>b</sup>. Available at:

<http://www.macmillan.org.uk/Cancerinformation/Cancertypes/Leukaemiachroniclymphocytic/AboutCLL/WhatisCLL.aspx> [Accessed February 2014]

Macmillan<sup>c</sup>. Available at:

<http://www.macmillan.org.uk/Cancerinformation/Cancertypes/LymphomanonHodgkin/TypesofNHL/DiffuselargeB-cell.aspx> [Accessed October 2013]

Mahmood. T. Yang. PC. 2012. "Western Blot: Technique, Theory, and Troubleshooting." North American Journal of Medicinal Science **4(9)**: 429-434

Medicago AB. Available at <http://www.medicago.se/phosphate-buffered-saline-pbs-ph-74-and-72> [Accessed October 2013]

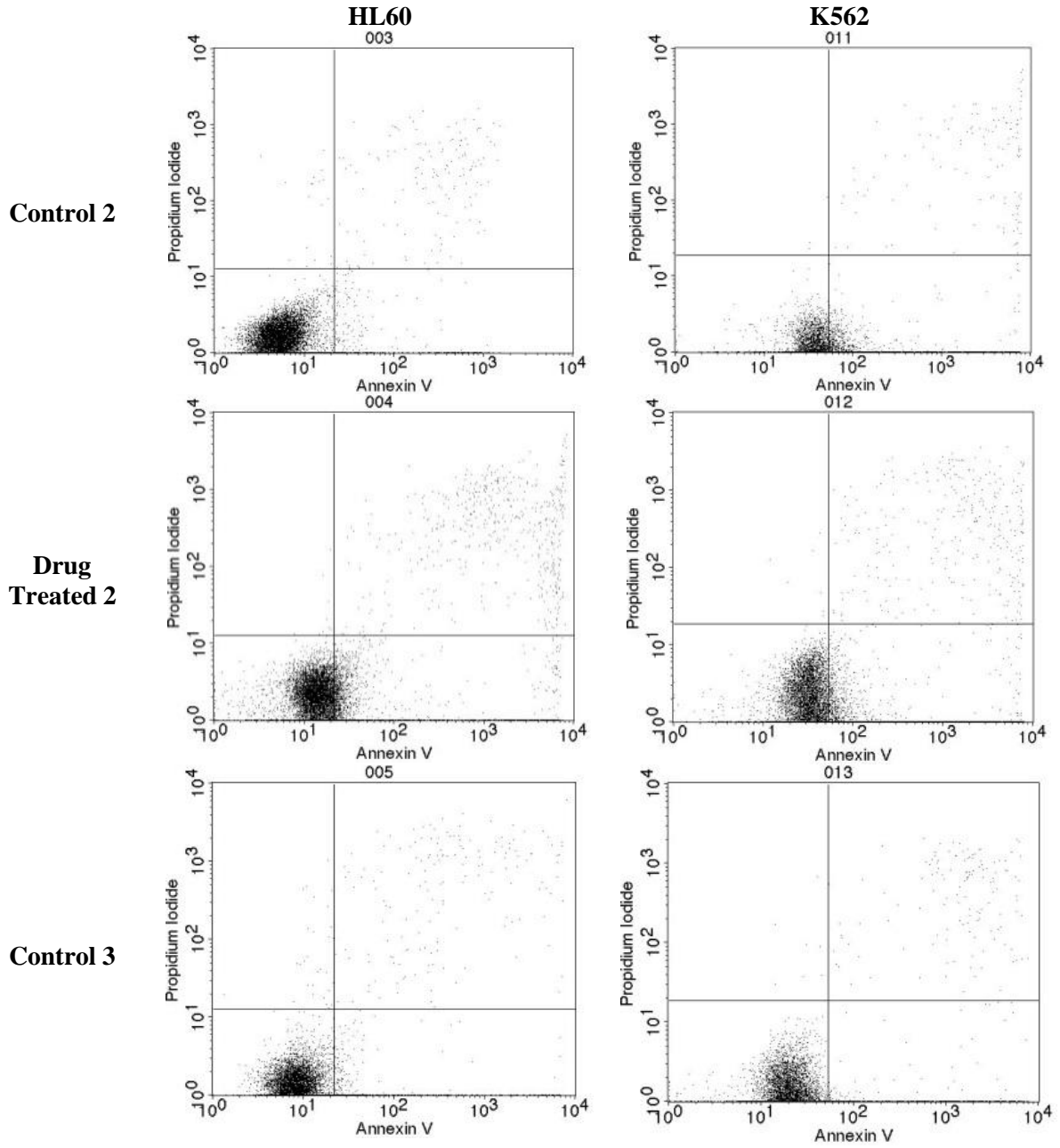
Rozman. C. and Montserrat. E (1995). "Chronic Lymphocytic Leukemia." New England Journal of Medicine **333**: 1052-1057

Thomson Reuters. 2012. "White Paper. Knowledge Based Drug Repositioning to Drive R&D Productivity."

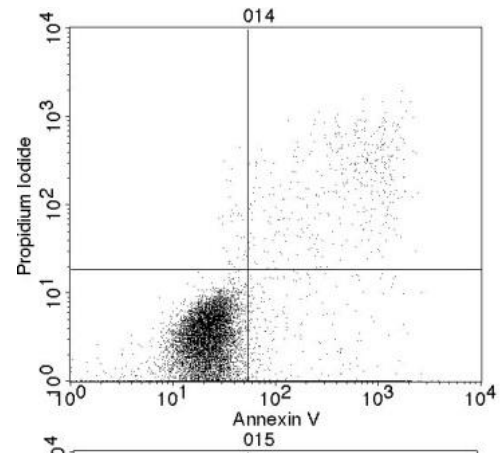
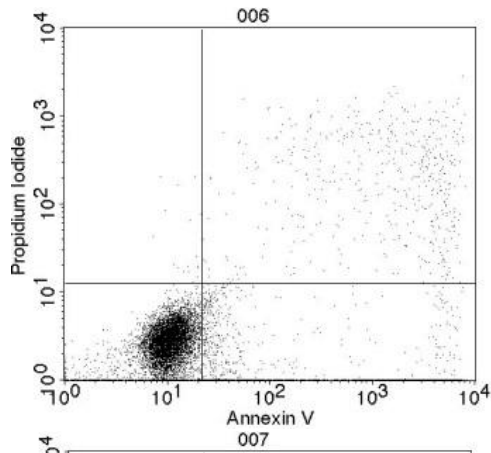
Wang. C. Rajput. S. Watabe, K. Liao. DF. Cao. D. 2010. "Acetyl-CoA carboxylase-a as a novel target for cancer therapy." Frontiers in bioscience **2**: 515-526

## Appendix I – Additional Data

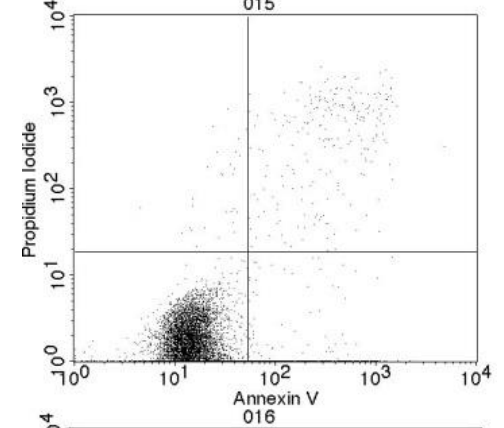
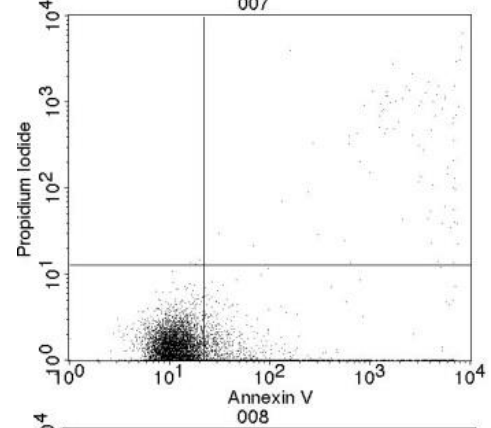
### AI.1: FACSCalibur Annexin V / Propidium Iodide Data (96-hour treatment)



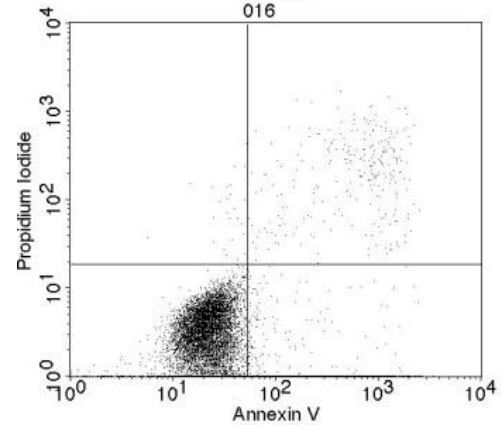
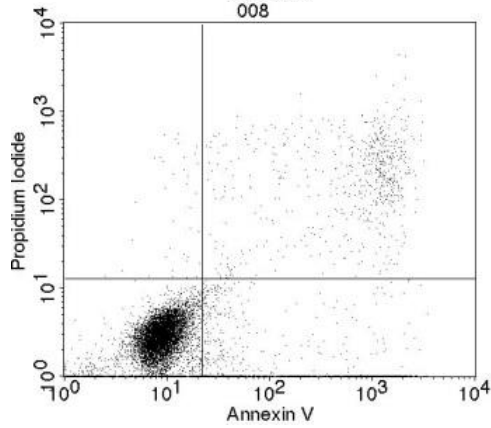
**Drug  
Treated 3**



**Control 4**

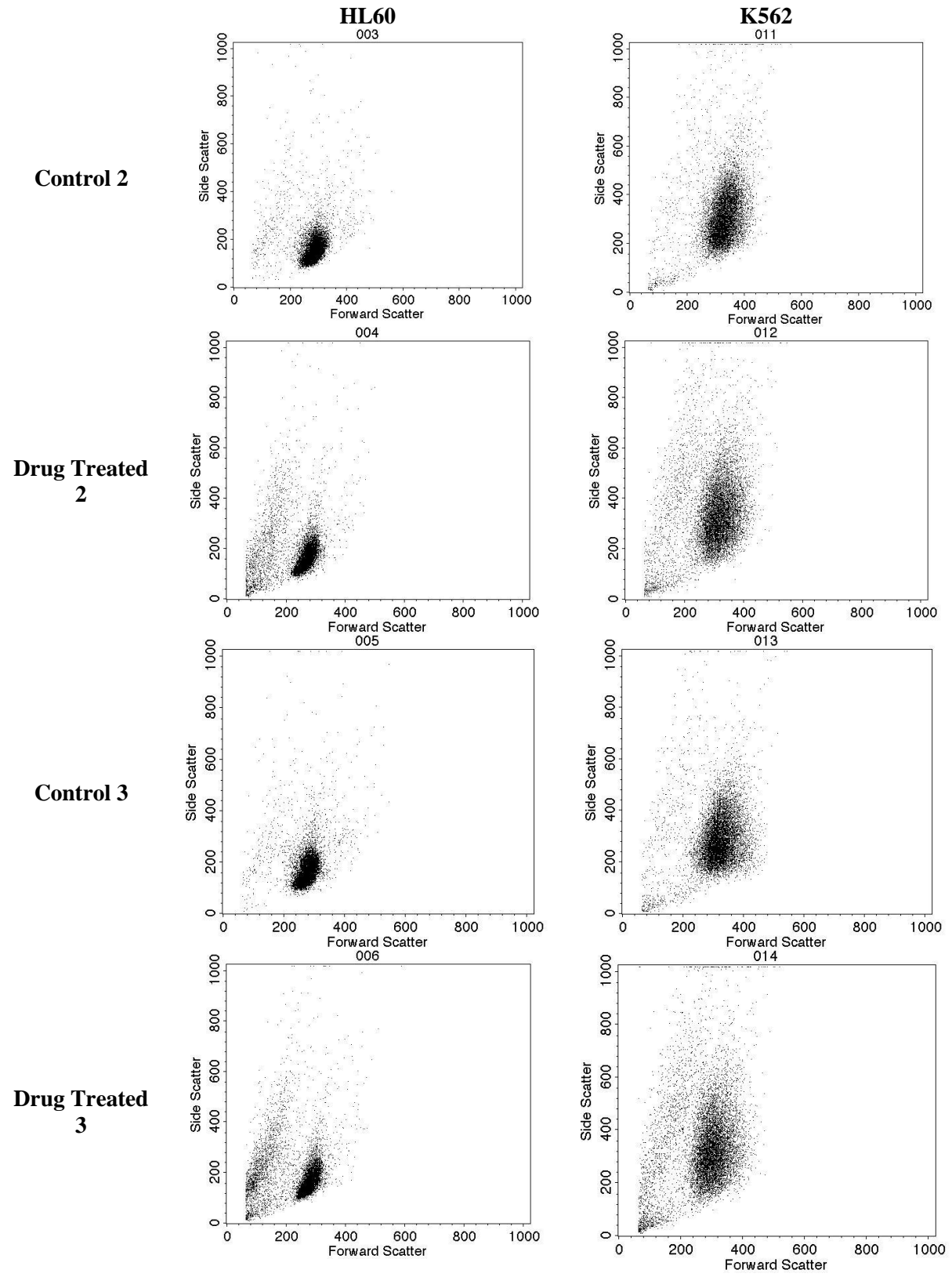


**Drug  
Treated 4**

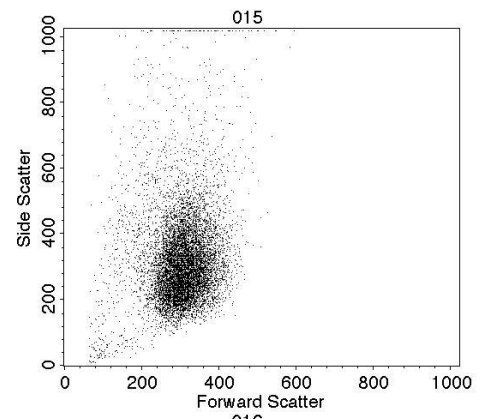
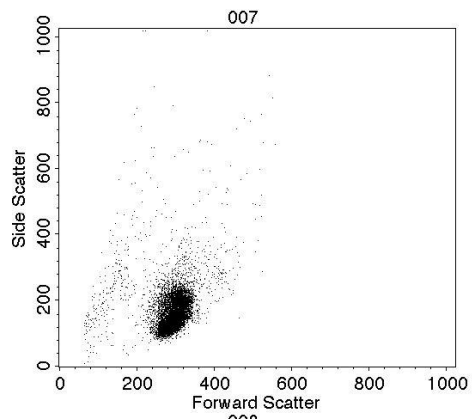


**AI.1** Additional data to support information shown by Figure 3.2. Annexin V and Propidium Iodide expression of HL60 cells shown in the left column, and K562 results shown in the right column. All control and BaP treated samples were treated for 96-hours.

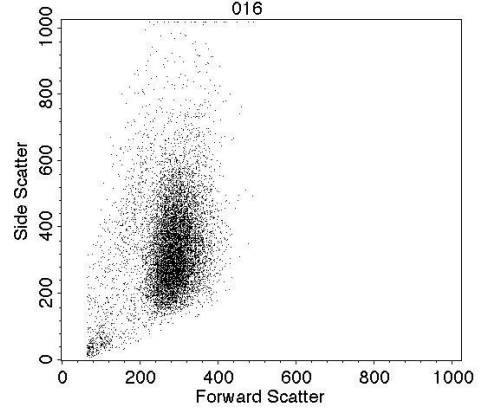
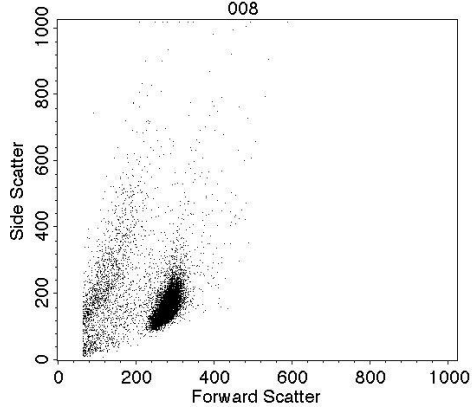
**AI.2: FACSCalibur Forward / Side Scatter Data (96-hour treatment)**



**Control 4**



**Drug Treated  
4**



**AI.2** Additional data to support information shown by Figure 3.3. Forward scatter and side scatter pattern of HL60 cells shown in the left column, and K562 results shown in the right column. All control and BaP treated samples were treated for 96-hours.

### AI.3 Palmitic Acid Rescue Data

Figure AI.3.1 72 hour Rescue Data

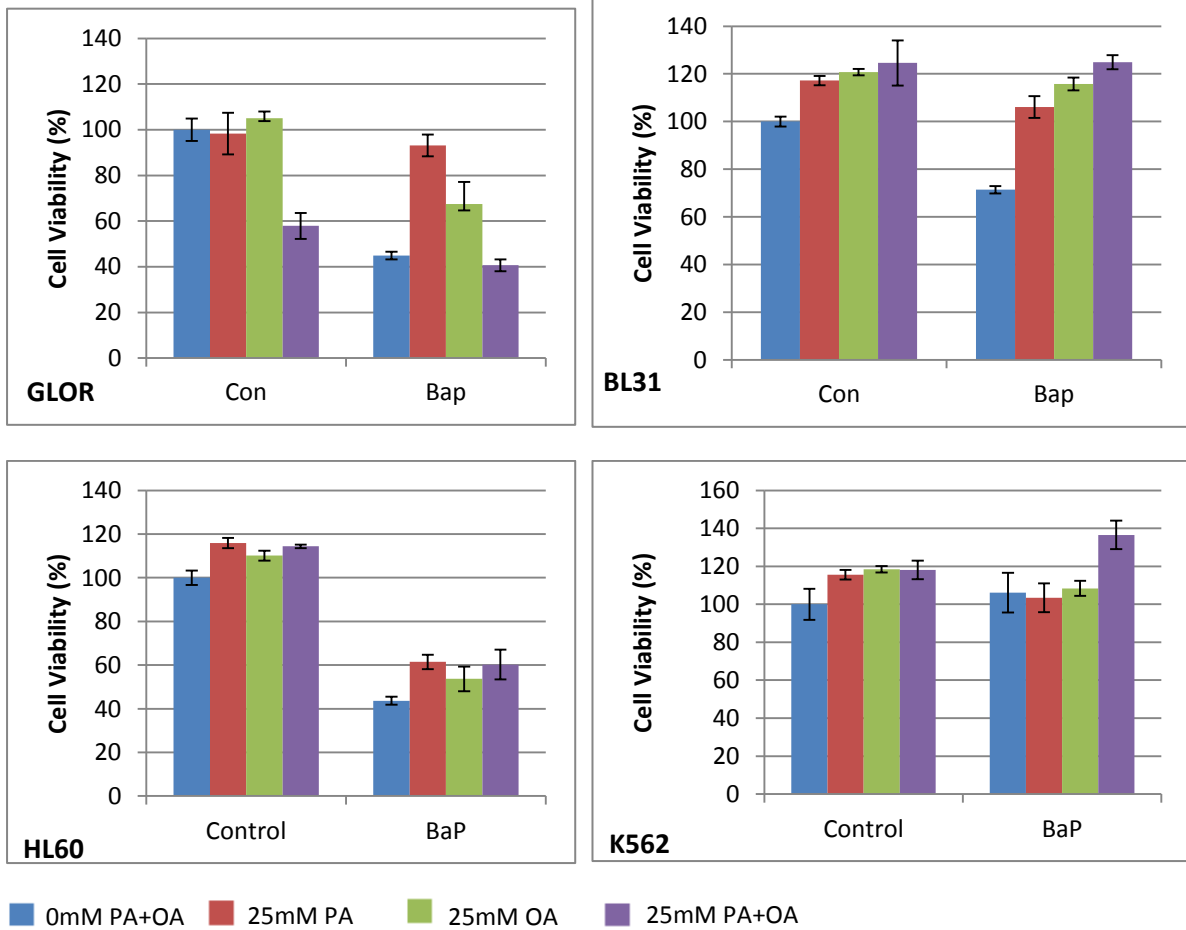
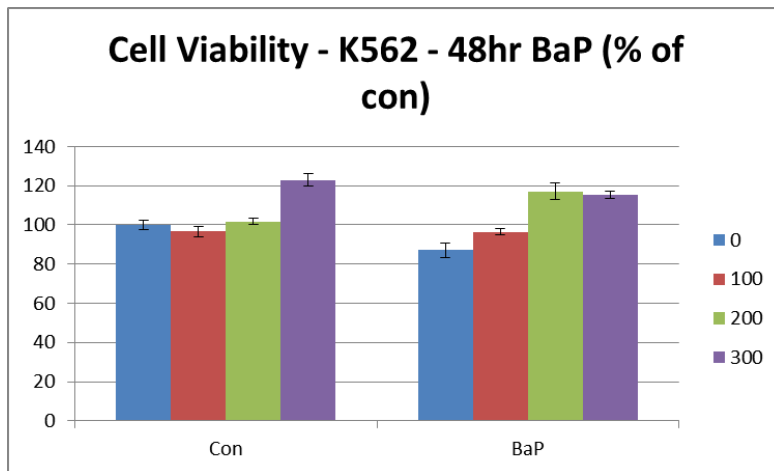


Figure AI.3.2 48 hour Rescue Data





**UNIVERSITY OF  
BIRMINGHAM**

**Analysis of Putative *cis*-Regulatory Elements in Type 2 Diabetes  
Associated Genes using Zebrafish Model**

**By**

**Julia Constantinou**

**Part 2 of 2: A research thesis submitted to the University of Birmingham as  
part of the requirement for the degree of MASTER OF RESEARCH in  
Molecular and Cellular Biology**

**College of Life and Environmental Sciences**

**School of Biosciences**

**University of Birmingham**

**August 2014**

## **ACKNOWLEDGEMENTS**

I would like to thank my supervisor Prof. Ferenc Müller for the giving me the opportunity to undertake this project and to Dr. Yavor Hadziev for his constant support, guidance and help though-out the duration of the project.

I would also like to thank the rest of the lab team; Nan Li, Rhiannon Hurst, Christopher Tyrrell, Agata Wieczorek, Stefania Santangeli and Hannah Edie for making the experience so rewarding.

Finally I would like to thank Irene Miguel-Escalada who made this project possible and was always willing to give advice and guidance when needed.

# CONTENTS

ABSTRACT.....	
1. INTRODUCTION.....	1
1.1 Diabetes.....	1
1.1.1 Type 1.....	1
1.1.2 Type 2.....	1
1.2 Transcription Regulates Gene Expression.....	2
1.2.1 Promoters.....	3
1.2.2 Enhancers.....	4
1.2.3 Silencers.....	5
1.3 Regulatory Elements in Disease Associated Disorders.....	6
1.4 Single Nucleotide Polymorphisms.....	7
1.4.1 Transcription Factor 7 like 2 (TCF7L2).....	8
1.4.2 Prospero Homeobox 1 (PROX1).....	8
1.4.3 Zinc Finger AN1 Domain 3 (ZFAND3).....	8
1.4.4 C2 Calcium Dependent Domain Containing 4A (C2CD4A).....	9
1.5 Zebrafish as a Model Organism.....	10
1.5.1 Zebrafish in Research.....	10
1.5.2 Zebrafish as a model for consolidating putative enhancers related to T2D, Preliminary Data.....	10
1.6 Aims and Objectives.....	14
2. MATERIALS AND METHODS.....	15
2.1 Materials.....	15
2.1.1 Antibiotics.....	15
2.1.2 Chemical Reagents.....	15
2.1.3 Consumables.....	15
2.1.4 Enzymes.....	15
2.1.5 Kits.....	16
2.1.6 Buffers and Solutions.....	16
2.1.7 Equipment.....	16
2.2 Identifying Transgenic Zebrafish.....	16

2.2.1 In-crossing Zebrafish.....	17
2.2.2 Screening F1 generation.....	17
2.2.3 F1 generation Image Acquisition .....	18
2.3 Whole-mount In Situ Hybridization (WISH).....	19
2.3.1 Obtaining positive zebrafish embryos .....	19
2.3.2 Fixation of embryos .....	19
2.3.3 Permeabilization of embryos.....	19
3. RESULTS .....	23
3.1 Identifying Founding Transgenic Fish Figure 3.1: Transmission Rate of In-Crossed Transgenic Fish.....	23
4. DISCUSSION .....	31
4.1 PhiC31 integrase facilitates targeted integration in Zebrafish model .....	31
4.2 Potential differences observed between PROX-G and PROX-A lines .....	31
4.3 C2CD4A enhancers may be too weak to drive <i>hsp70</i> promoter .....	33
4.4 ZFAND3 and TCF7L2 lines did not produce transgenic F1 generation .....	34
4.5 Time-constraints hindered project progression .....	35
4.6 Outstanding Aims.....	37
5. CONCLUSION .....	39
REFERENCES.....	40
APPENDIX I – ADDITIONAL DATA.....	i
AI.1. Crossing Record.....	ii
AI.2. 48hpf Fluorescence Images.....	iv
AI.3. 72hpf Fluorescence Images.....	v

## List of Figures

Figure 1.1: Schematic of a typical gene regulatory region.....	3
Figure 1.2: PhiC31 integrase.....	12
Figure 1.3: PhiC31 mediated integration for creation of transgenic zebrafish lines.....	13
Figure 3.1: Transmission Rate of In-Crossed Transgenic Fish.....	23
Figure 3.2: Transmission Rate of Out-Crossed Transgenic Fish.....	24
Figure 3.3: WISH Analysis of PROX-G and PROX-A embryos at 3dpf.....	25
Figure 3.4: WISH Analysis of PROX-G and PROX-A embryos at 30hpf.....	26
Figure 3.5: Fluorescent Expression of PROX-G and PROX-A lines at 25hpf.....	28
Figure 3.6: Fluorescent Expression of PROX-G and PROX-A lines at 48hpf.....	29
Figure 3.7: Fluorescent Expression of PROX-G and PROX-A lines at 72hpf.....	30

## List of Tables

Table 1.1: Disease associates <i>cis</i> -regulatory elements.....	7
Table 1.2: Constructs containing T2D-associated putative enhancers.....	13
Table 2.1: F0 Generation Transgenic Zebrafish.....	17
Table 2.2: Components of Hybridization Mix (50ml).....	20
Table 2.3: Alkaline Tris Buffer (50ml).....	21

## ABSTRACT

With the ever-expanding knowledge base obtained by genome-wide studies, the importance and complexity of transcription has become increasingly prominent. Advanced technology in the form of computer analysis can now predict the presence of *cis*-regulatory elements; however these *in silico* systems cannot validate such predictions. Here we have shown transgenic zebrafish can be used as a model to test functionality of human enhancers. Differences in expression patterns driven by two forms of the PROX enhancer, the common form (PROX-G) and also its type 2 diabetes associated SNP variant counter-part (PROX-A), were observed. These enhancers were integrated in to the genome using a targeted integration system mediated by PhiC31 integrase and showed promising transmission rate, as well as over-coming problems associated with other transgenesis systems, most notably position effect.

When examined by fluorescence microscopy, differences in expression of the reporter in the pancreatic islet at 25hpf (hours post fertilisation) appears to show earlier development in embryos containing the enhancer with disease associated SNP variant compared to embryos containing the common form of the enhancer. By 30hpf, *in situ* analysis showed pancreatic islet present in both lines. This subtle difference may hint at a role in disease progression, however a time-course experiment would have to be performed to identify precise timings of development.

The use of zebrafish as a model to elucidate enhancer function, alongside other *cis*-regulatory elements, appears to be a promising tool and warrants further investigation.

# 1. INTRODUCTION

## 1.1 Diabetes

Diabetes is the body's inability to regulate blood sugar levels and it is a lifelong condition. In the UK it affects approximately 2.9 million people, with an additional 850,000 thought to suffer undiagnosed diabetes (NHS, accessed May 2014). Two types of diabetes exist;

### 1.1.1 Type 1

Type 1 Diabetes (T1D) is an autoimmune condition that affects approximately 400,000 people in the UK and often develops before the age of 40. T1D is referred to as insulin-dependent as it is caused by the pancreas' inability to produce insulin. Insulin is the hormone that regulates blood glucose levels, and if glucose levels remain too high it can cause diabetic ketoacidosis and damage to organs, therefore T1D sufferers receive insulin injections on a regular basis to achieve a healthy balanced blood glucose level (NHS, accessed May 2014).

### 1.1.2 Type 2

Type 2 Diabetes (T2D) is the most common form of the disease and accounts for approximately 90% of all adult diabetes sufferers. T2D is referred to as insulin-resistant as the pancreas either does not produce enough insulin or the body cannot use the insulin that is produced to perform its normal role of regulating biological processes (NHS, accessed May 2014).

Extensive research including numerous Genome Wide Association Studies (GWAS) have identified susceptibility to and progression of T2D to be linked to genetic predisposition (Florez et al., 2006, Groves et al., 2006, Lyssenko et al., 2007, Pomerantz et al., 2009, Fujita et al., 2012, Smemo et al., 2014).

Due to the sheer number of T2D cases in the UK alone and the surmounting evidence showing genetic predisposition to the disease, including changes in gene expression, research into genes involved in the development of T2D must be undertaken to identify possible therapeutic agents.

## **1.2 Transcription Regulates Gene Expression**

Spatial and temporal activation of genes are of key importance for carrying out biological processes, as shown by the frequent consequence of disease when dysregulation occurs (Maston et al., 2006). It is widely accepted that transcriptional regulatory elements play a functional role in the spatial and temporal expression of genes.

Transcription is the initial phase of gene expression. Transcription is where an ‘unzipped’ DNA strand, known as the template strand, containing at least one gene is copied in to RNA by RNA Polymerase. The nucleotides of the DNA are matched with their corresponding RNA pair; where cytosine (C), guanine (G), thymine (T) and adenine (A) are paired with G, C, A and U (uracil) respectively. The transcribed RNA can ultimately relay in to a protein via translation, non-coding RNA genes, ribosomal RNA or transfer RNA.

In eukaryotes, RNA Polymerase II (RNA Pol II) is responsible for the transcription of protein-encoding genes. There are two bodies of *cis*-regulatory elements (CREs) that ensure transcription is controlled. Firstly, a body of promoters composed of a core promoter and proximal promoter elements located upstream; and secondly, distal regulatory regions consisting of enhancers, silencers, insulators or locus control regions (Maston et al., 2006).



Mammalian core promoters are characterised by either a T/A rich region known as the TATA-box or a C/G rich, largely unmethylated region known as a CpG island (Yamamoto et al., 2007, Deaton and Bird, 2011).

Clusters of multiple TSSs have been shown to exist in a single promoter region, the shape of which can affect the profile and expression of the corresponding gene. Mammalian TATA-promoters are described as sharp due to containing a chief TSS cluster that directs tissue-specific expression. CpG associated promoters often exist in TATA-less regions and express ubiquitously with broad TSS-clusters. Such activity describes a differentiated and complementary role between mammalian TATA-box and CpG-island promoter regions (Yamamoto et al., 2007).

### **1.2.2 Enhancers**

Transcription of heterologous human genes containing promoters are actively increased by the activity of enhancers. Enhancers regulate in a spatial or temporal specific manner and are highly dynamic during development. They can regulate transcription of specific genes independent of proximity to or orientation in relation to the corresponding promoter. Approximately 12-21% of enhancers appear to miss non-expressed neighbouring genes in order to regulate more distal genes, whilst the other 79-88% of enhancers regulate neighbouring genes, suggestive of CREs organised locally in domains supported by chromosomal domains, insulator binding and genome evolution (Maston et al., 2006, Kvon et al., 2014).

Distinct enhancer elements can act on a promoter at different times, in different tissue and as a result of various stimuli. They comprise a cluster of transcription factor binding sites whereby spatial organisation and orientation regulate the enhanced transcription activity.

The role of the enhancer appears to cross-over with the functional role of proximal promoter elements, however a distinctive difference is the enhancers ability to exert functional activity when located distally from the core promoter; including upstream or downstream of the promoter, in an intron or beyond the 3' end of the gene (Maston et al., 2006). For example, the enhancer element that drives sonic hedgehog (*Shh*) expression is located 1Mb away from the target gene (Lettice et al., 2003).

A favoured understanding of distal enhancer activity is that of the DNA-looping model. It is believed that the 'looping out' of DNA brings the enhancer and promoter in to close proximity allowing the enhancer to act upon the promoter to increase transcription activity, as represented in Figure 1.1 (Maston et al., 2006).

### **1.2.3 Silencers**

Silencing and repression of gene expression can occur due to negative regulation of transcription of the target genes by silencers. Silencers are sequence-specific elements that typically function individually from distance and orientation to the promoter, much like enhancer elements. The location of silencers can vary as they have been found to be situated as part of a proximal promoter or distal enhancer, but have also been identified as a separate distal regulatory module.

Silencers bind repressors and co-repressors which are negative transcription factors. There are multiple mechanisms of action that repressors can take to exert silencing activity. In some

cases, they act as inhibitors and block activator binding or compete for the same site. In other cases, repressors have been shown to establish a repressive chromatin structure via histone modification or chromatin stabilizing factors, preventing activator and/or general transcription factor binding (Maston et al., 2006).

### **1.3 Regulatory Elements in Disease Associated Disorders**

As previously described, execution of biological processes requires exquisite control of transcription for the correct expression of target genes. Mutations in key CREs can result in aberrations of transcriptional control which are often linked to disease.

There are many examples of cancers caused by irregular linkages between enhancers/promoters and oncogenes which are a result of chromosomal translocations. The linkages result in changed expression of the oncogenic protein. A clear example of this is the multifaceted oncogene *c-Myc* which plays a causal role in Burkitts lymphoma (BL). *c-Myc* is over expressed in BL due to its translocation under promoter regions of heavy or light chain immunoglobulin genes (Miller et al., 2012).

Another example is the case of  $\beta$ -thalassemia where a mutation in the core promoter (affecting the TATA, CACCC and EKLF binding regions) results in disrupted expression of the *HBB* gene (Epstein, 2009). These examples represent clearly the effect dysregulation of transcription via altered CREs has on the pathogenesis of disease types.

**Table 1.1:** Disease associated *cis*-regulatory elements

Gene	Disease	Location of rSNP	TF-binding site affected	References
<i>HBB</i>	$\beta$ -thalassemia	Promoter	Several (TATA, CACCC, EKLF)	[13]
<i>F9</i>	Hemophilia B	Promoter	Several (HNF4, C/EBP)	[13]
<i>LDLR</i>	Familial hypercholesterolemia	Promoter	Several (SPI, SRE repeat)	[13]
<i>Coll1A1</i>	Osteoporosis	Intron I (+2kb)	SPI (gain)	[14]
<i>RET</i>	Hirschprung	Intron1 (+9.7 kb)	Unknown	[23]
<i>HBA</i>	$\alpha$ -thalassemia	Upstream (-13 kb)	GATA1 (gain)	[25]
<i>SHH</i>	Preaxial polydactyly	Upstream (-1 Mb)	Unknown	[29]
<i>SHH</i>	Holoprosencephaly	Upstream (-470 kb)	Six3	[37]
<i>SOX9</i>	Pierre Robin Sequence	Upstream (-1.5 Mb)	Msx1	[41]
<i>IRF6</i>	Nonsyndromic cleft lip	Upstream (-14kb)	Ap2	[42]

Table 1.1 reproduced from Epstein, 2000.

## 1.4 Single Nucleotide Polymorphisms

In many human diseases it is the increased susceptibility to a disease or developed disease progression caused by complex interactions of numerous genes and variations that lead to its success as opposed to a single mutation on a singular gene.

Present in the human genome at approximately every 1000bp, the most common type of genetic predisposition to diseases are allele variations known as single nucleotide polymorphisms (SNPs). SNPs can be found in coding and noncoding regions, however 93-96% of variations identified via genome wide association studies (GWAS) have existed in non-coding regions thought to be in non-coding CREs such as enhancers (Maston et al., 2006, Corradin et al., 2014).

77% of 349 human cell types showed GWAS SNPs to be located in open chromatin when analysed via epigenomic profiling, specifically DNase I hypersensitivity site profiling. These open chromatin sites are thought to contain enhancer elements (Maurano et al., 2012, Corradin et al., 2014). Furthermore, in recent years GWAS SNPs have revealed a relationship with H3K4me1, H3K27ac, and H3K4me3 marked enhancer elements in relevant disease associated cell types (Ernst et al., 2011, Akhtar-Zaidi et al., 2012, Trynka et al., 2013,

Corradin et al., 2014). Research in to functional CREs in the human genome has obvious implications for potential future therapeutic targets.

#### **1.4.1 Transcription Factor 7 like 2 (TCF7L2)**

TCF7L2 encodes a transcription factor involved in the Wnt signalling pathway.

Polymorphisms in TCF7L2 have been shown to be associated with susceptibility to Type 2 Diabetes (Florez et al., 2006).

It was identified that SNP variants (rs12255372 G>T; rs7903146 C>T) in TCF7L2 aided the progression of T2D with association to impaired  $\beta$ -cell function but not with insulin resistance (Florez et al., 2006).

Extensive research on the link between TCF7L2 SNP variants and T2D has been performed, identifying a strong link between the two (Florez et al., 2006, Groves et al., 2006, Lyssenko et al., 2007, Wang et al., 2014).

Open chromatin regions are often a tell-tale sign of enhancer locations, and a SNP present in an islet specific open chromatin region in TCF7L2 showed higher enhancer activity in vitro in the diabetes risk allele (C>T, SNP ref rs7903146) (Gaulton et al., 2010)

#### **1.4.2 Prospero Homeobox 1 (PROX1)**

PROX1 was identified as a novel fasting glucose loci after meta-analysis of GWAS covering glucose and insulin related traits was performed (Hu et al., 2010).

#### **1.4.3 Zinc Finger AN1 Domain 3 (ZFAND3)**

ZFAND3 was identified as a potential T2D associated loci after reaching genome-wide significance during a meta-analysis of GWAS in an Asian population. The elucidation of the

role of ZFAND3 has yet to be achieved, however ZFAND6, a member of the same family, alongside FAH had been identified at a previously detected T2D locus. The risk allele was identified as rs9470794 (T>C) (Cho et al., 2012).

#### **1.4.4 C2 Calcium Dependent Domain Containing 4A (C2CD4A)**

C2CD4A has been linked to T2D susceptibility since 2011 after combined GWAS of East Asian and European populations associated C2CD4A-C2CD4B with T2D at significant levels, with an overall p value of  $8.78 \times 10^{-14}$ , with statistical relevance levels being  $<0.05$  (Yamauchi et al., 2010).

The following years saw a release of a wealth of evidence supporting the role of SNPs found in C2CD4A relating to susceptibility to T2D (Grarup et al., 2011, Cui et al., 2011, Strawbridge et al., 2011, Iwata et al., 2012).

#### **1.4.5 Type 2 Diabetes as a Genetic Disorder**

The definition of T2D as a genetic disease is one of debate. Although clear linkages between disease susceptibility and progression and genetic variation exist (as discussed above), it is the combination of genetic factors together with environmental factors ('risk factors' including age, obesity, diet (low fibre, high saturated fat), smoking, etc.) that are a primary cause; that is, even with the genetic disposition it is not necessarily guaranteed that T2D will develop without being exposed to certain environmental factors (Freeman and Cox, 2006, Lyssenko and Laakso, 2013). This is what makes T2D so challenging.

However, the identification of T2D-associated genetic predispositions and understanding of how these genetic variations work allows for the identification of risk prior to development of the disease and therefore can result in avoidance of disease development, or alternatively

provide elucidation of the mechanism by which T2D progresses and relay in to specialised therapeutic treatment resulting in more effective treatment.

## **1.5 Zebrafish as a Model Organism**

Zebrafish (*Danio rerio*) is a fast increasing model for an array of research, with an estimated number of zebrafish used in research reaching far in to the millions (Reed and Jennings, 2010).

### **1.5.1 Zebrafish in Research**

Zebrafish are often used for early stage embryonic studies due to embryogenesis in zebrafish being similar to higher vertebrates whilst the embryos develop externally in a transparent chorion. The embryos remain transparent for the first few days allowing visual analysis of early development processes easily *in vivo*. Additionally, high fecundity (pairs can lay ~200-300 eggs per week) and fast development make them an ideal model for genetic analysis (Dooley and Zon, 2000).

Furthermore, with the completion of the zebrafish genome-sequencing project it was possible to identify that 70% of human genes have at least 1 recognizable orthologue in zebrafish. It was shown that 84% of human disease causing genes can be found in zebrafish, identifying them as a useful model for human genetic disorder studies (Howe et al., 2013).

### **1.5.2 Zebrafish as a model for consolidating putative enhancers related to T2D, Preliminary Data**

Irene Miguel-Escalada (PhD student, Müller research laboratory, University of Birmingham Medical School) proposed the use of transgenic zebrafish embryo as a model to elucidate functionality of putative pancreatic-specific human enhancers that had been identified via a combination of chromatin signatures, bidirectional transcription and TF binding events with

the aim of identifying subtle changes caused by T2D disease-associated SNP variants. Zebrafish are an ideal model to investigate T2D as they have a common pancreatic structure with humans and contain conserved expression and function of pancreas-specific transcription factors, including PDX1, NKX6.1, NKX2.2, FOXA2 and MAFB.

A targeted integration system facilitated by PhiC31 integrase was used to improve the reliability of zebrafish transgenesis and circumvented the major issue of position effect variability. Using this method it was possible to identify a novel zebrafish enhancer (Roberts et al., 2014).

To ensure PhiC31 integrase facilitated targeted integration *in vivo*, a PhiC31 plasmid containing an attB site was inserted in to an attP site in zebrafish and was detected by reporter activity in lens. To do this, PhiC31 mRNA transcribed *in vitro* was co-injected with attB-mCherry construct in to single cell embryos from the Tol2-based transgenic recipient line Tg(Xla.crygc:attP-GFP).

Tol2 is an active autonomous vertebrate transposon isolated from the fish *Orzias latipes* which does not require co-injection of plasmid with transposase mRNA. These qualities mean introduction of Tol2 is less toxic therefore results in higher viability of transgenic embryos compared to other methods (Hamlet et al., 2006, Roberts et al., 2014). However, it has been observed that Tol2 does not have a target site of preference therefore can often lead to random integration (Hamlet et al., 2006).

**Figure 1.2: PhiC31 Integrase**

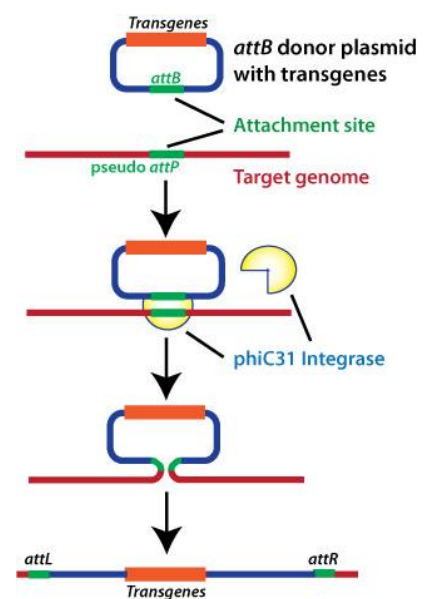
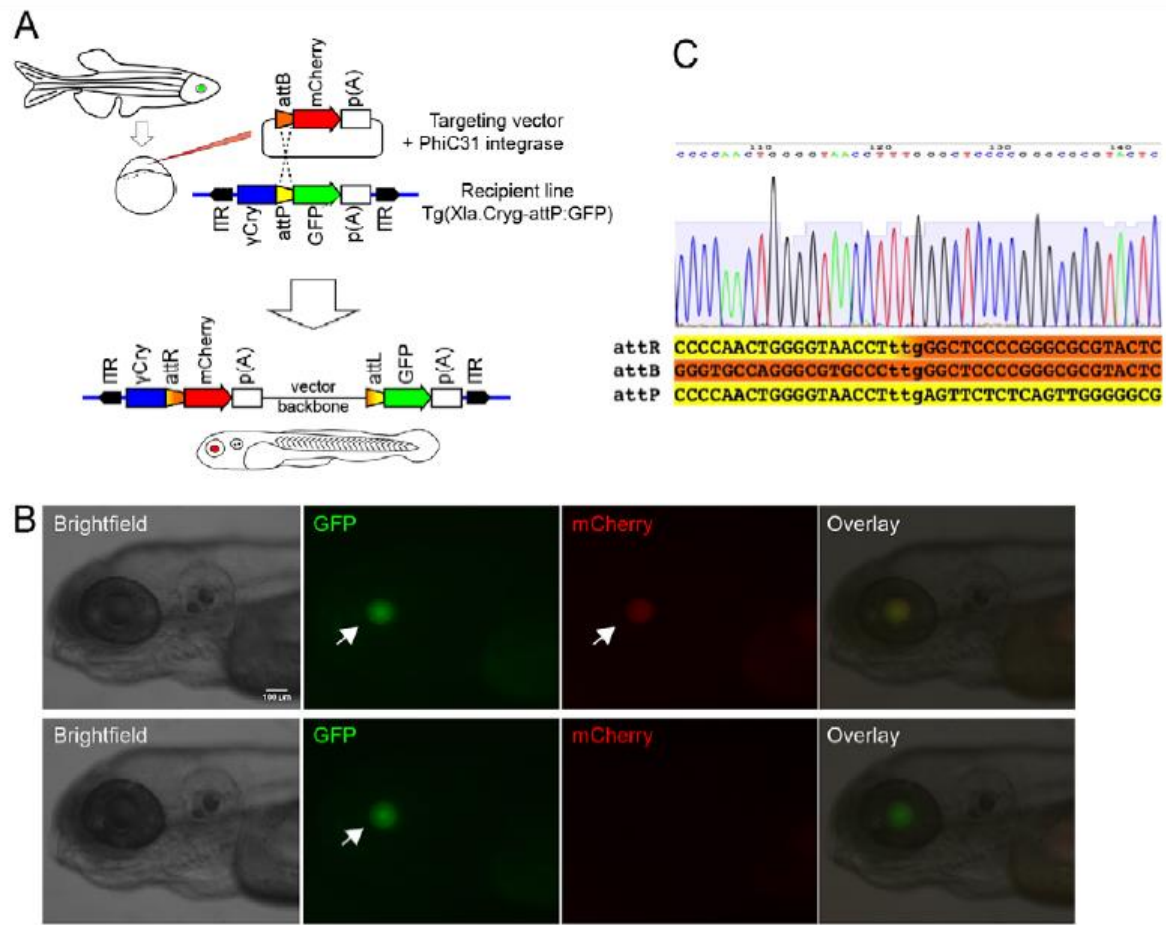


**Figure 1.2:** Reproduced from <http://www.systembio.com/phi31>

The use of PhiC31 can limit this random integration when used in combination with Tol2 by the use of the attP docking site in the genome and the attB site of the targeted plasmid (see Figure 1.2).

The addition of fluorescent reporter markers means that screening for desired site-specific integration can be performed and eliminates confusion with integrations at pseudo attP sites. Roberts et al (2014) found that 66.7% of normal developing larvae were positive for mCherry expression when co-injected with PhiC31 mRNA and targeting construct pJET-attBmCherry (n=258). Comparatively, of embryos injected with the same targeting construct minus PhiC31 integrase, 0% were positive for mCherry expression in the lens (n=302); see Figure 1.3B. These results suggest the lens colour change is due to integrase-mediated recombination events at docking sites in the recipient transgenic locus. PCR amplification and sequencing of the attL and attR sites that result from attP and attB site recombination was used to confirm integrase-dependent transgene integration (Roberts et al., 2014), see Figure 1.3A,C.

**Figure 1.3:** PhiC31 mediated integration for creation of transgenic zebrafish lines



Following the successful identification of targeted PhiC31 integrase mediated integration, the following constructs were created using PhiC31 technology;

**Table 1.2:** Constructs containing T2D-associated putative enhancers

Gene	Transgenic Line	Common/SNP
<b>PROX1</b>	Tg(ycry-ATTR-mCherry,Hs.PROX1-G-prox1:YFP:ATTR-GFP)	Common
<b>PROX1</b>	Tg(ycry-ATTR-mCherry,Hs.PROX1-A-prox1:YFP-ATTR-GFP)	Rare SNP Variant
<b>C2CD4A</b>	Tg(ycry-ATTR-mCherry,Hs.C2CD4A-C-hsp70:YFP-ATTR)	Common
<b>C2CD4A</b>	Tg(ycry:ATTR-mCherry,Hs.C2CD4A-T-hsp70:YFP-ATTR)	Rare SNP Variant
<b>ZFAND3</b>	Tg(cry:ATTR-mCherry,Hs.ZFAND3-C-hsp70:YFP-ATTR-GFP)	Common
<b>ZFAND3</b>	Tg(cry:ATTR-mCherry,Hs.ZFAND3-T-hsp70:YFP-ATTR-GFP)	Rare SNP Variant
<b>TCF7L2</b>	Tg(cry:ATTR-mCherry,Hs.TCF7L2-C-tcf7l2:YFP-ATTR)	Common
<b>TCF7L2</b>	Tg(cry:ATTR-mCherry,Hs.TCF7L2-T-tcf7l2:YFP-ATTR)	Rare SNP Variant

\*Rare SNP variants produced via site directed mutagenesis

The constructs were microinjected in to wild-type zebrafish embryos at 10 minutes post fertilisation. The embryos were screened daily for up to 5dpf, by which point red lens should have been visible for those with successful integration of the transgene. Those expressing red lens ('founders') were grown to maturity (F0 generation) with the aim to analyse F1 generation expression.

## **1.6 Aims and Objectives**

Advancements in genome-wide research and biotechnological capabilities have allowed a much improved identification system of potential CREs such as enhancers. However, these *in silico* systems cannot fully characterise the CREs or the effect of variations in disease susceptibility and progression, therefore an *in vivo* model is essential for validation. Zebrafish has great potential for such validation studies. The aim of this study is to utilise the zebrafish model to determine the role of putative enhancers in T2D disease progression. Stable transgenic zebrafish lines containing common or rare SNP variants of T2D associated putative enhancers attached to fluorescent markers will be crossed and fluorescent transgenic expression patterns will be compared and analysed. Any variation in expression observed between the common and disease-associated SNP could elucidate mechanisms by which T2D progresses and may relay in to a therapeutic drug target.

## 2. MATERIALS AND METHODS

### 2.1 Materials

All materials used were of a certified molecular biology grade.

List adapted from Irene Migeul-Escalada PhD thesis.

#### 2.1.1 Antibiotics

Gentamycin	BPE918-1	Fisher Bioreagents, UK
------------	----------	------------------------

#### 2.1.2 Chemical Reagents

Agarose	BIO-41025	Bioline Ltd., UK
5-Bromo 4-chloro 3 indolyl phosphate (BCIP)	11383221001	Roche Diagnostics, UK
dNTPs 10mM	R0192	Thermo Scientific, UK
Ethyl 3-aminobenzoate methanesulfonate 98% (MESAB)	E10521	Sigma-Aldrich, UK
Fetal Bovine Serum Heat Inactivated	A11-104	PAA Cell Culture, UK
Formamide (deionized)	AM9342	Ambion, UK
Gel Loading Dye, Blue 6X	B7021S	NEB, UK
Glycerol	G6279	Sigma-Aldrich, UK
Heparin sodium salt	H3393	Sigma-Aldrich, UK
N-Phenylthiourea Grade I (PTU)	P7629	Sigma-Aldrich, UK
Nitro blue tetrazolium (NBT)	11383213001	Roche Diagnostics, UK
Paraformaldehyde	P6148	Sigma-Aldrich, UK
SSC buffer substance	85639	Sigma-Aldrich, UK
Sheep serum	013000121	Interchim SA
Tween-20	P1379	Sigma-Aldrich, UK
UltraPure™ 1M Tris-HCl, pH 8.0	15568-025	Invitrogen, UK

#### 2.1.3 Consumables

Graduated Pasteur Pipette, 3ml	E1414-0300	Star Lab Group
Needle hypodermic regular bevel sterile 19G x 25mm	12379179	Fisher Scientific, UK
Petri dish resistance glass 60mm x 12mm	12901408	Fisher Scientific, UK

#### 2.1.4 Enzymes

Protinase K	Sigma Life Science	39450-01-6
RNase Polymerase T7	Roche	10 881 775 001

### 2.1.5 Kits

DIG RNA Labelling Kit (SP6/T7)      Roche      11 175 025 910

### 2.1.6 Buffers and Solutions

- E3 Medium: 0.5 mM NaCl, 0.17 mM KCl, 0.33 mM CaCl<sub>2</sub>, 0.33 mM MgSO<sub>4</sub>.
- 4% Paraformaldehyde (PFA): PFA dissolved in sterile PBS at 60° with constant stirring.
- PBST: PBS, 0.1% Tween-20.
- WISH Blocking Solution: 1x PBST, 2% sheep serum (v/v), 2 mg/ml BSA
- WISH Hybridization Buffer (+): 50% deionized formamide, 5X SSC, 0.1% Tween-20, 50 µg/ml of heparin bile salts, 500 µg/ml of extensively extracted RNase-free tRNA adjusted to pH 6.0 by adding citric acid (460 µl of 1 M citric acid solution per 50 ml of hybridization buffer).
- WISH Hybridization Buffer (-): 50% deionized formamide, 5X SSC, 0.1% Tween-20
- WISH Staining Buffer: 1 M Tris-HCl, adjusted to pH 9.5, 50 mM MgCl<sub>2</sub>, 100 mM NaCl, 0.1% Tween-20.
- WISH Staining Solution: Dilute 225 µl of 50 mg/ml NBT and 175 µl of 50 mg/ml BCIP with 50 ml of WISH Staining Buffer (Light sensitive).
- WISH Stop solution: PBS pH 5.5, 1 mM EDTA, 0.1% Tween-20.
- Antibody staining blocking buffer: 10% NBCS in PBST.

### 2.1.7 Equipment

Digital microINJECTOR System	MINJ-1	Tritech Research, US
Incubator		Heraeus, Germany
Leica TCS LSI zoom confocal microscope	LSI6000	Leica, UK
NanoDrop ND-1000 Spectrophotometer	ND-1000	NanoDrop Technologies
Digital Sight Nikon SMZ1500	DS-Qi1Mc	
Scan <sup>^</sup> R High-Content Screening Station for Life Science	scan <sup>^</sup> r	Olympus, Germany

## 2.2 Identifying Transgenic Zebrafish

The following 8 lines of transgenic zebrafish had been created and established by Irene Miguel-

Escalada;

**Table 2.1:** F0 Generation Transgenic Zebrafish

Gene	Transgenic Line	Common/SNP
<b>PROX1</b>	Tg(ycry-ATTR-mCherry,Hs.PROX1-G-prox1:YFP:ATTR-GFP)	Common
<b>PROX1</b>	Tg(ycry-ATTR-mCherry,Hs.PROX1-A-prox1:YFP-ATTR-GFP)	Rare SNP Variant
<b>C2CD4A</b>	Tg(ycry-ATTR-mCherry,Hs.C2CD4A-C-hsp70:YFP-ATTR)	Common
<b>C2CD4A</b>	Tg(ycry:ATTR-mCherry,Hs.C2CD4A-T-hsp70:YFP-ATTR)	Rare SNP Variant
<b>ZFAND3</b>	Tg(cry:ATTR-mCherry,Hs.ZFAND3-C-hsp70:YFP-ATTR-GFP)	Common
<b>ZFAND3</b>	Tg(cry:ATTR-mCherry,Hs.ZFAND3-T-hsp70:YFP-ATTR-GFP)	Rare SNP Variant
<b>TCF7L2</b>	Tg(cry:ATTR-mCherry,Hs.TCF7L2-C-tcf7l2:YFP-ATTR)	Common
<b>TCF7L2</b>	Tg(cry:ATTR-mCherry,Hs.TCF7L2-T-tcf7l2:YFP-ATTR)	Rare SNP Variant

**Table 2.1:** F0 generation created via microinjection. Injections comprised 15 ng/μl of high-quality plasmid DNA, 30 ng/μl of CFP mRNA, 15 ng/μl of PhiC31 integrase mRNA, filtered phenol red solution (0,2%) and nuclease-free water up to 10 μl.

### 2.2.1 In-crossing Zebrafish

To determine founders (positive for the transgene) from F0 generation, pairs of zebrafish were in-crossed in 1 litre crossing tanks. The pairs were placed in the crossing tanks post-feeding and left over-night. The tanks contained an in-lay which acted as a guard to inhibit the fish from eating the embryos. Lighting would commence at 8.30am which acts as a breeding trigger. Labels were given to each pair that had laid and the embryos were carefully collected in labelled 60mm petri-dishes by filtering the water from each crossing tank with a net.

Once collected, the embryos were transferred in to medium comprising E3 buffer and 0.5% gentamycin which acts as a fungicide and helps protect the embryos from infection. The embryos were stored in an incubator at 28.5°C. After 18 hours the embryos were transferred in to fresh media containing E3 buffer, 0.5% gentamycin and 5% PTU to remove pigmentation and allow visualisation. To avoid bacterial infection PTU medium was changed daily and dead embryos removed.

### 2.2.2 Screening F1 generation

The constructs contain fluorescent markers which are detectable if the construct has successfully integrated in to the target loci. A Nikon SMZ1500 was used to detect green fluorescence protein (GFP) in the lens in embryos up to 4 days post fertilisation (dpf), after which founding embryos expressed red lens (mCherry). mCherry is 30% of the intensity of

GFP therefore a period of 5dpf is usually needed for a detectable level of mCherry to be achieved.

After pancreas development, expression of TCF7L2 constructs, if successfully integrated, should express GFP in the pancreas. Variation in expression pattern between the common and SNP variant should then be compared. The PROX1 constructs contain GFP that should express in the neurons which develop from 18 somites and is also known to express in the pancreas and liver. Expression patterns for C2CD4A and ZFAND3 have yet to be characterised however differences between the common and SNP variant should still be possible.

Pairs of fish that produced transgenic F1 generation were separated from those that did not and were kept as founders.

The founders were later out-crossed with AB-wild type zebrafish which have a defined genotype. The same method for in-crossing was used to out-cross.

### **2.2.3 F1 generation Image Acquisition**

PTU-treated transgenic embryos were mounted on to 1% agarose in a 96-well plate along with negative embryos that act as a control.

#### **2.2.3.1 Making 1% agarose 96-well plate**

1g Agarose was added to 100ml water and heated until clear. In a 96-well plate, 80µl agarose was added to each well followed by a small amount of 100% ethanol. Agarose solution has high surface tension; by adding ethanol the tension is reduced allowing the agarose to set evenly. A brass template was inserted in to the 96-well plate and the agarose allowed to set. The template created grooves in the agarose producing a channel in which to orient embryos ready for imaging.

### **2.2.3.2 Image Acquisition**

Single embryos were plated in to the 96-well plate and oriented dorsally followed by laterally.

The embryos were imaged using the Scan<sup>^</sup>r microscope using brightfield, YFP and RFP filters.

## **2.3 Whole-mount In Situ Hybridization (WISH)**

WISH utilises a probe containing complementary RNA to localise a specific DNA or RNA tissue, for this project particularly, RNA in the pancreas and neurons in zebrafish embryos.

### **2.3.1 Obtaining transgenic zebrafish embryos**

The previously identified founders were in-crossed using the same method as described in Section 2.1.1. The embryos were collected and stored in fresh media containing E3 buffer and 0.5% gentamycin for the first 18 hours and then transferred in to media containing E3 buffer, 0.5% gentamycin and 5% PTU until they reached 3dpf.

### **2.3.2 Fixation of embryos**

At 3dpf embryos were fixed in 4% paraformaldehyde and left at room temperature for 2 hours then stored at 4°C over night. The embryos were washed twice in 2ml PBS followed by 100% methanol and stored at -20°C until used.

### **2.3.3 Permeabilization of embryos**

The in situ hybridization was performed using the Thisse protocol (Thisse and Thisse., 2008).

Firstly, the embryos must be permeabilized to enable the successful uptake of the probe.

#### **2.3.3.1 Rehydration**

The embryos were stored in 100% methanol at -20°C. 100% methanol was removed and the following washes were performed for 3 minutes:

1 x 75% methanol – 25% PBS

1 x 50% methanol – 50% PBS

1 x 25% methanol – 75% PBS

4 x PBT (PBS with 0.1% tween20)

### 2.3.3.2 *Permeabilization of embryos*

Embryos were digested with 10µg/ml proteinase K (PK) in PBT.

Embryos 24hours in age were digested for 10 minutes whilst embryos 48hours+ were digested for 30 minutes. To inhibit PK, embryos were exposed to 4%PFA-PBS for 20 minutes then washed 5 x 5 minutes in PBT.

### 2.3.3.3 *Prehybridization of embryos*

Hybridization mix (HM) was made as shown in Table 2.2:

**Table 2.2:** Components of Hybridization Mix (50ml)

Reagent	Volume	Final Concentration
Formamide	25.0ml	50% formamide
20xSSC	12.5ml	5xSSC
Heparin 5mg/ml	0.5ml	50µg/ml
tRNA 50mg/ml	0.5ml	500µg/ml
Tween20	50µl	0.1%
Citric Acid 1M	0.46ml	pH6
H <sub>2</sub> O	10.99	

Embryos were incubated in 2ml HM for 2.5hours at 70°C with constant gentle agitation.

### 2.3.3.4 *Hybridization*

The HM used for prehybridization was removed and replaced with 1ml HM containing 30ng antisense DIG labelled RNA (probe).

A nanodrop spectrophotometer was used to measure the background of YFP and mCherry probes prior to hybridization. A blank control of water was used to calibrate the measurements.

The embryos were incubated with the probes at 70°C overnight with constant gentle agitation.

### 2.3.3.5 *Removing antisense DIG labelled RNA probes*

A number of washes were performed in varying concentrations of HM minus tRNA and Heparin at 70°C for 10 minutes;

1 x 75% HM – 25% 2xSSC

1 x 50% HM - 50% 2xSSC

1 x 25% HM – 75% 2xSSC

1 x 2xSSC

The embryos were then washed twice in 0.2xSSC at 70°C for 30 minutes followed by a series of washes at room temperature for 10 minutes;

1 x 75% 0.2xSSC – 25% PBT

1 x 50% 0.2xSSC – 50% PBT

1 x 25% 0.2xSSC – 75% PBT

1 x PBT

#### **2.3.3.6 Incubation with Antibody**

Embryos were pre-incubated with 2mg/ml BSA with 2% sheep serum in PBT for 3 hours before being incubated with 1 in 5000 dilution alkaline phosphatase anti DIG antibody overnight at 4°C with agitation.

#### **2.3.3.7 Removal of unbound Antibody**

The embryos were washed 6 x 15 minutes in PBT at room temperature followed by 3 x 5 minutes in alkaline tris buffer comprising components shown in Table 2.3.

**Table 2.3:** Alkaline Tris Buffer (50ml)

<b>Reagent</b>	<b>Volume</b>	<b>Final Concentration</b>
<b>Tris HCl pH9.5 1M</b>	10ml	100mM
<b>MgCl<sub>2</sub> 1M</b>	5ml	50mM
<b>NaCl 5M</b>	2ml	100mM
<b>Tween20</b>	0.5ml	0.1%
<b>H<sub>2</sub>O</b>	32.5ml	

#### **2.3.3.8 Labelling embryos**

Embryos were transferred in to wells of a 24 well plate and excess alkaline tris buffer was removed. 700µl of labelling mix (comprising 225µl NBT, 50ml Alkaline Tris Buffer, 175µl BCIP) was added to each well. The plate was stored in the dark whilst the reaction occurred and embryonic fluorescence was monitored every 15 minutes for the first 60 minutes followed by every 30 minutes until the reaction was complete.

Once complete, the labelling reaction was inhibited by the removal of the labelling mix and washing 3 x 5 minutes in PBS pH5, EDTA 1mM.

The embryos were stored in glycerol at 4°C until imaged.

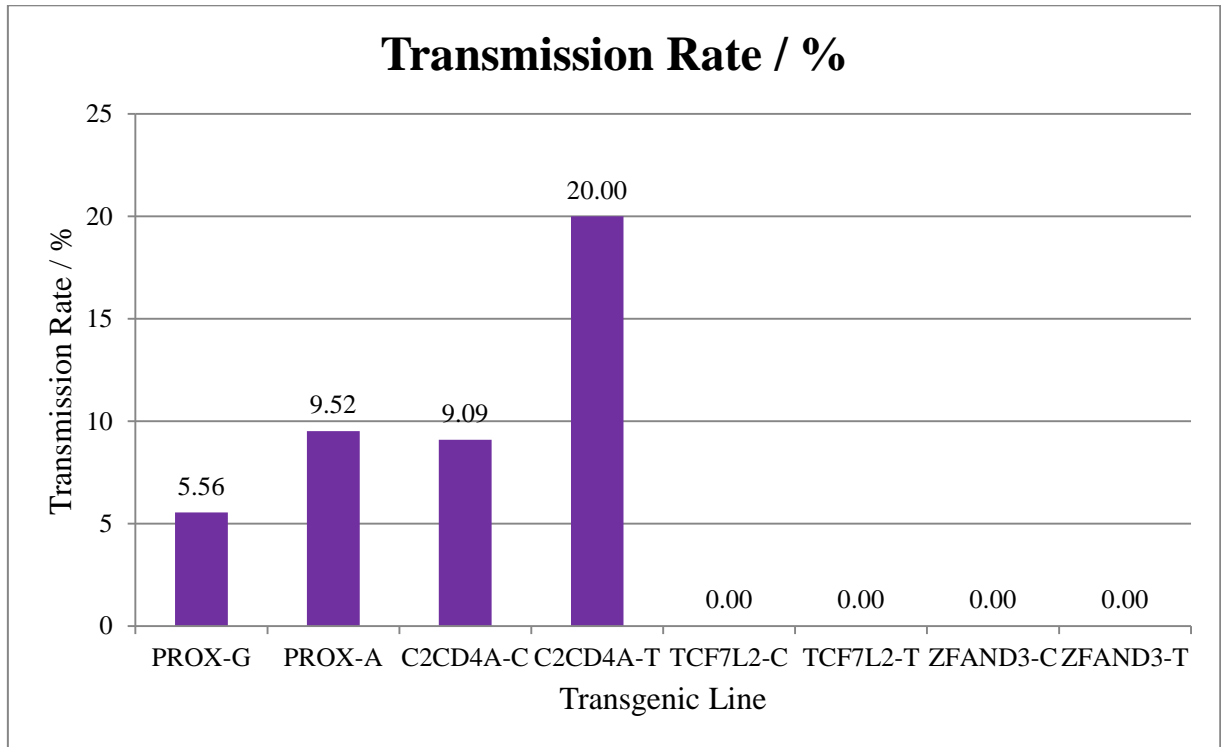
#### **2.3.3.9 Imaging fixed embryos**

Fixed embryos were mounted on to a slide in glycerol and imaged using a Leica TCS LSI zoom confocal microscope. Embryos were imaged in such a way that a view of the liver expression was clear in addition to dorsally and laterally.

### 3. RESULTS

#### 3.1 Identifying Transgenic Fish Founders

**Figure 3.1:** Transmission Rate of In-Crossed Transgenic Fish



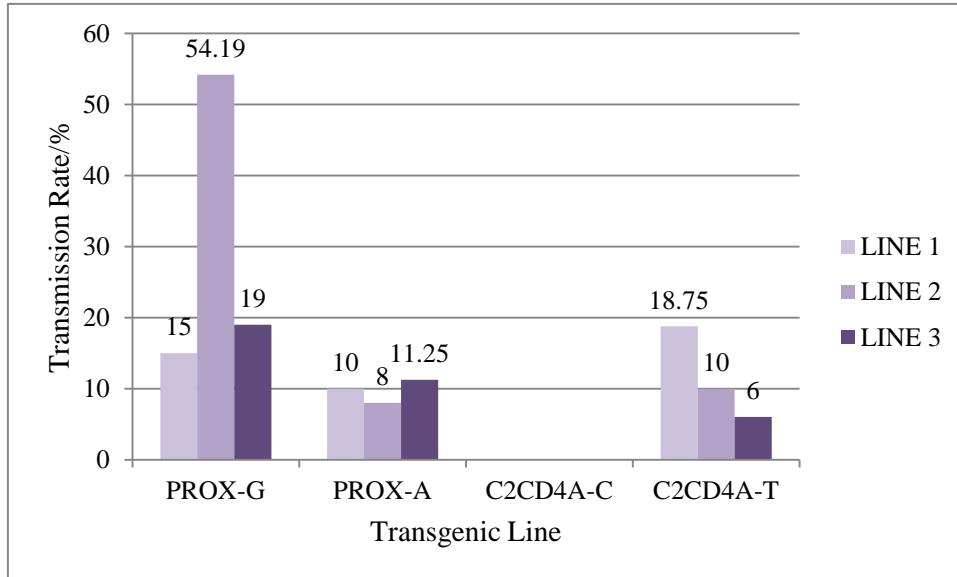
Transmission rate is calculated by the following equation;

$$\left[ \left( \frac{\text{Number of transgenic pairs identified}}{\text{Total number of pairs that laid}} \right) \div 2 \right] \times 100$$

For the PROX-G F0 generation, 3 of 27 in-crossed pairs that laid produced an F1 generation expressing red lens, due to potential for transgenic offspring being caused by a single parent of the pair being transgenic, 3 in 27 translates in to a transmission rate of 5.56%. PROX-A and C2CD4A-C gave similar transmission rates of 9.52% (4/21) and 9.09% (2/11) respectively. C2CD4A-T line showed the highest transmission rate as 20% (8/20) pairs

produced an F1 generation expressing red lens. 0% of TCF7L2-C, TCF7L2-T, ZFAND3-C and ZFAND3-T expressed red lens. Crossing record can be viewed in Appendix AI.1.

**Figure 3.2:** Transmission Rate of Out-Crossed Transgenic Fish



Founding zebrafish (those with F1 generation expressing red lens) were out-crossed with wild-type AB zebrafish to identify the transgenic members of each pair and to elucidate the pattern produced by a single transgenic zebrafish. Of the out-crossed zebrafish, transmission rate of transgenic embryos expressing red lens produced by 3 different fish with-in the same line were compared. To determine transmission rate with-in the line, the following equation was used;

$$\left( \frac{\text{Number of transgenic embryos}}{\text{Total number of embryos laid}} \right) \times 100$$

PROX-G transmission rate with-in the line appears highly variable with a range covering 15-54.19%. PROX-A transmission rate with-in the line stays moderately consistent around 10%.

Transmission rate of C2CD4A-C was not calculated due to time constraints of the project. C2CD4A-T achieves a transmission rate range of 6-18.75%; falling in-line with PROX-A with an average of 10%.

**Figure 3.3:** WISH Analysis of PROX-G and PROX-A embryos at 3dpf

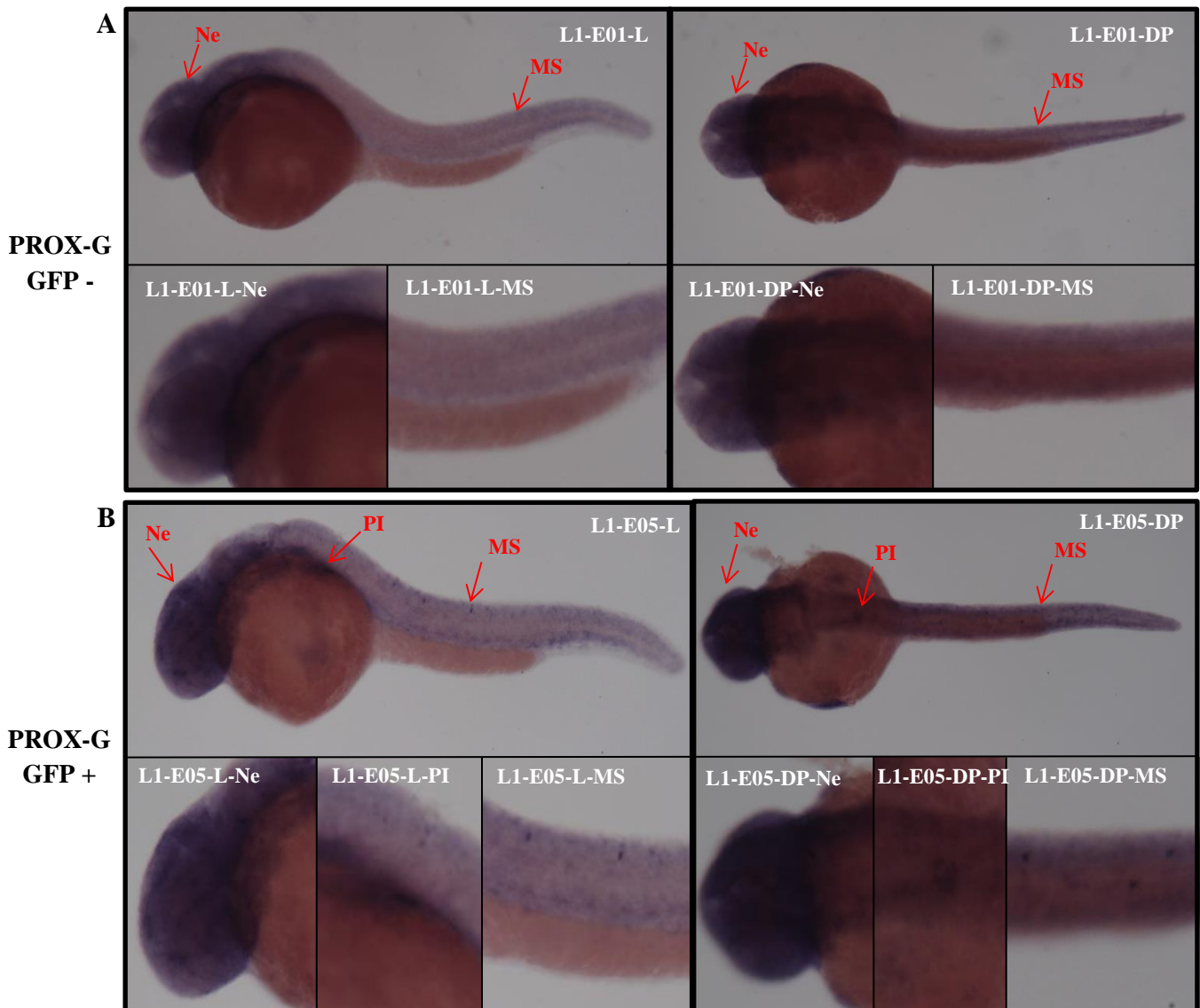


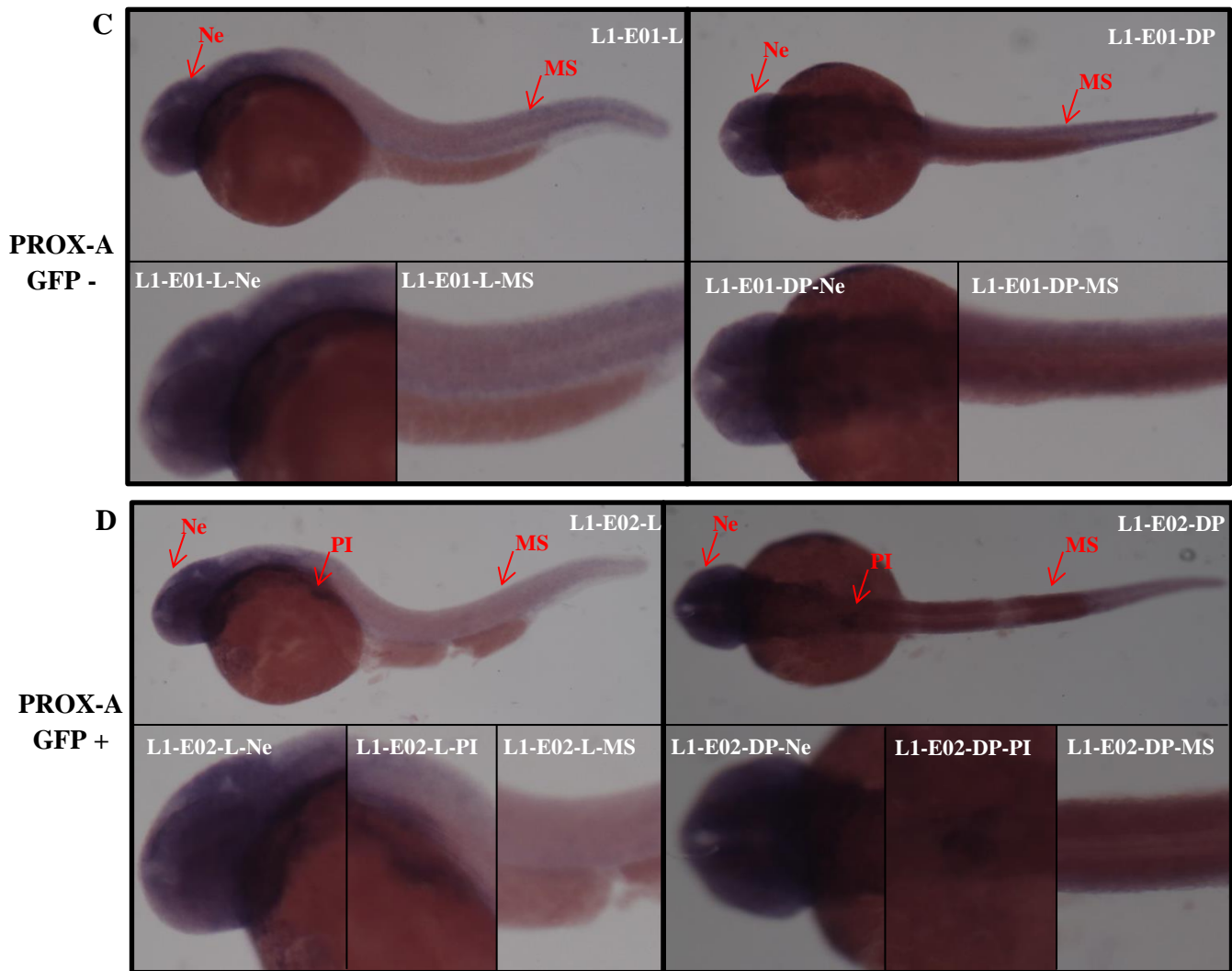
**Figure 3.3: WISH Analysis of PROX-G and PROX-A embryos at 3dpf:** A: Embryo from line containing PROX-G enhancer negative for *PROX* expression B: Embryo from line containing PROX-A enhancer negative for *PROX* expression C: Embryo from line containing PROX-A enhancer positive for *PROX* expression in liver and neurons. Arrows identify areas of interest. All embryos underwent whole-mount in situ hybridization stained with antisense DIG labelled RNA GFP and mCherry probe. Ne = Neuronal expression, Li = Liver expression.

Figure 3.3A shows the in situ results for embryos produced by the founders identified for the PROX-G line. Of 50 embryos, none showed expression through in situ testing, although red lens fluorescence was observed in 9 of the 50 prior to in situ analysis. Absence of PTU in the buffer used to treat embryos from 1dpf lead to pigmentation which made visualisation of mCherry in the lens difficult. Figure 3.3B represents 147/170 embryos laid from 2 founding PROX-A pairs. Similar to the PROX-G result, no expression was observed.

Figure 3.3C represents the remaining 23 embryos produced by PROX-A founders. These showed GFP expression in the liver and ubiquitous neuronal staining can also be observed.

**Figure 3.4:** WISH Analysis of PROX-G and PROX-A embryos at 30hpf





**Figure 3.4: Whole-mount in situ hybridization results. A:** PROX-G line 1 embryo 1 negative for GFP expression in pancreatic islet. **B:** PROX-G line 1 embryo 5 positive for GFP expression in pancreatic islet. **C:** PROX-A (SNP variant) line 1 embryo 1 negative for GFP expression in pancreatic islet. **D:** PROX-A (SNP variant) line 1 embryo 2 positive for GFP expression in pancreatic islet. Ne = Neuronal expression, MS = Mucous Secreting Cell, PI = Pancreatic Islet. L = lateral, DP = dorsal posterior. All embryos 30hpf.

Figure 3.4A shows the in situ results for embryos negative for pancreatic islet expression produced by out-crossed founders identified for the PROX-G line at 30hpf. Of 120 embryos, 67 showed no pancreatic islet expression through in situ testing. Figure 3.4B represents the remaining 54 embryos from the out-crossed PROX-G. These embryos showed pancreatic islet expression in addition to broad neuronal pattern and mucous secreting cells. Figure 3.4C and D show the same results respectively for the PROX-A line, representing 72/81 and 9/81.

**Figure 3.5:** Fluorescent Expression of PROX-G and PROX-A lines at 25hpf

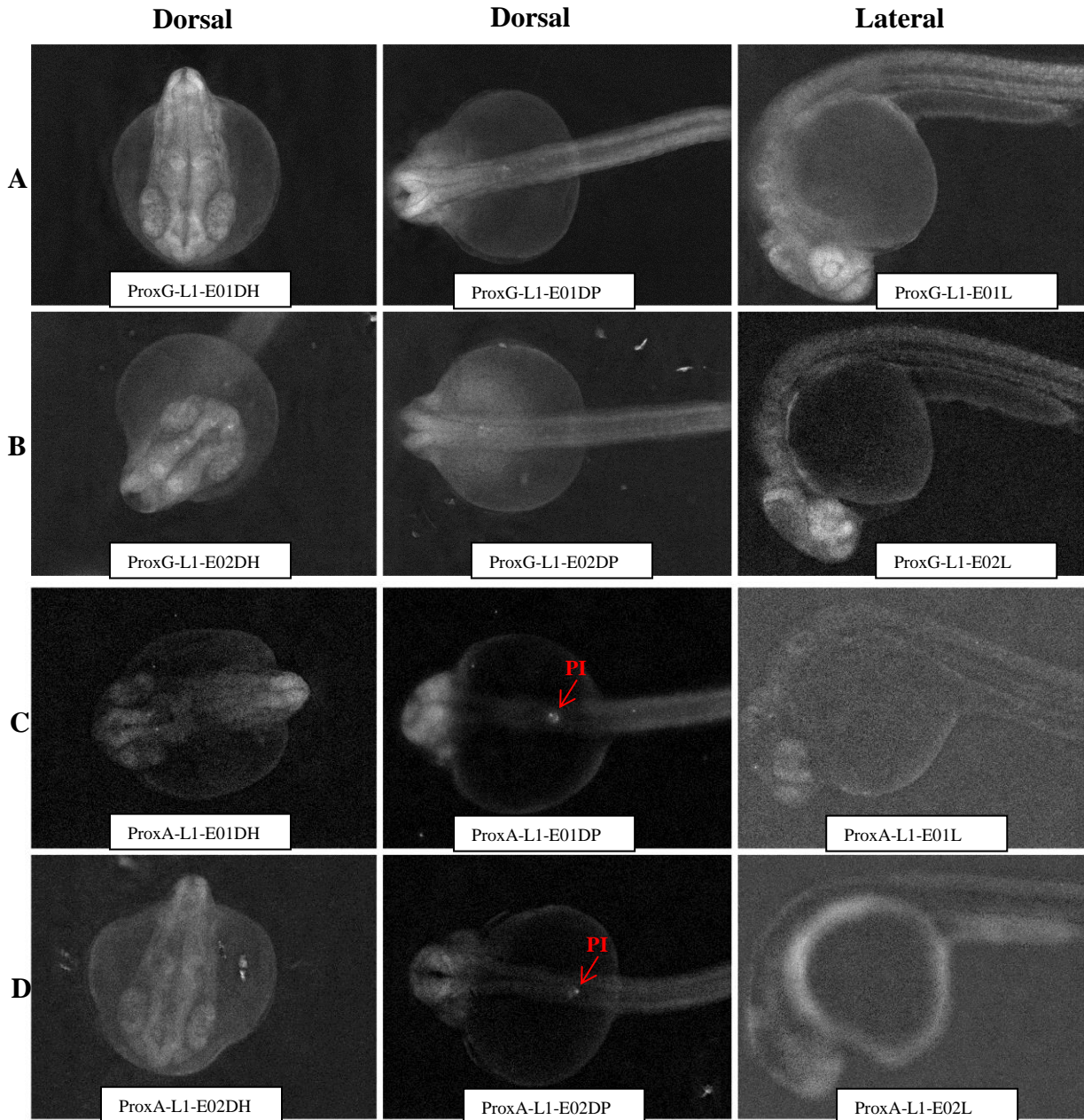


**Figure 3.5:** A and B represent GFP expression of PROX-G (common) line at 25hpf. C and D represent GFP expression of PROX-A (SNP variant) line at 25hpf. First image positioned dorsally. Second image positioned dorsally posterior to the left. Third image positioned laterally to the left. Image 6x magnification using Scan<sup>R</sup>. PI = Pancreatic Islet.

Pancreatic islet can be visualised by fluorescence microscopy in positive PROX-A embryos at 25hpf. Positive PROX-G embryos do not show pancreatic islet expression at this stage. Broad neuronal fluorescence can be seen in both PROX-G and PROX-A lines. High levels of background can also be observed.

**Figure 3.6:** Fluorescent Expression of PROX-G and PROX-A lines at 48hpf

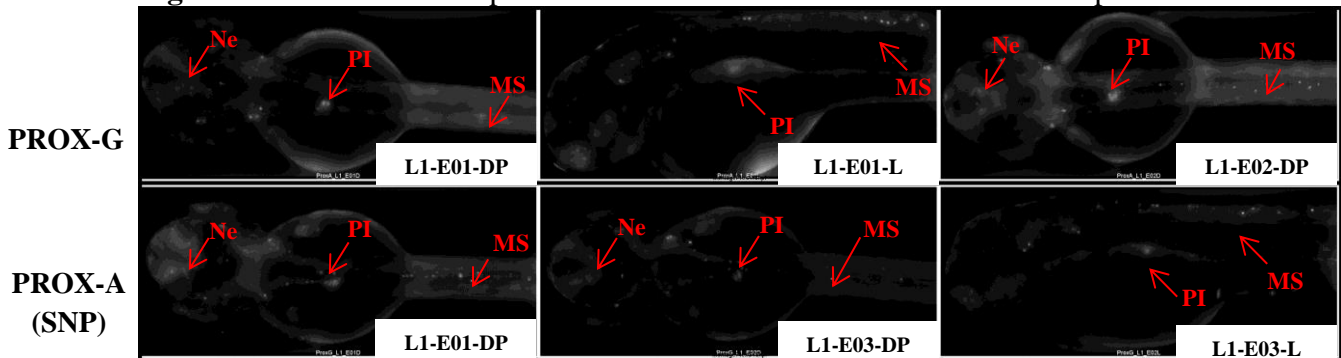


**Figure 3.6:** A: GFP expression of positive PROX-G (common) line at 48hpf. First image embryo 1 from Line 1 positioned dorsally anterior to the left. Second image embryo 1 from Line 1 positioned laterally anterior to the left. Third image embryo 2 from Line1 positioned dorsally anterior to the left. B represents GFP expression of positive PROX-A (SNP variant) line at 48hpf. . First image embryo 1 from Line 1 positioned dorsally anterior to the left. Second image embryo 3 from Line 1 positioned dorsally anterior to the left. Third image embryo 3 from Line1 positioned laterally anterior to the left. Image 6x magnification using Scan<sup>R</sup>. PI = Pancreatic Islet, Ne = Neuronal expression, MS = Mucous Secreting Cells.

Pancreatic islet can clearly be identified in both PROX-G and PROX-A lines, although appears slightly stronger in PROX-A embryos, see arrows labelled PI. A scattered pattern of mucous secreting cells can be observed in addition to broad neuronal expression in both lines (labelled MS and Ne). High levels of background can be observed. For further images of positive and negative embryos for both lines see Appendix AI.2.

**Figure 3.7:** Fluorescent Expression of PROX-G and PROX-A lines at 72hpf

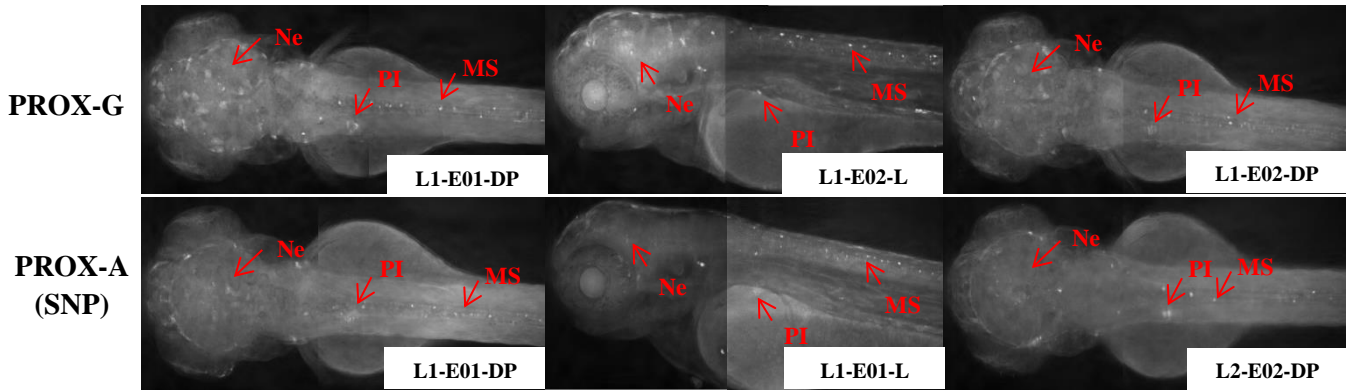


**Figure 3.7:** A: YFP expression of positive PROX-G (common) line at 72hpf. First image embryo 1 from Line 1 positioned dorsally posterior to the left. Second image embryo 2 from Line 1 positioned laterally anterior to the left. Third image embryo 2 from Line 1 positioned dorsally anterior to the left. B represents YFP expression of positive PROX-A (SNP variant) line at 72hpf. . First image embryo 1 from Line 1 positioned dorsally posterior to the left. Second image embryo 1 from Line 1 positioned laterally. Third image embryo 2 from Line 2 positioned dorsally posterior to the left. Image 6x magnification using Scan<sup>R</sup>. PI = Pancreatic Islet, Ne = Neuronal expression, MS = Mucous Secreting Cells.

Pancreatic islet can clearly be identified in both PROX-G and PROX-A lines, although appears slightly stronger in PROX-A embryos. A scattered pattern of mucous secreting cells can be observed in addition to broad neuronal expression in both lines. High levels of background can be observed. For further images of positive and negative embryos for both lines see Appendix AI.3.

## **4. DISCUSSION**

### **4.1 PhiC31 integrase facilitates targeted integration in Zebrafish model**

Of the PROX-G and PROX-A F1 generation analysed, all those identified as expressing GFP in pancreatic islet, neurons and mucous secreting cells also expressed red lens. No embryos were found to express red lens or GFP pattern independent of each other therefore indicative of successful targeted integration mediated by PhiC31 integrase.

Average transmission rate falls between 10-20% as shown by Figures 3.1 and 3.2 which is comparable to the most commonly used mediator of integration, Tol2 transposon; which achieves an average transmission rate between 15-20% (Clark et al., 2011). However, Tol2 mediated transgenesis often causes position effects due to allowing random integration in to the genome. In animal model, such as zebrafish, exogenous genes are often randomly integrated in chromatin. In the circumstance that gene constructs do not fulfil requirements for truthful gene locus activation, the result is variable expression levels and alterations in temporal and spatial expression patterns, known collectively as genomic position effect (Bonifer et al., 1996).

The apparent ability of PhiC31 integrase to overcome position effect whilst maintaining a comparable transmission rate makes it a preferential integration mediator to Tol2.

### **4.2 Potential differences observed between PROX-G and PROX-A lines**

Analysis via fluorescence microscopy and whole mount in situ hybridization did not show any clear significant differences between common PROX-G line and SNP variant PROX-A line in pancreatic islet, neuronal or mucous secreting cell expression, however, some slight

differences in timing of pancreatic islet expression observed hold promise for future elucidation.

The founding zebrafish identified by initial in-crossing were out-crossed with wild-type AB zebrafish which have a defined genotype in order to eliminate potential interference in expression pattern in embryos.

The neuronal expression observed in the head of the embryo is broad and mosaic making it difficult to identify if a pattern is present. Fluorescence analysis at 72hpf in PROX-G embryos showed neuronal expression more strongly when compared to PROX-A embryos of the same developmental stage, see Figure 3.7. However, due to time constraints of the project it remains unclear if these are a particular group of neurons with a specific function or if they cross multiple groups and obligate many functions. Without knowing the function of these neurons that are expressed it cannot be concluded if the difference observed between the common and SNP variant lines is of significant value.

Furthermore, the staining apparent along the spinal cord of the embryos is inconsistent and patchy (Figure 3.7), unlike normal neuronal expression patterns. Under further analysis, it is believed that this expression is of mucous secreting cells as identified by Thisse *et al* (2001). Mucous secreting cells are expressed differently by each individual zebrafish therefore making the variation in the spinal cord expression null for the purpose of this research.

Fluorescence microscopy of embryos at 25hpf (hours post fertilisation) (Figure 3.5) showed a potential difference in the timing of pancreatic islet development between PROX-G and PROX-A lines. At this stage in development, pancreatic islet was visible by fluorescence microscopy in PROX-A embryos but not visible in PROX-G lines, therefore it may be

plausible that the disease associated SNP variant causes an alteration in pancreas development. By 30hpf in situ analysis identified pancreatic islet in both lines.

To elucidate any alterations in development of the pancreatic islet, it would be beneficial to monitor expression over time. By identifying the average stage at which the islet is visible via fluorescence for both lines, it would be possible to identify how accelerated development is as a result of the SNP variant. Although the initial aim of the study was to identify differing patterns between the lines, it may be that it is not difference in spatial expression, but actually the difference in temporal expression that causes T2D susceptibility associated with the SNP.

#### **4.3 C2CD4A enhancers may be too weak to drive the *hsp70* promoter**

Both C2CD4A-C and CDCD4A-T lines produced F1 generation expressing red lens but no other expression was observed. The common C2CD4A-C line achieved a transmission rate 9.09% (2/11 pairs produced transgenic embryos) whilst C2CD4A-T achieved a rate of 20% (8/20 pairs produced transgenic embryos). Further elucidation of C2CD4A-T founders identified a range of 6-18% transmission rate across 2 lines. The design of the constructs allows gamma crystalline ( $\gamma$ -Cry) to drive expression of mCherry whilst downstream the putative enhancer acts on the promoter to drive gene expression (Figure 1.3A). The construct must be successfully integrated for expression to occur therefore mCherry expression in the lens identifies that integration has been accomplished. The observed lack of GFP/YFP expression suggests that the enhancers, which comprise a cluster of transcription factor binding sites, fail to attract transcription factors to the promoter to a high enough level resulting in failed transcription and therefore lack of gene expression.

Alternatively, GFP/YFP expression may be so low that it cannot be detected by the low sensitivity of fluorescence imaging. Whole-mount In Situ Hybridization (WISH) analysis

presents a solution to this issue. Embryos fixed at the developmental stage of interest can be exposed to a probe containing complementary RNA to localise specific RNA in pancreatic islet and neurons. WISH provides a more sensitive method for enhancer activity and so provides an alternative method of analysis for zebrafish with weak enhancer driven expression.

#### **4.4 ZFAND3 and TCF7L2 lines did not produce transgenic F1 generation**

Of the 18 and 13 pairs that laid for ZFAND3-C (Z.C) and ZFAND3-T (Z.T) respectively, no transgenic embryos were produced. With 10-20% transmission rate appearing for other lines, at least 1 transgenic pair from each line was expected, or alternatively an approximate expectation of 170 and 100 transgenic embryos for the corresponding 1720 (Z.C) and 1060 (Z.T) embryos screened.

For TCF7L2 lines, lower numbers of embryos were screened. In total, 13 pairs laid from the TCF7L2 lines (6 and 7 for TCF7L2-C and TCF7L2-T respectively) therefore it would be expected that at least one of the pairs would produce transgenic F1 generation. A total of 870 embryos (450 and 420 for TCF7L2-C and TCF7L2-T respectively) would result in an expected 80 transgenic embryos to have been observed.

A reason for failed expression may be due to single-copy integration at the docking site. A single copy integration site, namely Xla.crygc:attP-GFP, was specifically achieved for the recipient transgenic lines so that a stable, reproducible and single standardized landing site was attained. The lab identified a line (uobL6) that contained a single copy of this integration site therefore uobL6 was chosen for the creation of the enhancer-containing lines used throughout this project. Additionally, the enhancers may not work in the genomic context of uobL6. To overcome these issues the multi-copy line designated uobL12 could be used.

Southern blot analysis of uobL12 performed by Irene Miguel-Escalada identified integration of the desired transgene (Xla.crygc:attP-GFP integration site) with an approximate copy number of 11.6.

Alternatively, a technical problem at the establishment of transgenesis may otherwise be the cause for the apparent negative result for this line. However, as all other variables remain consistent and only the enhancer sequence differs between all of the lines created; there is no obvious technical cause for lesser efficiency of targeted recombination.

Finally, considering the low number of zebrafish screened for TCF7L2 lines, it may be possible that negative selection has occurred and so by chance only non-transgenic zebrafish have been crossed, thus in the event of more zebrafish being screened transgenic founders may be identified.

#### **4.5 Time-constraints hindered project progression**

As is the nature of working with animals, some activity is unpredictable. With this project it was not always possible to obtain embryos when crosses were set-up. In the process of identifying founders, as many crosses as possible were set up, however on average only 50% of the pairs produced embryos. For example, 55 pairs of PROX-G were in-crossed with only 27 producing embryos. Of those 27 pairs, only 3 zebrafish have been identified as transgenic (positive for red lens and pancreatic islet expression). For PROX-A, 44 pairs were in-crossed and only 21 pairs laid, resulting in 4 transgenic zebrafish being recognized. The PROX lines were the most mature of the F0 generation transgenic lines and so these zebrafish were crossed first; they showed high fecundity and as a result achieved the highest level of screening.

A summary of the other lines laying record is as follows; C2CD4A-C line had a total of 22 pairs set-up with only 11 producing embryos. Of these 11 pairs, 2 transgenic zebrafish have been identified. C2CD4A-T line had a total of 33 pairs set-up with 20 producing embryos. Of these 20 pairs, 8 zebrafish have been identified as transgenic. ZFAND3-C had 18/26 pairs produce embryos and ZFAND3-T 13/21 with no transgenic zebrafish positive for red lens expression identified. Finally, 6/23 and 7/12 pairs laid for TCF7L2-C and TCF7L2-T respectively again resulting in no transgenic zebrafish positive for red lens expression, see crossing record in Appendix AI.1 for further details.

With only 50% of crosses set up producing embryos, it leaves many zebrafish unscreened. In addition to this, due to the sheer number of F0 generation it was not possible to cross all of the available zebrafish for each line therefore opportunity for identifying transgenic zebrafish has been missed.

Moreover, once the zebrafish have been crossed, they are kept in breeding tanks for up to 5 days until embryos have been screened for red lens. Once the transgenic F1 generation has been identified, the founding zebrafish were separated from the negative zebrafish ready to be out-crossed with wild-type AB. Having been recently crossed and kept in a 1 litre breeding tank for 5 days, the zebrafish take 7 days to recover and therefore cannot be crossed again in this time, resulting in a week-long delay before out-crossing can begin. Once again, when out-crossed there is no guarantee that all of the zebrafish will lay and therefore to obtain a minimum of 3 transgenic lines for each construct to be compared via fluorescence microscopy is extremely time consuming and success is unpredictable.

The difficulties and delays in obtaining embryos for positively identified transgenic zebrafish for each line resulted in insufficient numbers obtained and time available for the attempt to

quantify potential difference between PROX-G and PROX-A variant activity in WISH or fluorescence data. A minimum of 3 lines (3 transgenic zebrafish) for each variant is required for comparison to detect the degree of variation of activity between lines of the same construct versus variation between lines with different constructs.

#### **4.6 Outstanding Aims**

It would be beneficial to screen the remaining un-crossed zebrafish for each F0 transgenic line in order to fully elucidate transgenic potential. Further identification of transgenic zebrafish positive for red lens for PROX and C2CD4A lines will provide a solid platform for the identification of any potential differences in spatial and temporal expression that may occur between the common and SNP variant lines.

Furthermore, complete screening of TCF7L2 lines will eliminate the possibility of negative selection and identify if integration has been successful or unsuccessful. If successful, analysis of spatial and temporal differences can be obtained as with PROX and C2CD4A lines. If integration is found to be unsuccessful, it may be possible to use multi-copy line uobL12 as opposed to single-copy uobL6 to create transgenic lines for TCF7L2 and ZFAND3.

Potential differences in temporal expression can be observed in pancreatic islet at 25hpf, see Figure 3.5. Visual analysis identifies expression of pancreatic islet in PROX-A (SNP variant) embryos but not in PROX-G (common) embryos. This difference at such an early stage in development suggests the SNP may cause alteration in the timing of pancreas development, which in turn may be linked to T2D susceptibility and progression associated with the SNP. A

time-course of fluorescence images should be captured in order to identify the developmental stage that pancreatic islet develops in both PROX-G and PROX-A lines to determine the magnitude of change in temporal expression appearing to be caused by the T2D-associated SNP. A minimum of 3 replicates would be required to support reliability of timing results.

Similarly, potential differences in intensity of expression can be observed in pancreatic islet at 72hpf (see Figure 3.7), whereby intensity of pancreatic islet expression in PROX-A lines appear comparatively stronger than in PROX-G lines. To quantify this difference, it would be possible to perform densitometry analysis on fluorescence images using ImageJ software. As a control, the same analysis could be performed on embryos negative for pancreatic islet expression. The results of densitometry would give a numeric value for controls that are negative for pancreatic islet expression therefore providing a result for 'background', whilst providing numeric value for expression in positive embryos. These numeric values can be used to quantify the magnitude of difference between pancreatic islet expression in both common and SNP lines. Again, a minimum of 3 replicates (from 3 founding zebrafish) would be needed to ensure magnitude of change is representative of the entire transgenic line as opposed to singularly representative of that embryo or founding zebrafish.

An observable change in expression patterns between the PROX common and SNP variant lines is not obvious from the experiments undertaken within this project to date. However, at 72hpf, fluorescence imaging identified a slightly more defined neuronal pattern in PROX-G embryos. Due to the difficulty in getting zebrafish to lay and the time it takes to image the embryos, only embryos from one pair of PROX-G zebrafish positive for red lens were imaged, therefore it is not conclusive if the neuronal expression is singular to the founding zebrafish that laid or if it is representative of the PROX-G line.

## 5. CONCLUSION

The use of zebrafish as an *in vivo* validation tool for putative enhancers remains unconfirmed but provides promising results thus far. Enhancer elements in the PROX lines clearly drive expression in pancreatic islet, neurons and mucous secreting cells. Although no discerning pattern between common and SNP variant lines has been observed in this project, it may not be spatial expression that is altered but perhaps alterations to temporal activity as indicated by the noticeable difference of pancreatic islet expression by fluorescence microscopy at 25hpf. It appears as though GFP is expressed in the pancreatic islet by the SNP variant line, PROX-A, whilst is much weaker in the common PROX-G line at 25hpf. By 48hpf, both lines express pancreatic islet, however expression appears slightly stronger in PROX-A embryos, followed at 72hpf by a similar pattern. Elucidation of this difference in expression could be achieved by monitoring reporter expression over time.

Time constraints prevented the complete screening of all lines therefore transgenic zebrafish are likely to have been missed. This task should be completed in order to identify all transgenic zebrafish for PROX and C2CD4A lines, as well as any eventual ZFAND3 or TCF7L2 transgenic zebrafish.

## REFERENCES

### Scientific Journal

- AKHTAR-ZAIDI, B., LARI, R. C. S., CORRADIN, O., SAIAKHOVA, A., BARTELS, C. F., BALASUBRAMANIAN, D., MYEROFF, L., LUTTERBAUGH, J., JARRAR, A., KALADY, M. F., WILLIS, J., MOORE, J. H., TESAR, P. J., LAFRAMBOISE, T., MARKOWITZ, S., LUPIEN, M. & SCACHERI, P. C. 2012. Epigenomic Enhancer Profiling Defines a Signature of Colon Cancer. *Science*, 336, 736-739.
- BONIFER, C., HUBER, M. C., JAGLE, U., FAUST, N. & SIPPEL, A. E. 1996. Prerequisites for tissue specific and position independent expression of a gene locus in transgenic mice. *Journal of Molecular Medicine-Imm*, 74, 663-671.
- CHO, Y. S., CHEN, C. H., HU, C., LONG, J. R., ONG, R. T. H., SIM, X. L., TAKEUCHI, F., WU, Y., GO, M. J., YAMAUCHI, T., CHANG, Y. C., KWAK, S. H., MA, R. C. W., YAMAMOTO, K., ADAIR, L. S., AUNG, T., CAI, Q. Y., CHANG, L. C., CHEN, Y. T., GAO, Y. T., HU, F. B., KIM, H. L., KIM, S., KIM, Y. J., LEE, J. J. M., LEE, N. R., LI, Y., LIU, J. J., LU, W., NAKAMURA, J., NAKASHIMA, E., NG, D. P. K., TAY, W. T., TSAI, F. J., WONG, T. Y., YOKOTA, M., ZHENG, W., ZHANG, R., WANG, C., SO, W. Y., OHNAKA, K., IKEGAMI, H., HARA, K., CHO, Y. M., CHO, N. H., CHANG, T. J., BAO, Y., HEDMAN, A. K., MORRIS, A. P., MCCARTHY, M. I., TAKAYANAGI, R., PARK, K. S., JIA, W. P., CHUANG, L. M., CHAN, J. C. N., MAEDA, S., KADOWAKI, T., LEE, J. Y., WU, J. Y., TEO, Y. Y., TAI, E. S., SHU, X. O., MOHLKE, K. L., KATO, N., HAN, B. G., SEIELSTAD, M., CONSORTIUM, D. & MU, T. C. 2012. Meta-analysis of genome-wide association studies identifies eight new loci for type 2 diabetes in east Asians. *Nature Genetics*, 44, 67-U97.
- CLARK, K. J., URBAN, M. D., SKUSTER, K. J. & EKKER, S. C. 2011. Transgenic Zebrafish Using Transposable Elements. *In: DETRICH, H. W., WESTERFIELD, M. & ZON, L. I. (eds.) Zebrafish: Genetics, Genomics and Informatics, 3rd Edition.*
- CORRADIN, O., SAIAKHOVA, A., AKHTAR-ZAIDI, B., MYEROFF, L., WILLIS, J., LARI, R. C. S., LUPIEN, M., MARKOWITZ, S. & SCACHERI, P. C. 2014. Combinatorial effects of multiple enhancer variants in linkage disequilibrium dictate levels of gene expression to confer susceptibility to common traits. *Genome Research*, 24, 1-13.
- CUI, B., ZHU, X. L., XU, M., GUO, T., ZHU, D. L., CHEN, G., LI, X. J., XU, L. Y., BI, Y. F., CHEN, Y. H., XU, Y., LI, X. Y., WANG, W. Q., WANG, H. F., HUANG, W. & NING, G. 2011. A Genome-Wide Association Study Confirms Previously Reported Loci for Type 2 Diabetes in Han Chinese. *Plos One*, 6(7).
- DEATON, A. M. & BIRD, A. 2011. CpG islands and the regulation of transcription. *Genes & Development*, 25, 1010-1022.
- DOOLEY, K. & ZON, L. I. 2000. Zebrafish: a model system for the study of human disease. *Current Opinion in Genetics & Development*, 10, 252-256.
- EPSTEIN, D. J. 2009. Cis-regulatory mutations in human disease. *Briefings in functional genomics & proteomics*, 8, 310-6.
- ERNST, J., KHERADPOUR, P., MIKKELSEN, T. S., SHORESH, N., WARD, L. D., EPSTEIN, C. B., ZHANG, X. L., WANG, L., ISSNER, R., COYNE, M., KU, M. C.,

- DURHAM, T., KELLIS, M. & BERNSTEIN, B. E. 2011. Mapping and analysis of chromatin state dynamics in nine human cell types. *Nature*, 473, 43-U52.
- FLOREZ, J. C., JABLONSKI, K. A., BAYLEY, N., POLLIN, T. I., DE BAKKER, P. I. W., SHULDINER, A. R., KNOWLER, W. C., NATHAN, D. M., ALTSHULER, D. & DIABET PREVENTION PROGRAM RES, G. 2006. TCF7L2 polymorphisms and progression to diabetes in the Diabetes Prevention Program. *New England Journal of Medicine*, 355, 241-250.
- FREEMAN, H. & COX, R. D. 2006. Type-2 diabetes: a cocktail of genetic discovery. *Human Molecular Genetics*, 15, R202-R209.
- FUJITA, H., HARA, K., SHOJIMA, N., HORIKOSHI, M., IWATA, M., HIROTA, Y., TOBE, K., SEINO, S. & KADOWAKI, T. 2012. Variations with modest effects have an important role in the genetic background of type 2 diabetes and diabetes-related traits. *Journal of Human Genetics*, 57, 776-779.
- GAULTON, K. J., NAMMO, T., PASQUALI, L., SIMON, J. M., GIRESI, P. G., FOGARTY, M. P., PANHUIS, T. M., MIECZKOWSKI, P., SECCHI, A., BOSCO, D., BERNEY, T., MONTANYA, E., MOHLKE, K. L., LIEB, J. D. & FERRER, J. 2010. A map of open chromatin in human pancreatic islets. *Nature Genetics*, 42, 255-U41.
- GRARUP, N., OVERVAD, M., SPARSO, T., WITTE, D. R., PISINGER, C., JORGENSEN, T., YAMAUCHI, T., HARA, K., MAEDA, S., KADOWAKI, T., HANSEN, T. & PEDERSEN, O. 2011. The diabetogenic VPS13C/C2CD4A/C2CD4B rs7172432 variant impairs glucose-stimulated insulin response in 5,722 non-diabetic Danish individuals. *Diabetologia*, 54, 789-794.
- GROVES, C. J., ZEGGINI, E., MINTON, J., FRAYLING, T. M., WEEDON, M. N., RAYNER, N. W., HITMAN, G. A., WALKER, M., WILTSHIRE, S., HATTERSLEY, A. T. & MCCARTHY, M. I. 2006. Association analysis of 6,736 UK subjects provides replication and confirms TCF7L2 as a type 2 diabetes susceptibility gene with a substantial effect on individual risk. *Diabetes*, 55, 2640-2644.
- HAMLET, M. R. J., YERGEAU, D. A., KULIYEV, E., TAKEDA, M., TAIRA, M., KAWAKAMI, K. & MEAD, P. E. 2006. Tol2 transposon-mediated transgenesis in *Xenopus tropicalis*. *Genesis*, 44, 438-445.
- HOWE, K., CLARK, M. D., TORROJA, C. F., TORRANCE, J., BERTHELOT, C., MUFFATO, M., COLLINS, J. E., HUMPHRAY, S., MCLAREN, K., MATTHEWS, L., MCLAREN, S., SEALY, I., CACCAMO, M., CHURCHER, C., SCOTT, C., BARRETT, J. C., KOCH, R., RAUCH, G. J., WHITE, S., CHOW, W., KILIAN, B., QUINTAIS, L. T., GUERRA-ASSUNCAO, J. A., ZHOU, Y., GU, Y., YEN, J., VOGEL, J. H., EYRE, T., REDMOND, S., BANERJEE, R., CHI, J. X., FU, B. Y., LANGLEY, E., MAGUIRE, S. F., LAIRD, G. K., LLOYD, D., KENYON, E., DONALDSON, S., SEHRA, H., ALMEIDA-KING, J., LOVELAND, J., TREVANION, S., JONES, M., QUAIL, M., WILLEY, D., HUNT, A., BURTON, J., SIMS, S., MCLAY, K., PLUMB, B., DAVIS, J., CLEE, C., OLIVER, K., CLARK, R., RIDDLE, C., ELIOTT, D., THREADGOLD, G., HARDEN, G., WARE, D., MORTIMER, B., KERRY, G., HEATH, P., PHILLIMORE, B., TRACEY, A., CORBY, N., DUNN, M., JOHNSON, C., WOOD, J., CLARK, S., PELAN, S., GRIFFITHS, G., SMITH, M., GLITHERO, R., HOWDEN, P., BARKER, N., STEVENS, C., HARLEY, J., HOLT, K., PANAGIOTIDIS, G., LOVELL, J., BEASLEY, H., HENDERSON, C., GORDON, D., AUGER, K., WRIGHT, D., COLLINS, J., RAISEN, C., DYER, L., LEUNG, K., ROBERTSON, L., AMBRIDGE, K., LEONGAMORNLETT, D., MCGUIRE, S., GILDERTHORP, R., GRIFFITHS,

- C., MANTHRAVADI, D., NICHOL, S., BARKER, G., WHITEHEAD, S., KAY, M., et al. 2013. The zebrafish reference genome sequence and its relationship to the human genome. *Nature*, 496, 498-503.
- HU, C., ZHANG, R., WANG, C. R., WANG, J., MA, X. J., HOU, X. H., LU, J. Y., YU, W. H., JIANG, F., BAO, Y. Q., XIANG, K. S. & JIA, W. P. 2010. Variants from GIPR, TCF7L2, DGKB, MADD, CRY2, GLIS3, PROX1, SLC30A8 and IGF1 Are Associated with Glucose Metabolism in the Chinese. *Plos One*, 5(11).
- IWATA, M., MAEDA, S., KAMURA, Y., TAKANO, A., KATO, H., MURAKAMI, S., HIGUCHI, K., TAKAHASHI, A., FUJITA, H., HARA, K., KADOWAKI, T. & TOBE, K. 2012. Genetic Risk Score Constructed Using 14 Susceptibility Alleles for Type 2 Diabetes Is Associated With the Early Onset of Diabetes and May Predict the Future Requirement of Insulin Injections Among Japanese Individuals. *Diabetes Care*, 35, 1763-1770.
- KVON, E. Z., KAZMAR, T., STAMPFEL, G., YANEZ-CUNA, J. O., PAGANI, M., SCHERNHUBER, K., DICKSON, B. J. & STARK, A. 2014. Genome-scale functional characterization of Drosophila developmental enhancers in vivo. *Nature*, 512, 91-5.
- LETTICE, L. A., HEANEY, S. J. H., PURDIE, L. A., LI, L., DE BEER, P., OOSTRA, B. A., GOODE, D., ELGAR, G., HILL, R. E. & DE GRAAFF, E. 2003. A long-range Shh enhancer regulates expression in the developing limb and fin and is associated with preaxial polydactyly. *Human Molecular Genetics*, 12, 1725-1735.
- LYSSENKO, V. & LAAKSO, M. 2013. Genetic Screening for the Risk of Type 2 Diabetes Worthless or valuable? *Diabetes Care*, 36, S120-S126.
- LYSSENKO, V., LUPI, R., MARCHETTI, P., DEL GUERRA, S., ORHO-MELANDER, M., ALMGREN, P., SJOGREN, M., LING, C., ERIKSSON, K. F., LETHAGEN, A. L., MANCARELLA, R., BERGLUND, G., TUOMI, T., NILSSON, P., DEL PRATO, S. & GROOP, L. 2007. Mechanisms by which common variants in the TCF7L2 gene increase risk of type 2 diabetes. *Journal of Clinical Investigation*, 117, 2155-2163.
- MASTON, G. A., EVANS, S. K. & GREEN, M. R. 2006. Transcriptional regulatory elements in the human genome. *Annual Review of Genomics and Human Genetics*. Palo Alto: Annual Reviews.
- MAURANO, M. T., HUMBERT, R., RYNES, E., THURMAN, R. E., HAUGEN, E., WANG, H., REYNOLDS, A. P., SANDSTROM, R., QU, H. Z., BRODY, J., SHAFER, A., NERI, F., LEE, K., KUTYAVIN, T., STEHLING-SUN, S., JOHNSON, A. K., CANFIELD, T. K., GISTE, E., DIEGEL, M., BATES, D., HANSEN, R. S., NEPH, S., SABO, P. J., HEIMFELD, S., RAUBITSCHKE, A., ZIEGLER, S., COTSAPAS, C., SOTOODEHNIA, N., GLASS, I., SUNYAEV, S. R., KAUL, R. & STAMATOYANNOPOULOS, J. A. 2012. Systematic Localization of Common Disease-Associated Variation in Regulatory DNA. *Science*, 337, 1190-1195.
- MILLER, D. M., THOMAS, S. D., ISLAM, A., MUENCH, D. & SEDORIS, K. 2012. c-Myc and Cancer Metabolism. *Clinical Cancer Research*, 18, 5546-5553.
- POMERANTZ, M. M., AHMADIYEH, N., JIA, L., HERMAN, P., VERZI, M. P., DODDAPANENI, H., BECKWITH, C. A., CHAN, J. A., HILLS, A., DAVIS, M., YAO, K. L., KEHOE, S. M., LENZ, H. J., HAIMAN, C. A., YAN, C. L., HENDERSON, B. E., FRENKEL, B., BARRETINA, J., BASS, A., TABERNERO, J., BASELGA, J., REGAN, M. M., MANAK, J. R., SHIVDASANI, R., COETZEE, G. A. & FREEDMAN, M. L. 2009. The 8q24 cancer risk variant rs6983267 shows long-range interaction with MYC in colorectal cancer. *Nature Genetics*, 41, 882-884.

- ROBERTS, J. A., MIGUEL-ESCALADA, I., SLOVIK, K. J., WALSH, K. T., HADZHIEV, Y., SANGES, R., STUPKA, E., MARSH, E. K., BALCIUNIENE, J., BALCIUNAS, D. & MULLER, F. 2014. Targeted transgene integration overcomes variability of position effects in zebrafish. *Development*, 141, 715-724.
- SMEMO, S., TENA, J. J., KIM, K.-H., GAMAZON, E. R., SAKABE, N. J., GOMEZ-MARIN, C., ANEAS, I., CREDIDIO, F. L., SOBREIRA, D. R., WASSERMAN, N. F., LEE, J. H., PUVIINDRAN, V., TAM, D., SHEN, M., SON, J. E., VAKILI, N. A., SUNG, H.-K., NARANJO, S., ACEMEL, R. D., MANZANARES, M., NAGY, A., COX, N. J., HUI, C.-C., GOMEZ-SKARMETA, J. L. & NOBREGA, M. A. 2014. Obesity-associated variants within FTO form long-range functional connections with IRX3. *Nature*, 507, 371-5.
- STRAWBRIDGE, R. J., DUPUIS, J., PROKOPENKO, I., BARKER, A., AHLQVIST, E., RYBIN, D., PETRIE, J. R., TRAVERS, M. E., BOUATIA-NAJI, N., DIMAS, A. S., NICA, A., WHEELER, E., CHEN, H., VOIGHT, B. F., TANEERA, J., KANONI, S., PEDEN, J. F., TURRINI, F., GUSTAFSSON, S., ZABENA, C., ALMGREN, P., BARKER, D. J. P., BARNES, D., DENNISON, E. M., ERIKSSON, J. G., ERIKSSON, P., EURY, E., FOLKERSEN, L., FOX, C. S., FRAYLING, T. M., GOEL, A., GU, H. F., HORIKOSHI, M., ISOMAA, B., JACKSON, A. U., JAMESON, K. A., KAJANTIE, E., KERR-CONTE, J., KUULASMAA, T., KUUSISTO, J., LOOS, R. J. F., LUAN, J. A., MAKRILAKIS, K., MANNING, A. K., MARTINEZ-LARRAD, M. T., NARISU, N., MANNILA, M. N., OHRVIK, J., OSMOND, C., PASCOE, L., PAYNE, F., SAYER, A. A., SENNBLAD, B., SILVEIRA, A., STANCAKOVA, A., STIRRUPS, K., SWIFT, A. J., SYVANEN, A. C., TUOMI, T., VAN 'T HOOFT, F. M., WALKER, M., WEEDON, M. N., XIE, W. J., ZETHELIUS, B., ONGEN, H., MALARSTIG, A., HOPEWELL, J. C., SALEHEEN, D., CHAMBERS, J., PARISH, S., DANESH, J., KOONER, J., OSTENSON, C. G., LIND, L., COOPER, C. C., SERRANO-RIOS, M., FERRANNINI, E., FORSEN, T. J., CLARKE, R., FRANZOSI, M. G., SEEDORF, U., WATKINS, H., FROGUEL, P., JOHNSON, P., DELOUKAS, P., COLLINS, F. S., LAAKSO, M., DERMITZAKIS, E. T., BOEHNKE, M., MCCARTHY, M. I., WAREHAM, N. J., GROOP, L., PATTOU, F., GLOYN, A. L., DEDOISSIS, G. V., LYSENKO, V., MEIGS, J. B., BARROSO, I., WATANABE, R. M., INGELSSON, E., et al. 2011. Genome-Wide Association Identifies Nine Common Variants Associated With Fasting Proinsulin Levels and Provides New Insights Into the Pathophysiology of Type 2 Diabetes. *Diabetes*, 60, 2624-2634.
- TRYNKA, G., SANDOR, C., HAN, B., XU, H., STRANGER, B. E., LIU, X. S. & RAYCHAUDHURI, S. 2013. Chromatin marks identify critical cell types for fine mapping complex trait variants. *Nature Genetics*, 45, 124-130.
- WANG, X. H., LEI, X. G. & WANG, J. F. 2014. Malondialdehyde regulates glucose-stimulated insulin secretion in murine islets via TCF7L2-dependent Wnt signaling pathway. *Molecular and Cellular Endocrinology*, 382, 8-16.
- YAMAMOTO, Y. Y., ICHIDA, H., ABE, T., SUZUKI, Y., SUGANO, S. & OBOKATA, J. 2007. Differentiation of core promoter architecture between plants and mammals revealed by LDSS analysis. *Nucleic Acids Research*, 35, 6219-6226.
- YAMAUCHI, T., HARA, K., MAEDA, S., YASUDA, K., TAKAHASHI, A., HORIKOSHI, M., NAKAMURA, M., FUJITA, H., GRARUP, N., CAUCHI, S., NG, D. P. K., MA, R. C. W., TSUNODA, T., KUBO, M., WATADA, H., MAEGAWA, H., OKADA-IWABU, M., IWABU, M., SHOJIMA, N., SHIN, H. D., ANDERSEN, G., WITTE, D.

R., JORGENSEN, T., LAURITZEN, T., SANDBAEK, A., HANSEN, T., OHSHIGE, T., OMORI, S., SAITO, I., KAKU, K., HIROSE, H., SO, W. Y., BEURY, D., CHAN, J. C. N., PARK, K. S., TAI, E. S., ITO, C., TANAKA, Y., KASHIWAGI, A., KAWAMORI, R., KASUGA, M., FROGUEL, P., PEDERSEN, O., KAMATANI, N., NAKAMURA, Y. & KADOWAKI, T. 2010. A genome-wide association study in the Japanese population identifies susceptibility loci for type 2 diabetes at UBE2E2 and C2CD4A-C2CD4B. *Nature Genetics*, 42, 864-+.

### **Other Sources**

NHS [Accessed May 2014] Available at: <http://www.nhs.uk/Conditions/Diabetes-type1/Pages/Introduction.aspx>

REED, B., JENNINGS, M. 2010. Guidance on the housing and care of Zebrafish *Danio rerio*. *RSPCA*.

THISSE, B., PFLUMIO, S., FÜRTHAUER, M., LOPPIN, B., HEYVER, V., DEGRAVE, A., WOEHL, R., LUX, A., STEFFAN, T., CHARBONNIER, X.Q. and THISSE, C. (2001) Expression of the zebrafish genome during embryogenesis (NIH R01 RR15402). ZFIN Direct Data Submission (<http://zfin.org>).

THISSE, C., THISSE, B. (2008) High resolution in situ hybridization on whole-mount zebrafish embryo. *Nature Protocol*, 3, 59-69. Updated protocol available at: <https://wiki.zfin.org/display/prot/Thisse+Lab+-+In+Situ+Hybridization+Protocol+-+2010+update>

## **APPENDIX I – ADDITIONAL DATA**

AI.1. Crossing Record

Construct	SNP Type	Label	Date Crossed	No. Pairs that laid	Pair	No. Embryos Laid	Number of Transgenics from survivors					
<b>Tg(ycry-ATTR-mCherry,Hs.PROX1-G-prox1:YFP-ATTR-GFP)</b>	Common_G	P.G	30/03/2014	11/23	P.G 1	25	0					
					P.G 2	120	0					
					P.G 3	30	0					
					P.G 4	50	17 RL+GL					
					P.G 5	100	0					
					P.G 6	40	0					
					P.G 7	100	0					
					P.G 8	50	0					
					P.G 9	30	0					
					P.G 10	50	0					
					P.G 11	70	0					
					<b>Tg(ycry-ATTR-mCherry,Hs.PROX1-A-prox1:YFP-ATTR-GFP)</b>	Rare Variant_P.A		07/04/2014	18/28	P.A 1	30	0
										P.A 2	40	0
										P.A 3	20	0
										P.A 4	20	0
P.A 5	50	0										
P.A 6	60	0										
P.A 7	30	0										
P.A 8	20	0										
P.A 9	70	0										
P.A 10	10	0										
P.A 11	100	0										
P.A 12	80	1 RL, 1 RL+GL										
P.A 13	50	1 RL, 3 RL+GL										
P.A 14	10	0										
P.A 15	50	0										
P.A 16	10	0										
P.A 17	40	1 RL, 10 RL+GL										
P.A 18	30	2 RL+GL, 2 WRL										
<b>Tg(ycry-ATTR-mCherry,Hs.C2CD4A-C-hsp70:YFP-ATTR)</b>	Common_C	C.C	26/03/2014	11/22	C.C 1	50	0					
					C.C 2	20	0					
					C.C 3	25	0					
					C.C 4	80	50 RL					
					C.C 5	40	0					
					C.C 6	40	0					
					C.C 7	30	4 RL					
					C.C 8	70	0					
					C.C 9	50	0					
					C.C 10	60	0					
					C.C 11	50	0					
					<b>Tg(ycry:ATTR-mCherry,Hs.C2CD4A-T-hsp70:YFP-ATTR)</b>	Rare Variant_C.T		01/01/2014	20/33	C.T 1	50	1 RL, 1RL+GL
										C.T 2	15	0
										C.T 3	20	0
										C.T 4	50	1 RL
C.T 5	80	0										
C.T 6	20	5 RL, 6 RL+GL										
C.T 7	60	0										
C.T 8	90	0										
C.T 9	40	0										
C.T 10	50	0										

					C.T 11	60	1 RL	
					C.T 12	30		0
					C.T 13	30		0
					C.T 14	40	3 RL, 4 RL + GL	
					C.T 15	20		0
					C.T 16	20	1 RL, 1RL+GL	
					C.T 17	30		0
					C.T 18	50		0
					C.T 19	40	4 RL, 1 RL+GL	
					C.T 20	20	3 RL, 2 RL+GL	
<b>Tg(cry:ATTR-mCherry,Hs.ZFAND3-C-hsp70:YFP-ATTR-GFP)</b>	<b>Common_C</b>	<b>Z.C</b>	<b>09/04/2014</b>	<b>6/23</b>	Z.C 1	100		0
					Z.C 2	50		0
					Z.C 3	100		0
					Z.C 4	30		0
					Z.C 5	60		0
					Z.C 6	60		0
			13/07/2014	13/20	Z.C 7	100		0
					Z.C 8	300		0
					Z.C 9	100		0
					Z.C 10	60		0
					Z.C 11	80		0
					Z.C 12	50		0
					Z.C 13	40		0
					Z.C 14	70		0
					Z.C 15	200		0
					Z.C 16	70		0
					Z.C 17	100		0
					Z.C 18	50		0
					Z.C 19	100		0
<b>cry:ATTR-mCherry,Hs.ZFAND3-T-hsp70:YFP-ATTR-</b>	<b>Rare Variant_T</b>	<b>Z.T</b>	<b>09/04/2014</b>	<b>2/6</b>	Z.T 1	50		0
					Z.T 2	30		0
			13/07/2014	11/15	Z.T 3	50		0
					Z.T 4	80		0
					Z.T 5	90		0
					Z.T 6	60		0
					Z.T 7	60		0
					Z.T 8	60		0
					Z.T 9	50		0
					Z.T 10	100		0
					Z.T 11	200		0
					Z.T 12	80		0
					Z.T 13	150		0
<b>Tg(cry:ATTR-mCherry,Hs.TCF7L2-C-tcf7l2:YFP-ATTR</b>	<b>Common_C</b>	<b>T.C</b>	<b>24/03/2013</b>	<b>3/6</b>	T.C 1	100		0
					T.C 2	40		0
					T.C 3	50		0
			23/06/2014	2/11	T.C 1	50		0
					T.C 2	180		0
			15/07/2014	13/20	T.C 1	100		0
					T.C 2	300		0
					T.C 3	100		0
					T.C 4	60		0
					T.C 5	50		0
					T.C 6	50		0
					T.C 7	80		0
					T.C 8	70		0
					T.C 9	200		0
					T.C 10	70		0
					T.C 11	100		0
					T.C 12	50		0
					T.C 13	80		0
<b>Tg(cry:ATTR-mCherry,Hs.TCF7L2-T-tcf7l2:YFP-ATTR)</b>	<b>Rare Variant_T</b>	<b>T.T</b>	<b>23/06/2014</b>	<b>3/11</b>	T.C 1	200		0
					T.C 2	100		0
					T.C 3	150		0
			15/07/2014	11/15	T.C 1	50		0
					T.C 2	80		0
					T.C 3	40		0
					T.C 4	60		0
					T.C 5	60		0
					T.C 6	60		0
					T.C 7	50		0
					T.C 8	100		0
					T.C 9	200		0
					T.C 10	80		0
					T.C 11	150		0

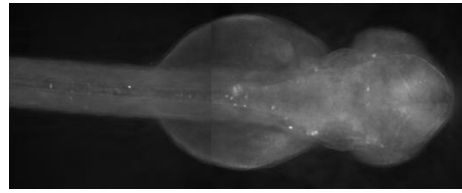
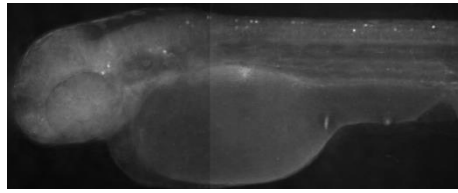
KEY

RL Red Lense  
GL Green Lense

## AI.2 48hpf FLUORESCENCE IMAGES

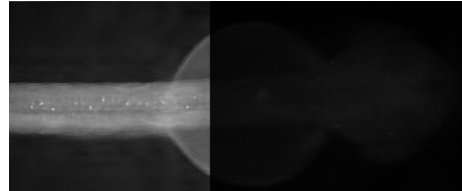
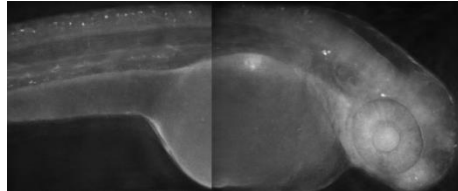
### PROX G

LINE1  
EMBRYO 2

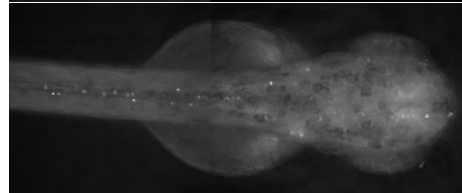
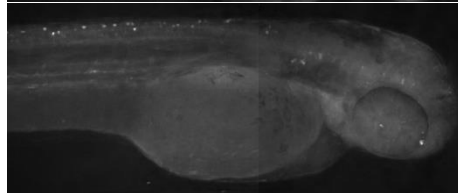


### PROX A

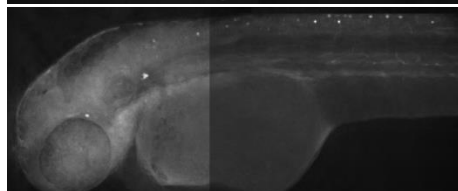
LINE 1  
EMBRYO 2



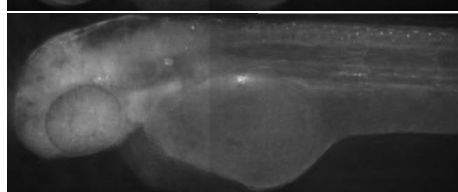
LINE 2  
EMBRYO 1



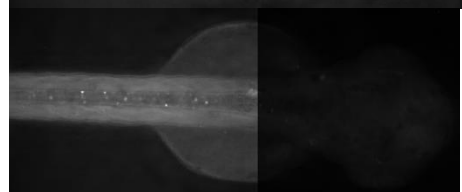
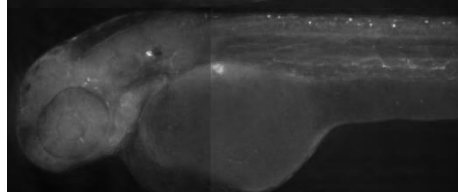
LINE 2  
EMBRYO 2



LINE 3  
EMBRYO 1



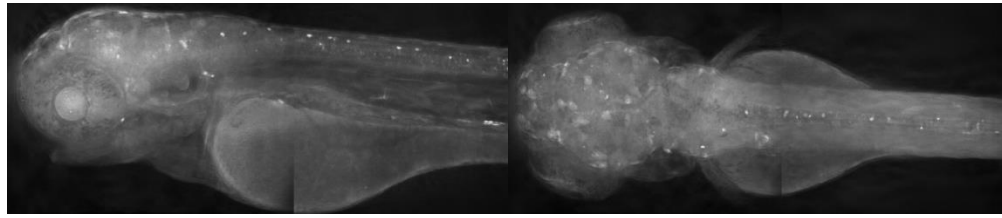
LINE 3  
EMBRYO 2



AI.3 72hpf FLUORESCENCE IMAGES

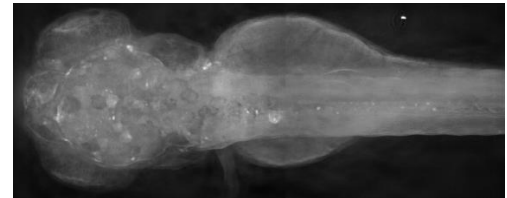
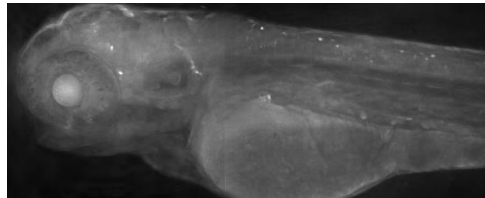
**PROX G**

LINE1  
EMBRYO 2

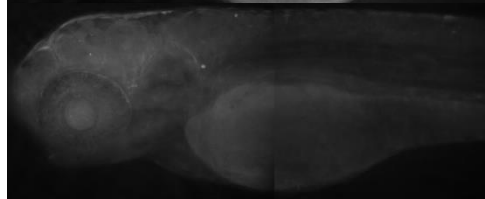


**PROX A**

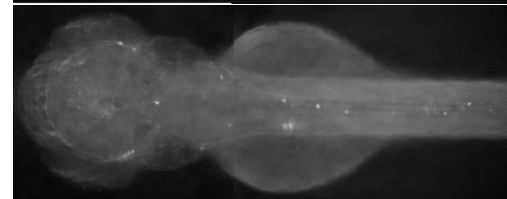
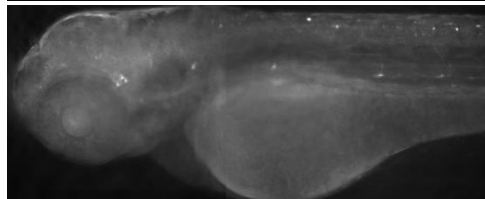
LINE 1  
EMBRYO 2



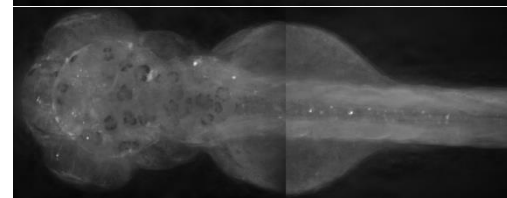
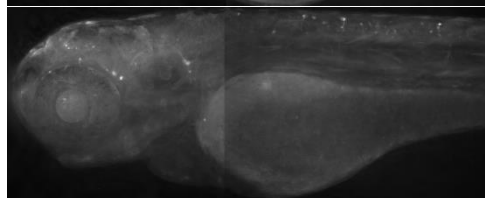
LINE 2  
EMBRYO 1



LINE 2  
EMBRYO 2



LINE 3  
EMBRYO 1



LINE 3  
EMBRYO 2

